

FY 2018

Gravitational Waves

Shinji Miyoki

**The University of Tokyo
Institute for Cosmic Ray Research
Astronomy and Gravity Division
KAGRA Observatory**

Contents

1. Special Relativity
2. **General Introduction of Challenge to direct detection of GWs**
3. Gravitational Waves from General Relativity
4. Gravitational Wave Sources and Wave Forms
5. Techniques to Treat Small Signals
6. Techniques of Gravitational Wave Detectors (GWD) (1)
 - Power Recycled Fabry-Perot Michelson Interferometer using Resonant Sideband Extraction Technique
 - Noise sources and its suppression
 - Control of GWDs
 - Next Generation (3rd) GWDs Outline.
7. Data Analysis
8. New fields explored by Advanced Techniques for GWDs.

General Introduction of Challenge to direct detection of GWs

■ What is Gravitational Wave (GW)

- History of Relativity verifications
- Gravitational Waves from General Relativity
- Why the direct detection of GW is desired ?

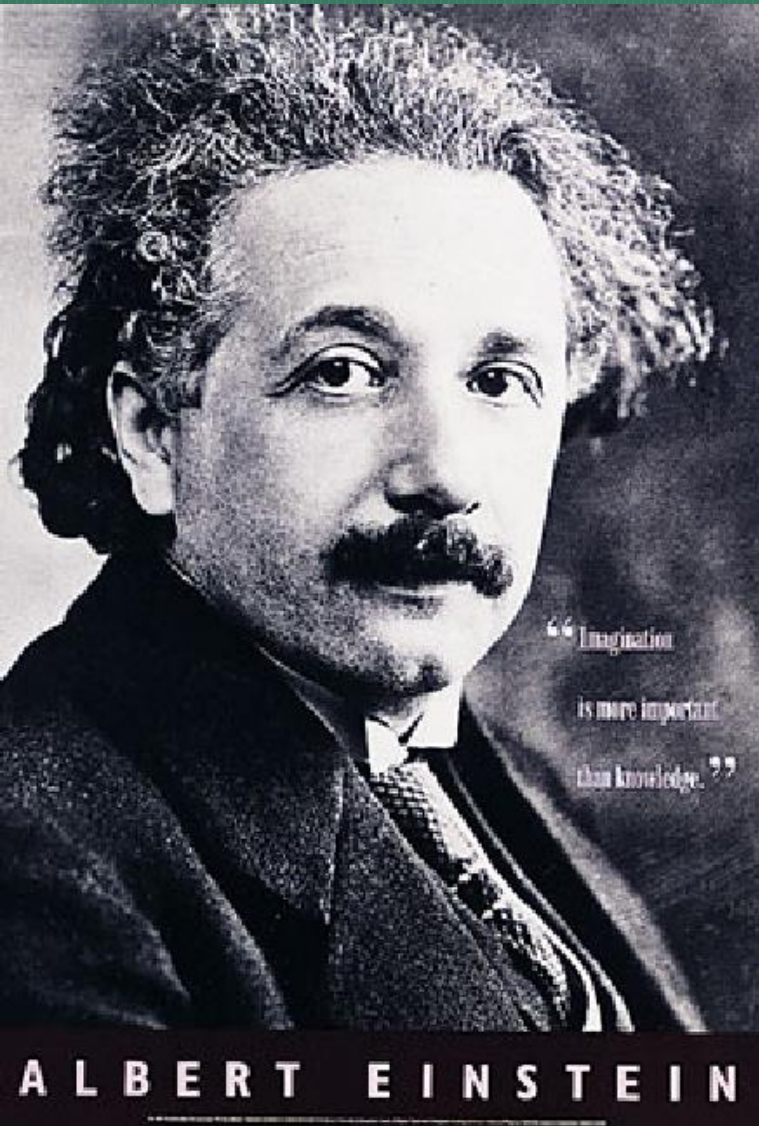
■ GW Sources

■ Development of GW detectors (GWDs)

- Resonant type GWDs
- Laser interferometer GWDs

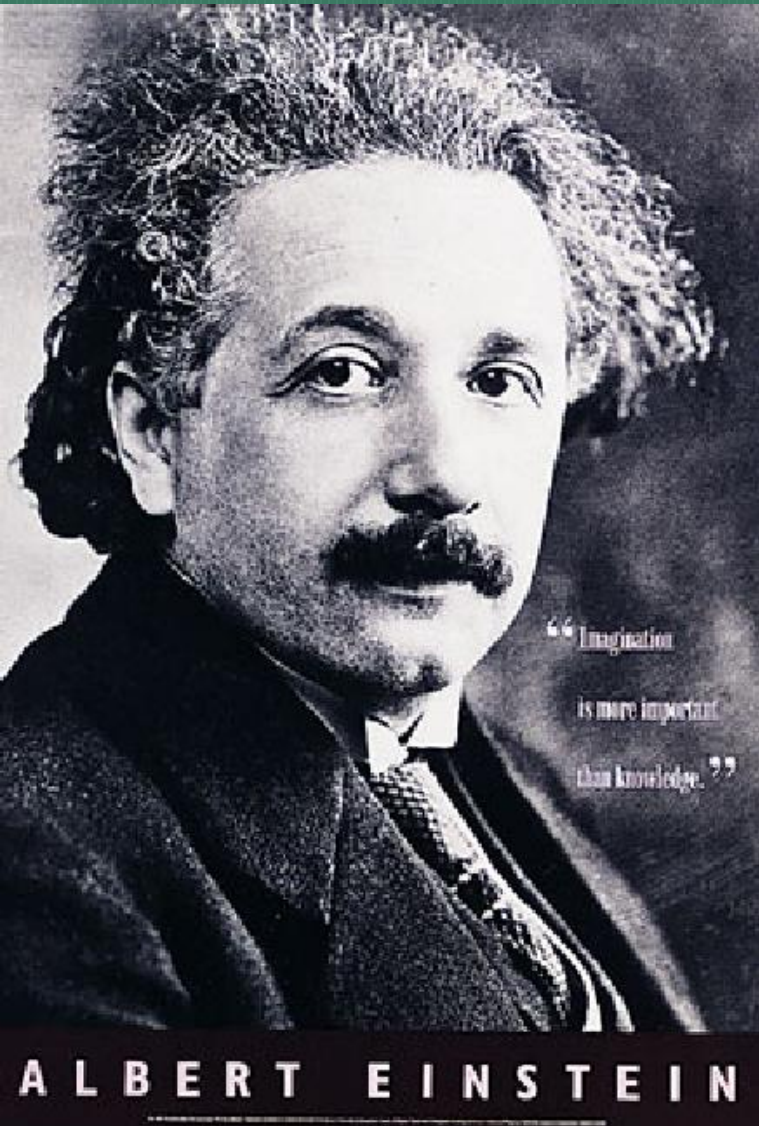
■ Km-scale GWDs in the world

What is GWs ?



- Ripple of space-time derived from Einstein's General Theory of Relativity.
- The speed of GWs is expected to be same with light speed.
- GW is transparent for any material, except gravity sources.

What is GWs ?



- Polarization of GWs is quadrupole because graviton is mono-pole, while dipole for EMWs because charge has two polarities.
- If GWs pass through the space-time, the distance between two free-falling mass seems to be extended and/or shrunk.
- GWs frequency varies for their origins. The first targeted GW frequencies are from 10 Hz to 1kHz.

Time Delay...

(History of Relativity Verifications 1)

- Special Relativity (Constant Light Speed, Inertia System Ideas)
 - Time Delay → Observation of life time extension of muon.
 - Lorentz Contraction

Muon

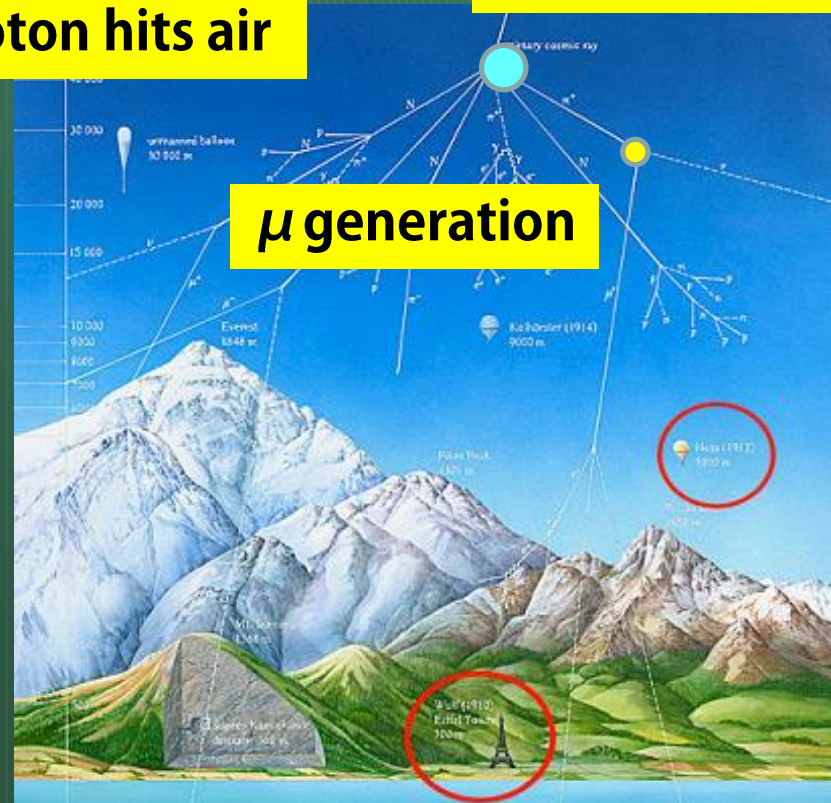
$$\begin{aligned}\mu^- &\rightarrow e^- + \nu_\mu + \bar{\nu}_e \\ \mu^+ &\rightarrow e^+ + \nu_e + \bar{\nu}_\mu\end{aligned} \quad dt' = \frac{1}{\sqrt{1 - (v/c)^2}} dt$$

- Muon life time is $\sim 2.2 \times 10^{-6}$ [sec].
- 660 m is the maximum travelling length. Muons cannot reach to the ground!
- However, the life is extended upto $\sim 10^{-4}$ [sec] because of the near light speed.

Proton hits air

π generation

μ generation



Curved Space-time

(History of Relativity Verifications 2)

■ General Theory of Relativity predicts Curved Space

- Gravity Lensing Effect (GL) → In 1919, Sir S. Eddington observed star position effects near the SUN before and after the eclipse. Recently, GL is used to observe the amount of Dark Matter in the space.
- Perihelion Shift → Observed in Mercury and compact binary systems, estimated in binary neutron star system.

LIGHTS ALL ASKEW IN THE HEAVENS

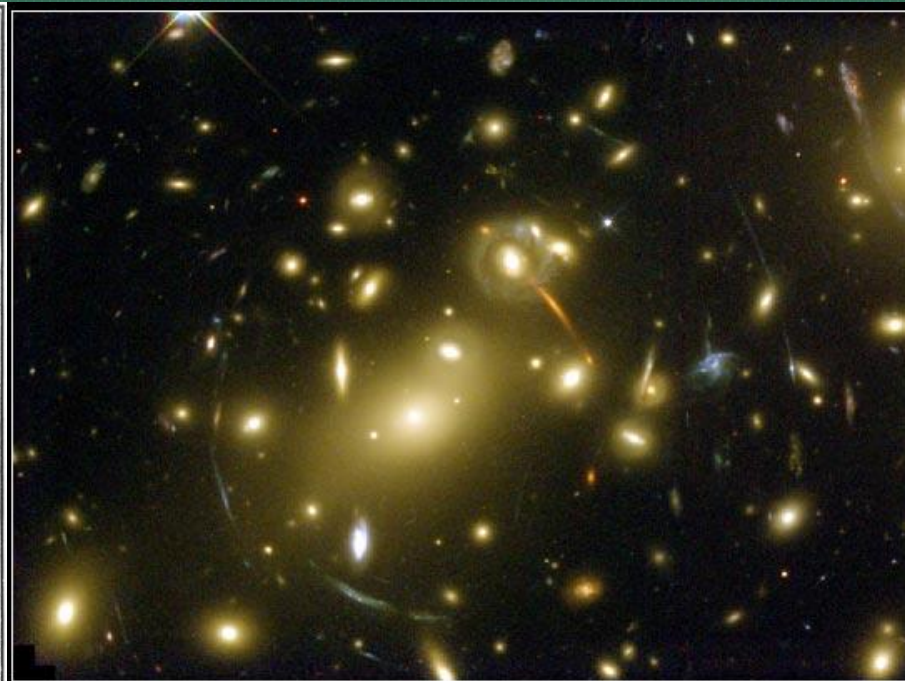
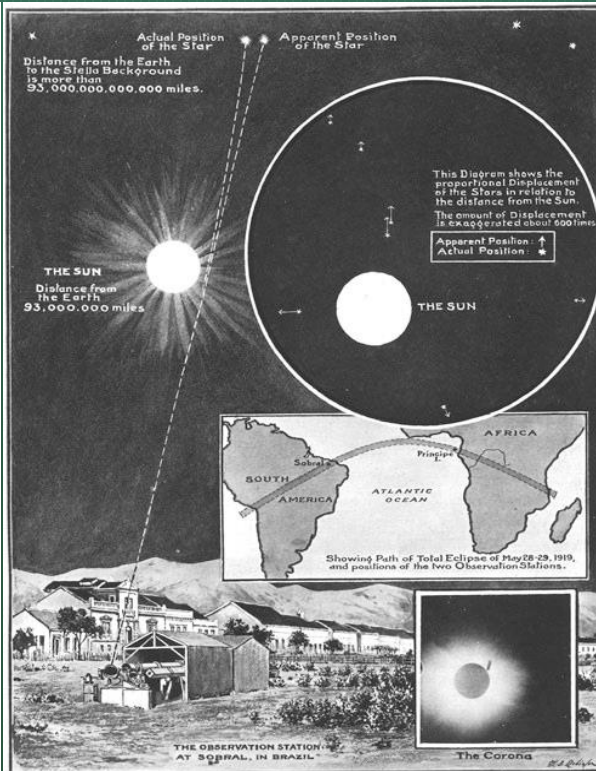
Men of Science More or Less
Agog Over Results of Eclipse
Observations.

EINSTEIN THEORY TRIUMPHS

Stars Not Where They Seemed
or Were Calculated to be,
but Nobody Need Worry.

A BOOK FOR 12 WISE MEN

No More in All the World Could
Comprehend It, Said Einstein When
His Daring Publishers Accepted It.



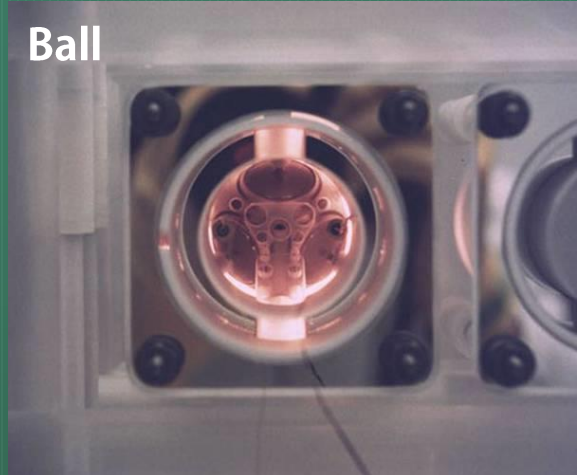
Galaxy Cluster Abell 2218

NASA, A. Fruchter and the ERO Team (STScI, ST-ECF) • STScI-PRC00-

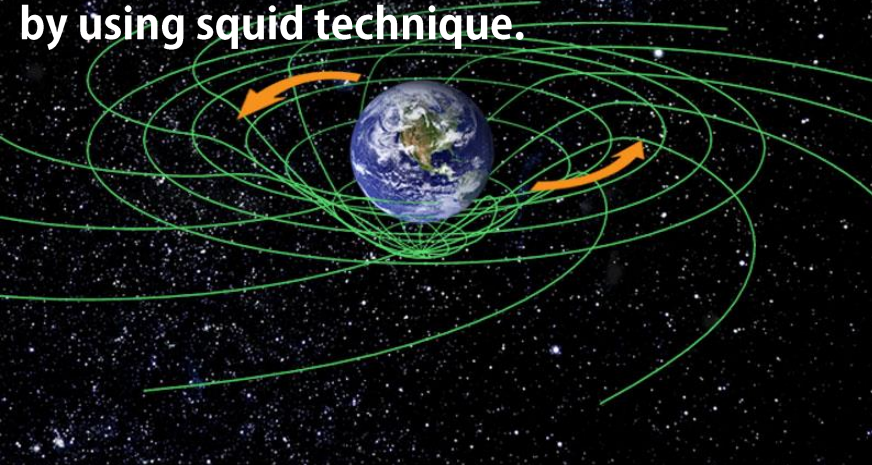
Twisted Space-time

(History of Relativity Verifications 3)

- Frame-Dragging Effect (FDE) → Gravity Probe-B observed FDE and Geodesic Effect as precession (0.000011 degree/year) of a Ball that has ultimate sphericity. (It take 40 years to make a ball !)



Rotate a ball that has ultimate sphericity (2mm roughness for the Earth scale ball !!), and monitor its precession motion by using squid technique.



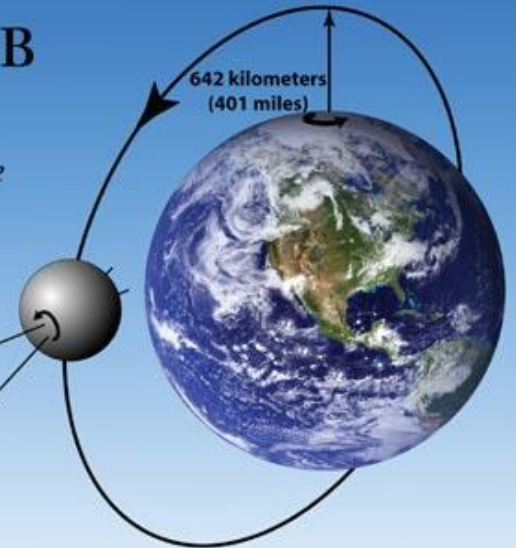
The Gravity Probe B Experiment

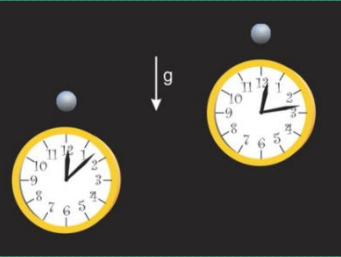
...testing Einstein's Universe

Frame-dragging Effect
39 milliarcseconds/year
(0.000011 degrees/year)

Guide Star
IM Pegasi
(HR 8703)

Geodetic Effect
6,606 milliarcseconds/year
(0.0018 degrees/year)





Gravitational Redshift

(History of Relativity Verifications 4)

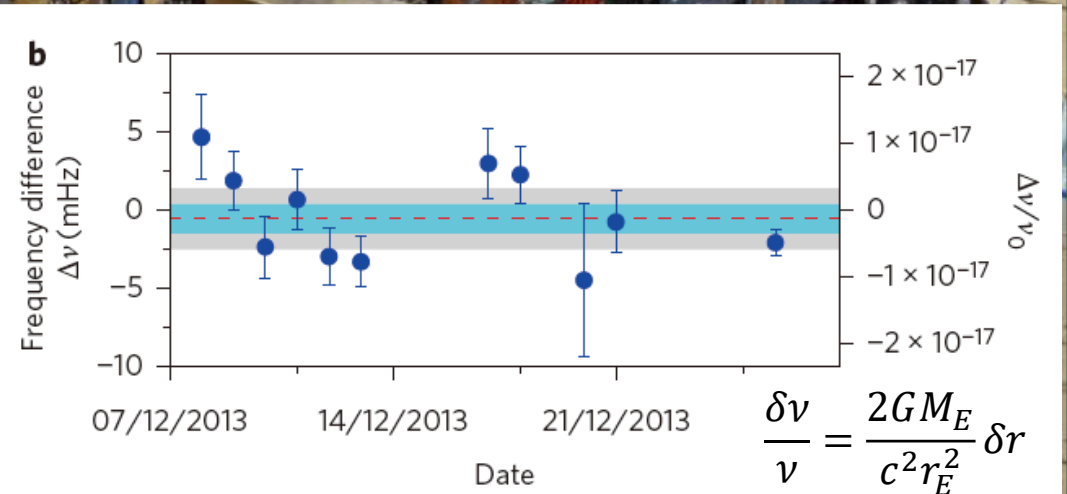
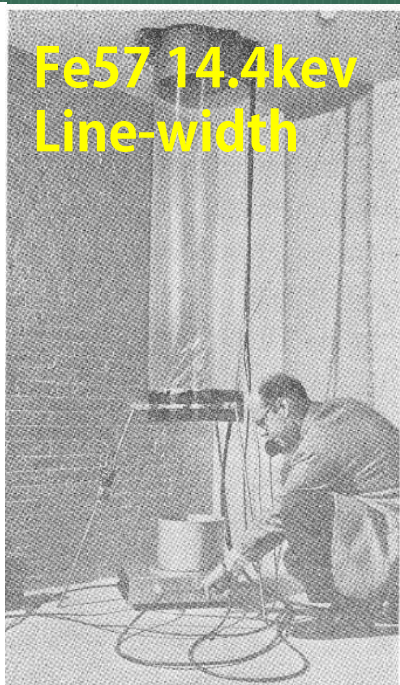
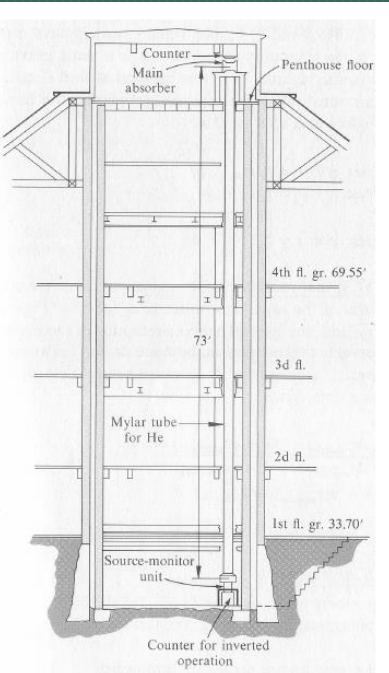
Gravitational Redshift

The strength of gravity affects the time progress.

1960-65 : The redshift between the 22.6 m altitude difference was detected by using Mössbauer Effect.

$$\Delta E = \frac{E_\gamma^2}{2Mc^2} \sim h\delta\nu_{shift}$$

2015 : Optical lattice clock can detects redshift bw the cm level altitude difference. (I.Ushijima et . al., Nature Photonics, 2015.5)

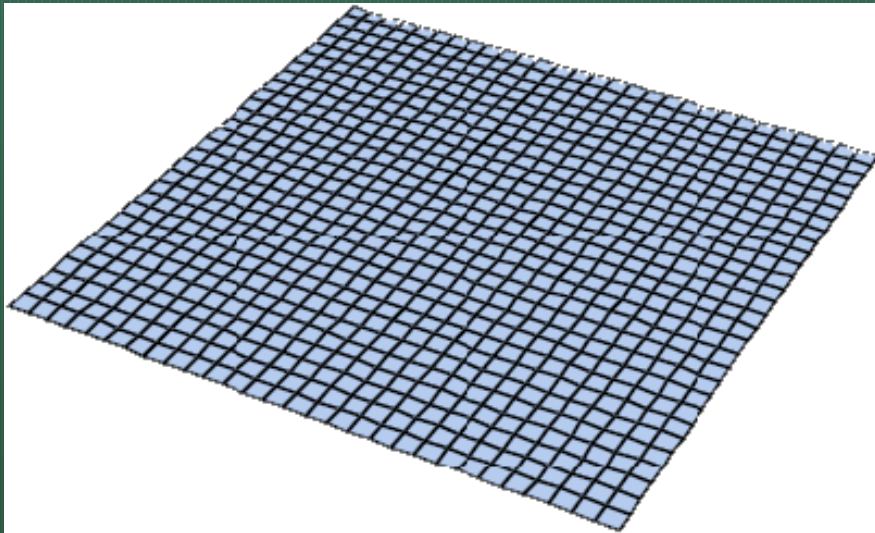


How to Generate GWs

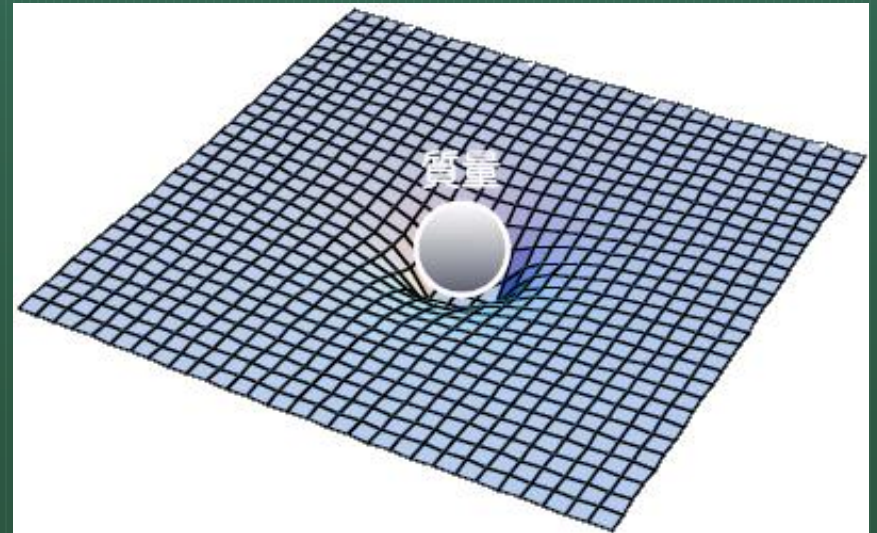
- Non axis-symmetrical motion is required -

■ Geodesic effect around a mass ...

Plane space-time
(assuming 2 dimension)



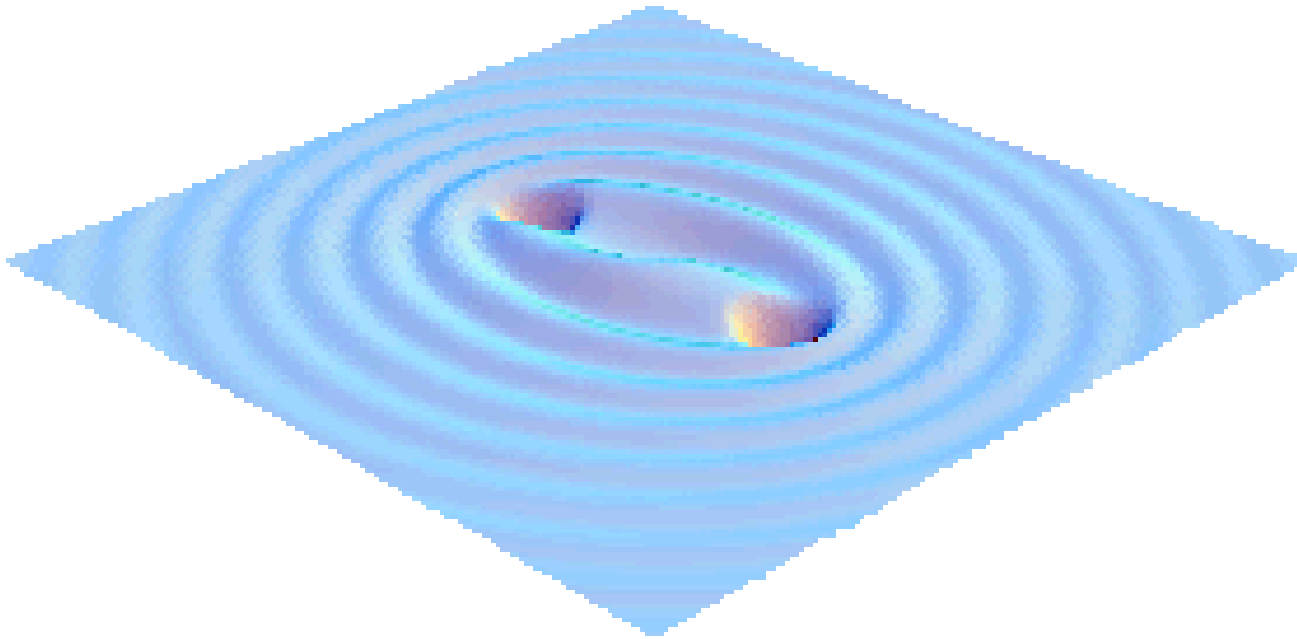
Curved space-time generation
by a spherical mass.
Rotation of this ball cannot
generate GWs.



How to Generate GWs

- Non axisymmetrical motion is required -

- Non axisymmetrical motion is required...
- For example, the compact binary system



(note : GW is not propagation of the change of gravity potential.)

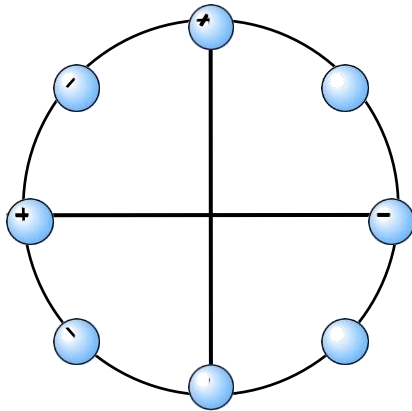
Effect of GWs and Units

- distance change between two free falling masses -

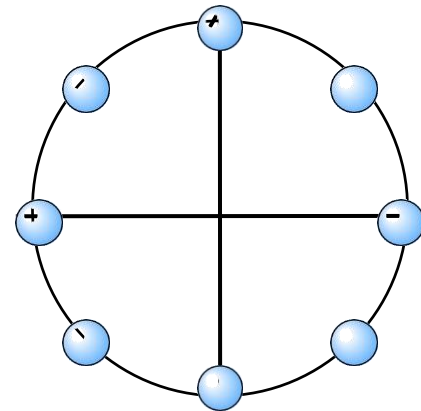
- Two polarization of GWs quadrupole.

Motion of Free Mass

+
mode



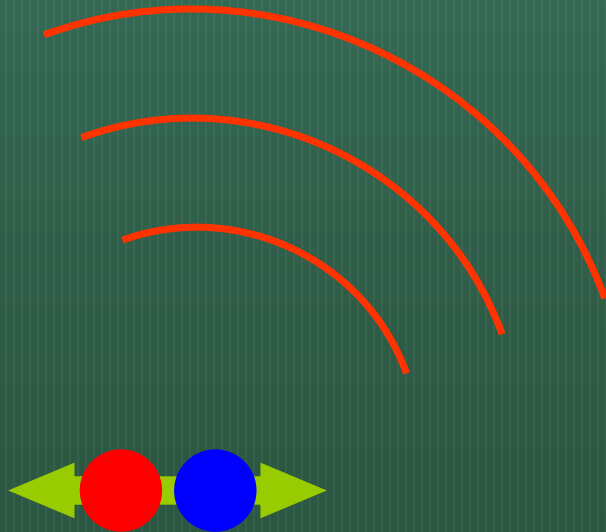
X
mode



Difference between EM and GW

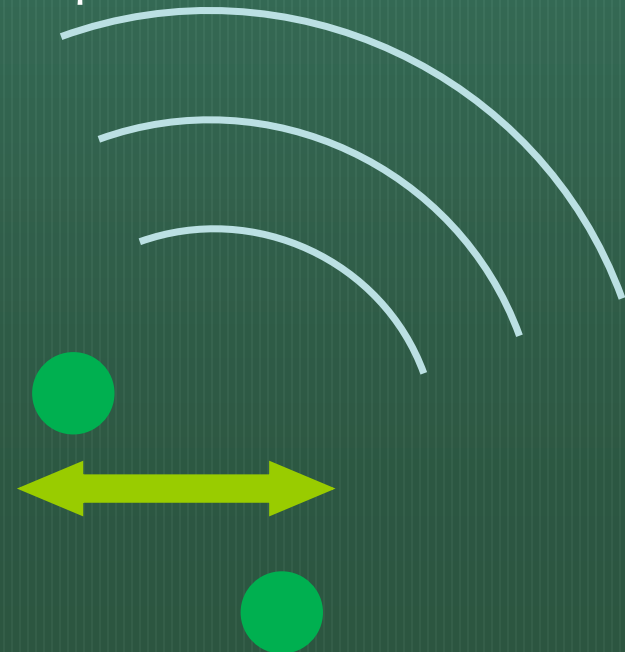
■ EM (Electrical Magnetic Wave)

- Solution of Maxwell Equation (1864)
- Speed of Light
- Verified by Herz (1868)
- Dipole Radiation due to +/- charged particle
- Two Polarizations.



■ GW (Gravitational Wave)

- Solution of Einstein Equation (1916)
- Also Speed of Light
- Indirectly verified by Hulse and Taylor (1982~1989)
- Quadrupole Radiation due to monopole mass.
- Two polarizations.

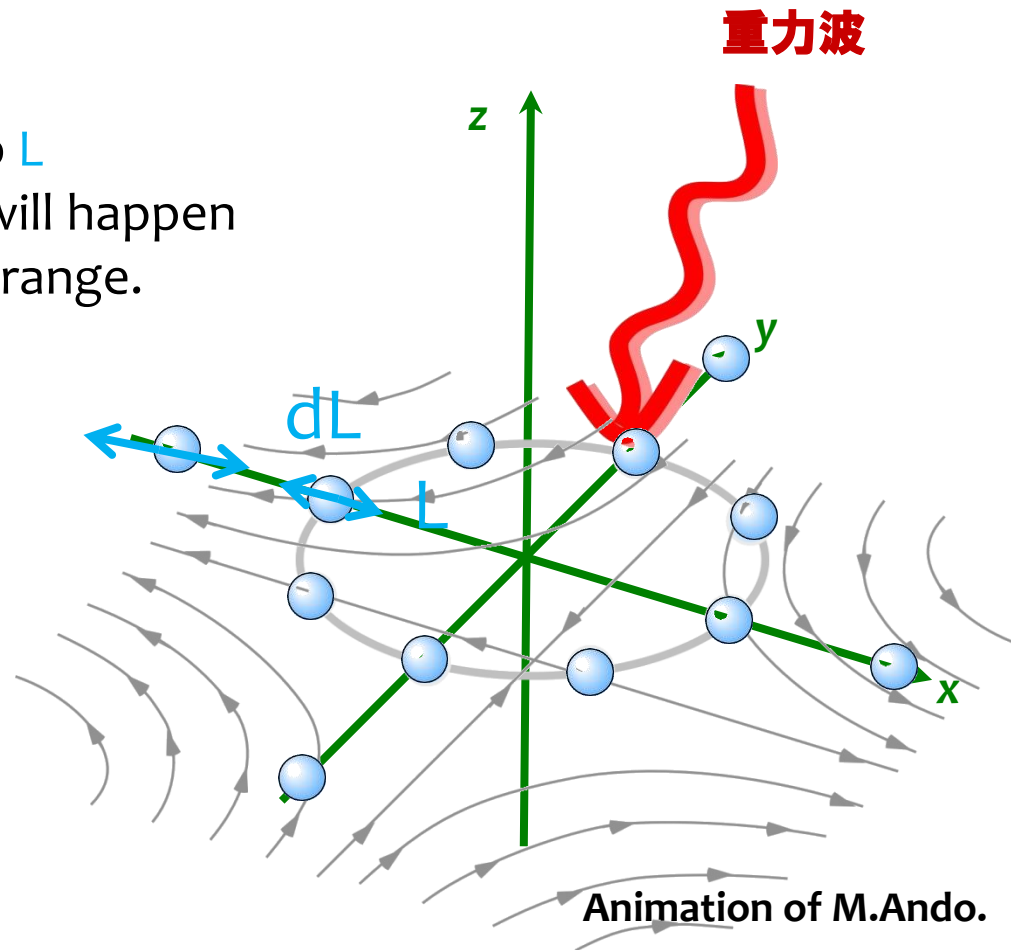


Effect of GWs and Units

- distance change between two free falling masses -

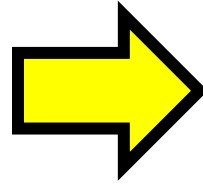
■ Orthogonal length of space-time changes oppositely. If one arm shrinks, the other will extend.

- Strain (h) = dL / L
- dL is proportional to L
- Signal cancellation will happen for some frequency range.

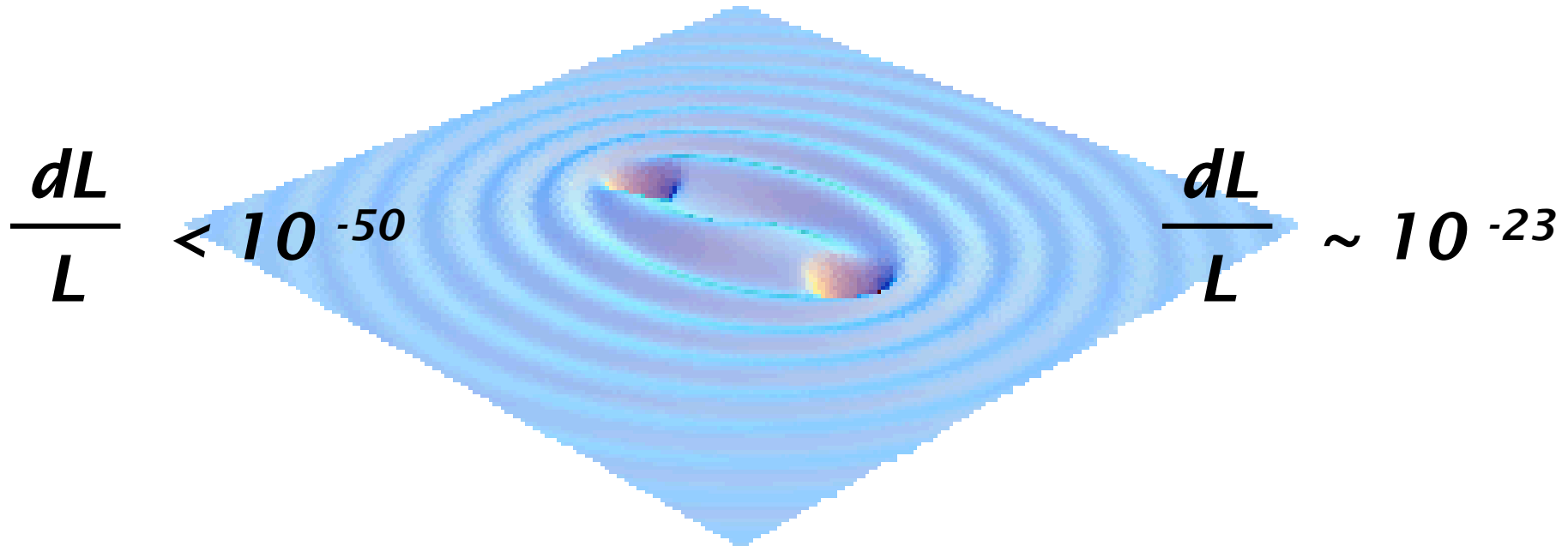


Mass of Star and Compactness are Required

You can generate undetectable small GWs by rolling your arm.

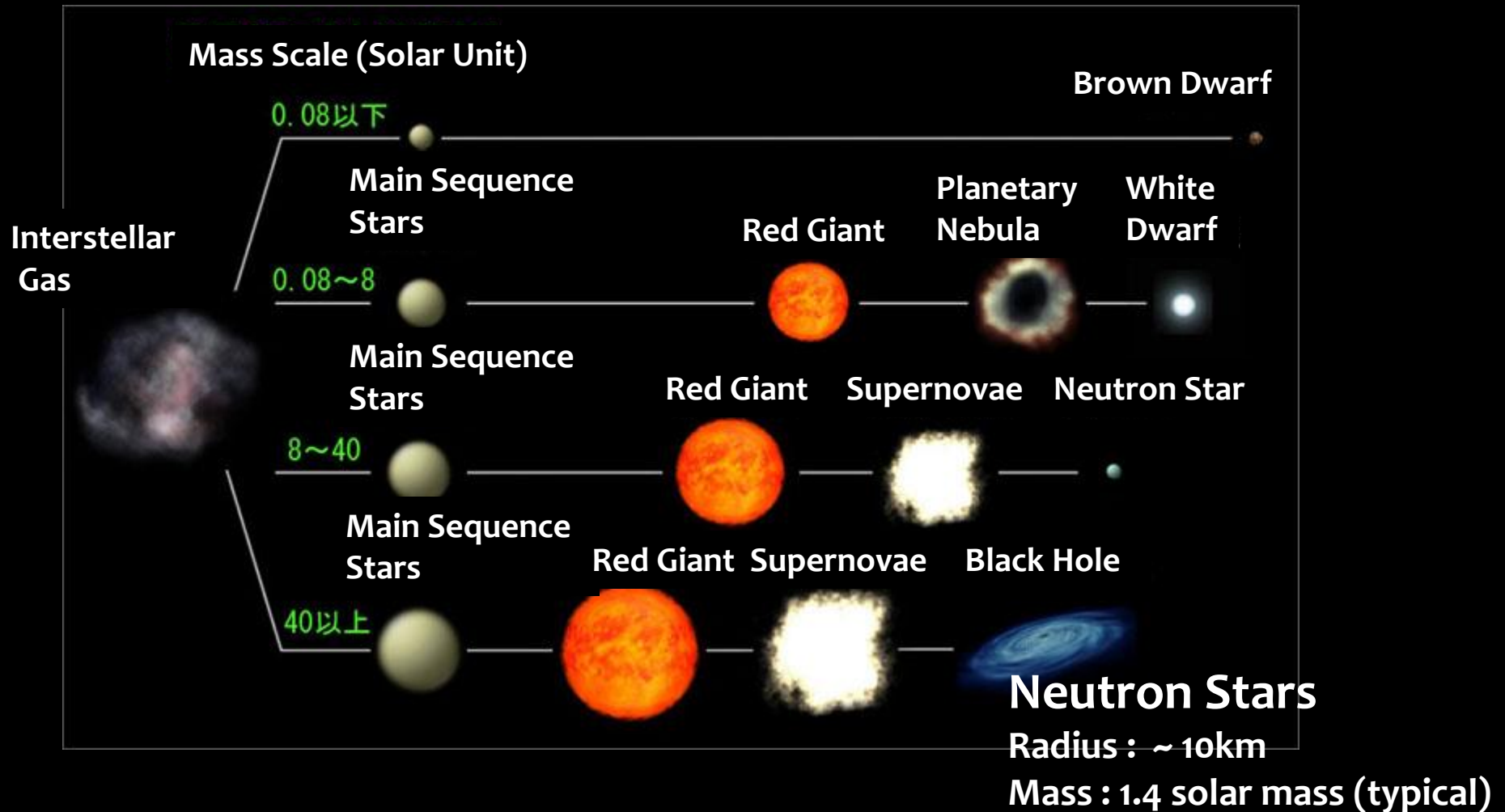


Mass of a star and its mass compactness are necessary to generate GWs that the humankind can detect.



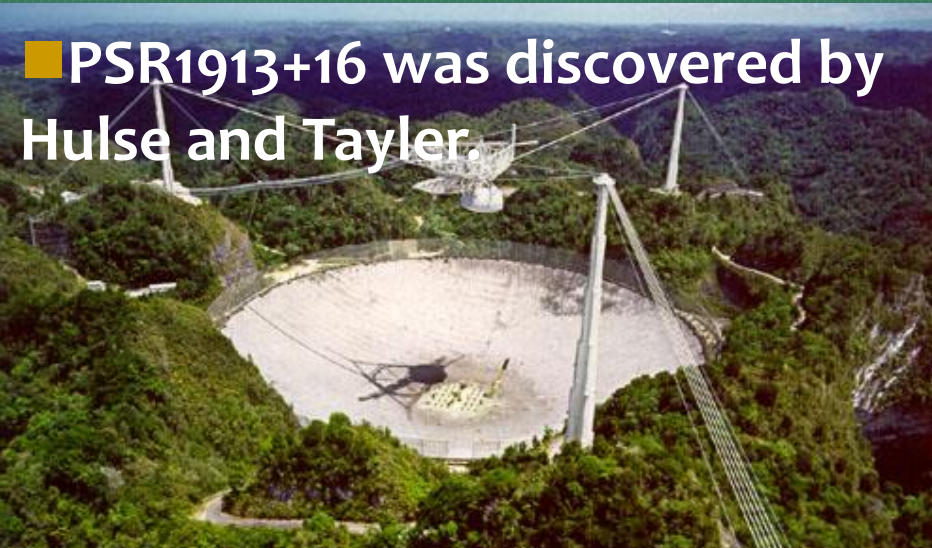
Such kind of compact binary star (Neutron stars (NS) and black holes (BK)) system dose exist ??

Binary Neutron Star System

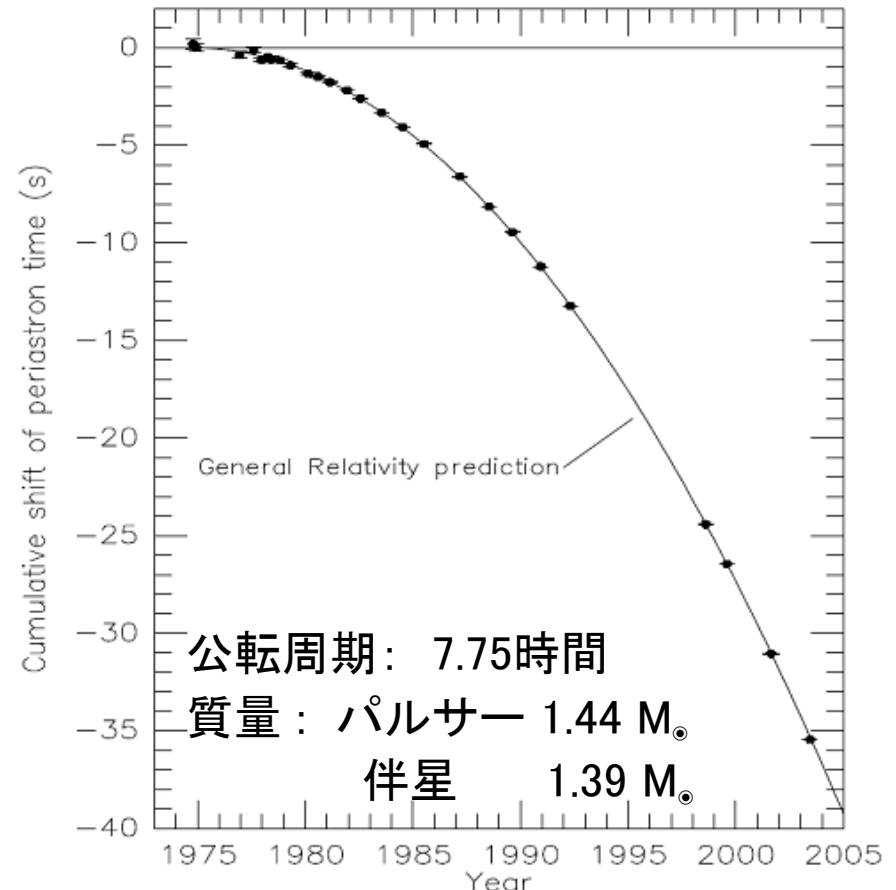


Indirect Evidence of GWs

Observation of the change of revolution time of PSR1913+16



The accumulated amount of periastron changes



Observation : $(-2.4056 \pm 0.0051) \times 10^{-12}$ [s/s]

Theory : $(-2.40242 \pm 0.00002) \times 10^{-12}$ [s/s]

Indirect Evidence of GWs



The Nobel Prize in Physics 1993

"for the discovery of a new type of pulsar, a discovery that has opened up new possibilities for the study of gravitation"



Russell A. Hulse



Joseph H. Taylor Jr.

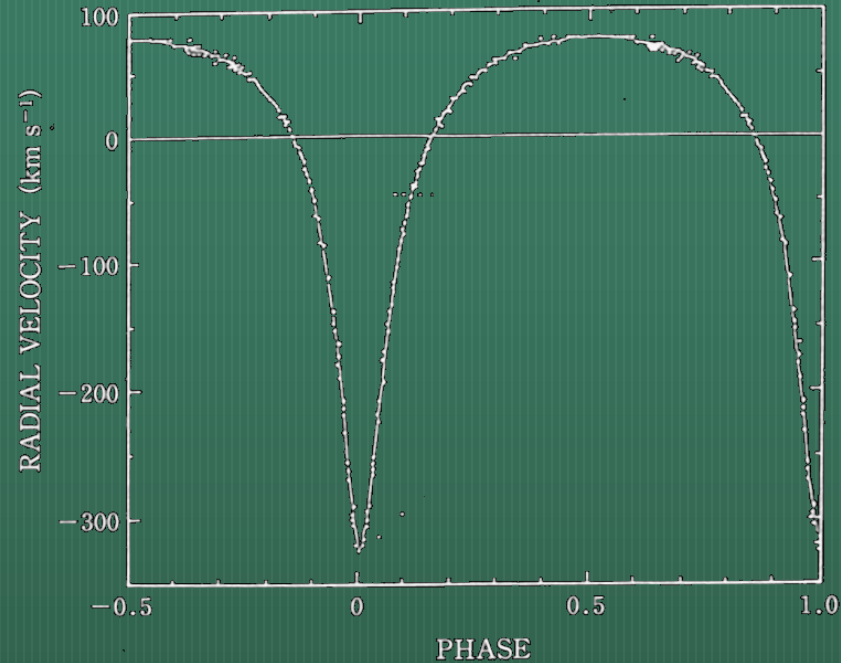
“Direct” detection of GWs are strongly desired !!

Orbital Parameter of PSR1913+16

- Kepler Motion -

- Firstly, a pulsar was found (59msec).
- Its pulse period was regularly modulated (7.75 hours).
- It's a Doppler shift due to **a binary star**.

Orbital parameters are obtained from the radial velocity, assuming Kepler motion.



No possibility except for NS-NS binary system from the obtained parameters,

- Orbital period : 7.751939106 hr (P)
- Eccentricity : 0.617131
- Semimajor axis : 1,950,100 km (a : 長半径)
- Periastron separation : 746,600 km (近星点)
- Apastron separation : 3,153,600 km (遠星点)

$$\frac{a^3}{P^2} = G \frac{M_1 + M_2}{4\pi^2}$$

- a can be estimated from
- orbital velocity
 - G
 - position of a main star
 - Mass of the main star

Orbital Parameter of PSR1913+16

- compensation assuming GR for M_1, M_2 estimation-

Post Kepler parameters...

(1) Change of Perihelion

$$\dot{\omega} = 2.1 \left(\frac{M_1 + M_2}{M_{\odot}} \right)^{2/3} \text{ [deg/year]}$$

(2) Red Shift

$$\gamma = 2.96 \frac{M_1 + 2M_2}{M_{\odot}} \frac{M_2}{M_{\odot}} \left(\frac{M_1 + M_2}{M_{\odot}} \right)^{-4/3} \text{ [msec]}$$

(3) Shapiro Delay

$$r = 5 \frac{M_2}{M_{\odot}} \text{ [\musec]} \quad s = 0.51 \left(\frac{M_2}{M_{\odot}} \right)^{-1} \left(\frac{M_1 + 2M_2}{M_{\odot}} \right)^{2/3} \text{ [msec]}$$

(4) Revolution time decrease due to GWs radiation

$$\dot{P}_b = -54.6 \frac{M_1 M_2}{M_{\odot}^2} \left(\frac{M_1 + M_2}{M_{\odot}} \right)^{-1/3} \text{ [\musec/year]}$$

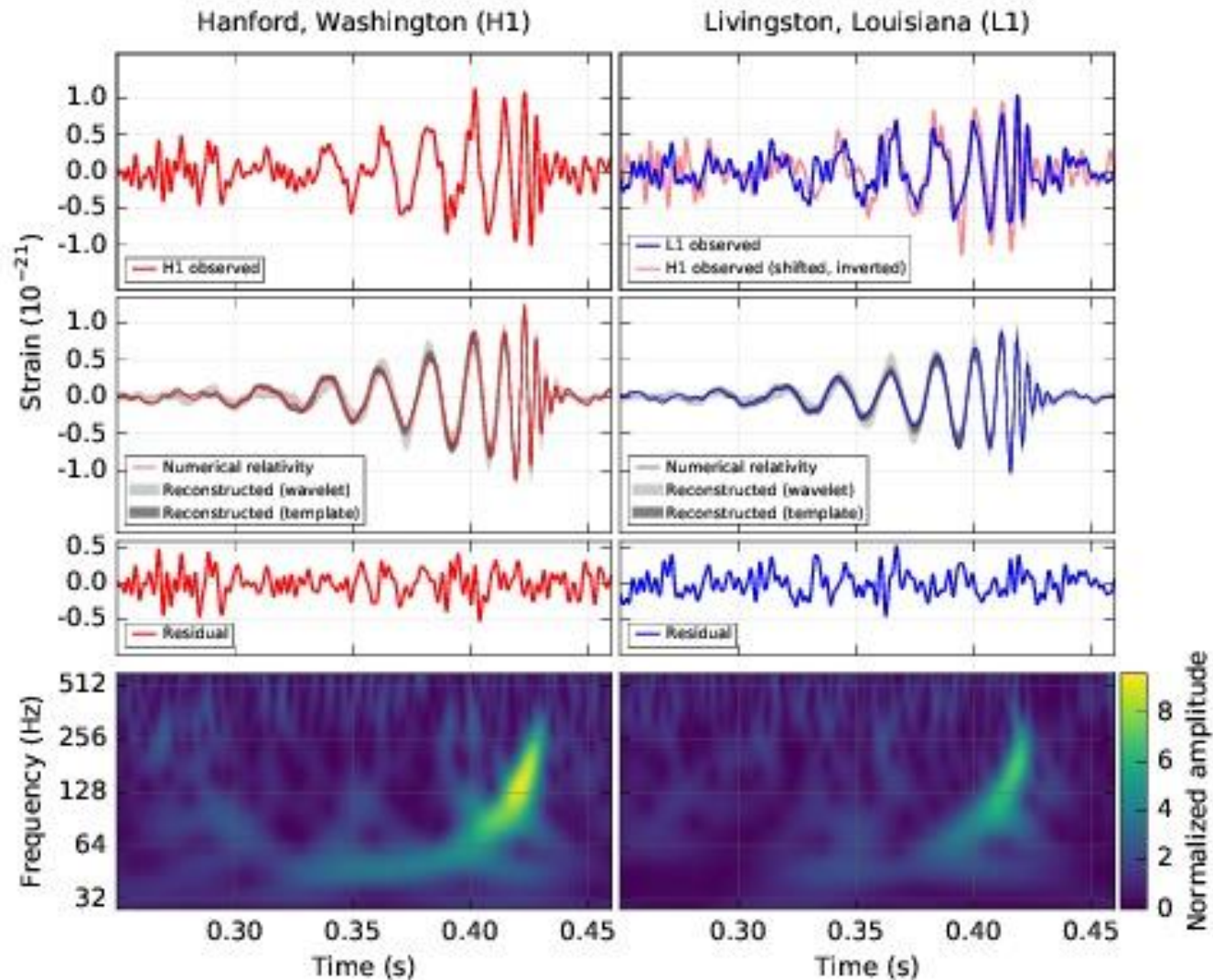
Using a least square methods for each parameters, M_1 and M_2 are decided.

$$M_1 : 1.441 M_{\odot}$$

$$M_2 : 1.387 M_{\odot}$$

Direct Detection of GWs form Binary Black Hole Coalescences by Adv.LIGO

GW150914 ($36M_{\odot} - 29M_{\odot}$) : SN~24, D ~ 440Mpc



Significance of LIGO GW direct detections (GW150914...)

- Direct Evidence of Black Holes
- Discovery of Mid-scale ($> 20M_{\odot}$) BHs
- Discovery of Binary BHs and their coalescences within cosmological time scale.
- Validity of GR in the very strong gravitational fields around $30M_{\odot}$ BHs.

The First Direct Evidence of GWs

Nobel Prize in Physics 2017



Barry C. Barish (Caltech)



Kip S. Thorne (Caltech)



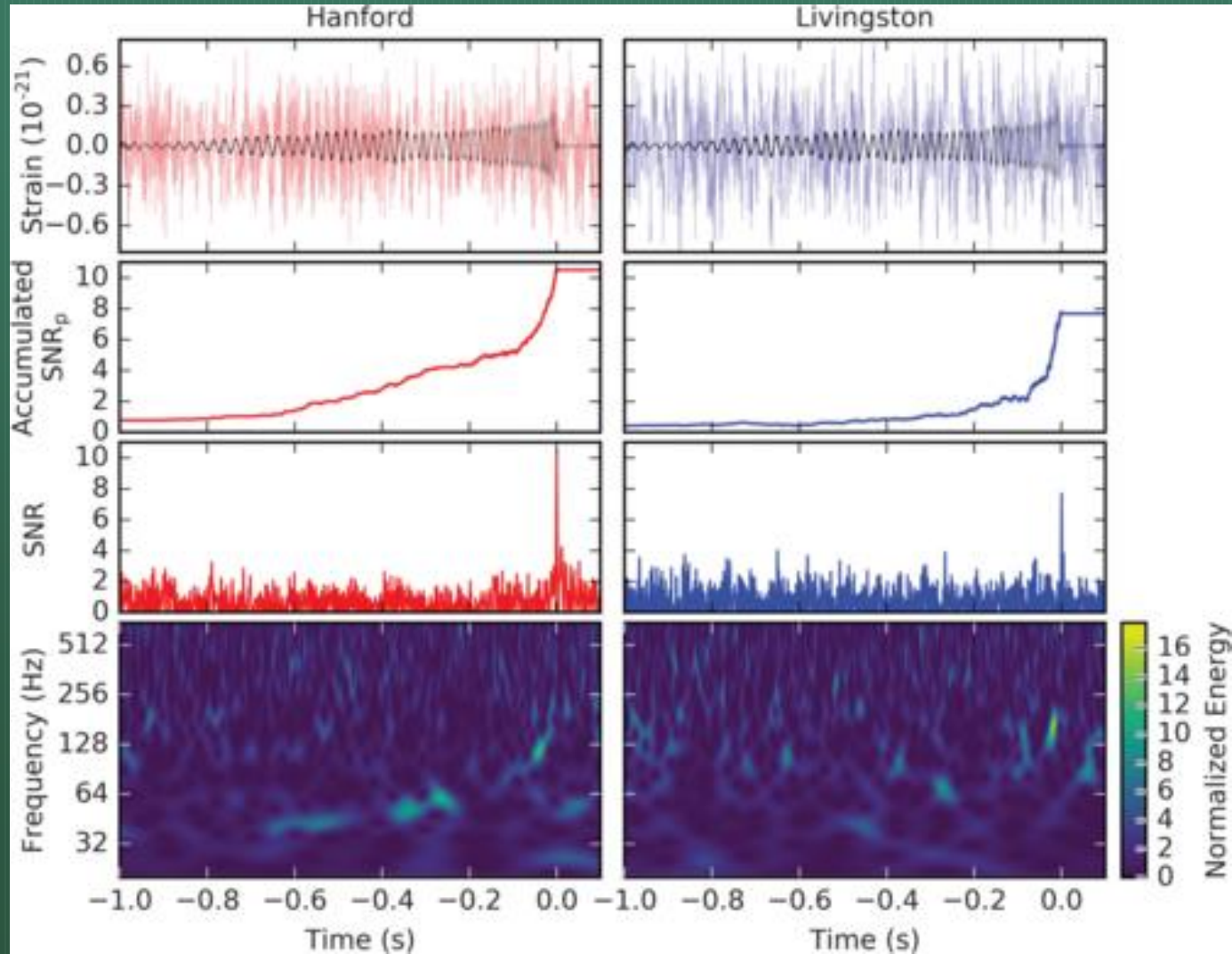
Rainer Weiss (MIT)



2017 Nobel Prize in Physics

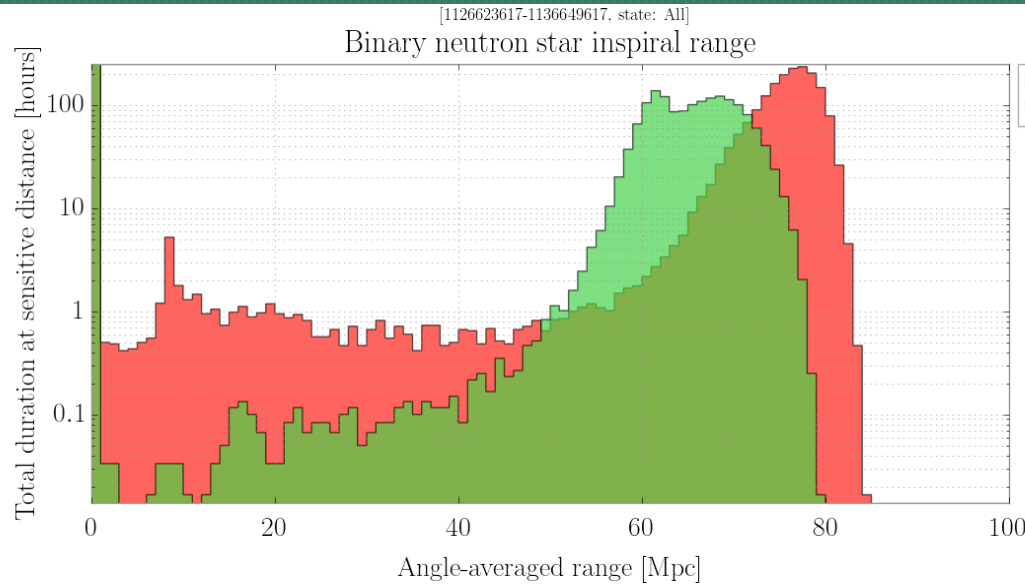
Direct Detection of GWs form BBH by Adv.LIGO

GW151226 ($14.2M_{\odot} - 7.5M_{\odot}$) : SN~13, D ~ 440Mpc



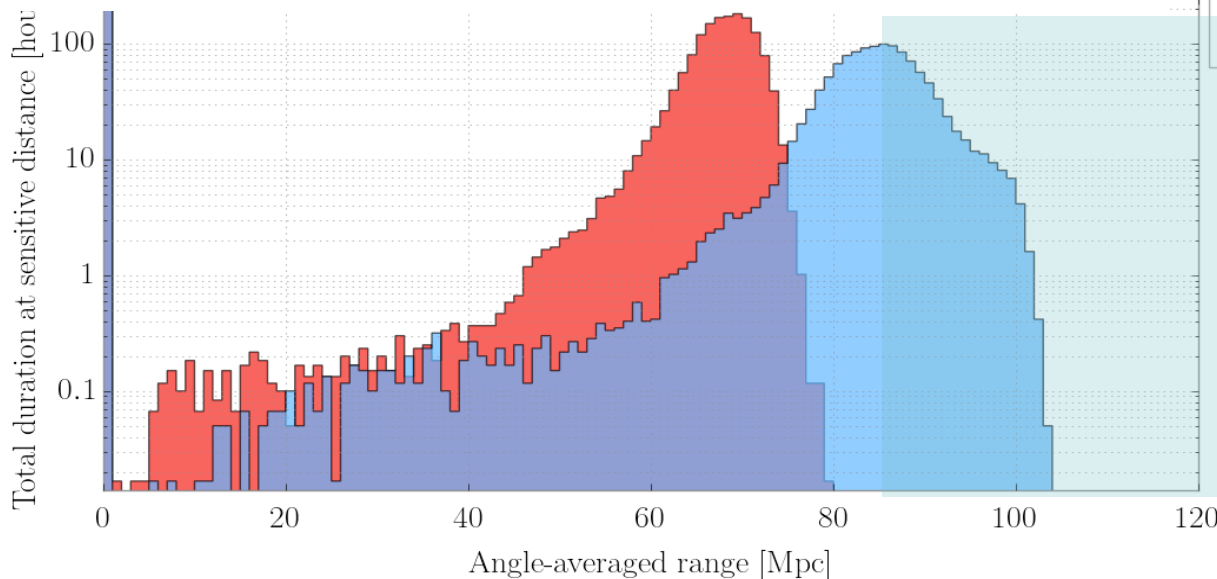
LIGO Observation 1 & 2 Binary Range

(by D.Sigg in GWADW2017)



O1

Volume-Time product now about the same for O1 & O2

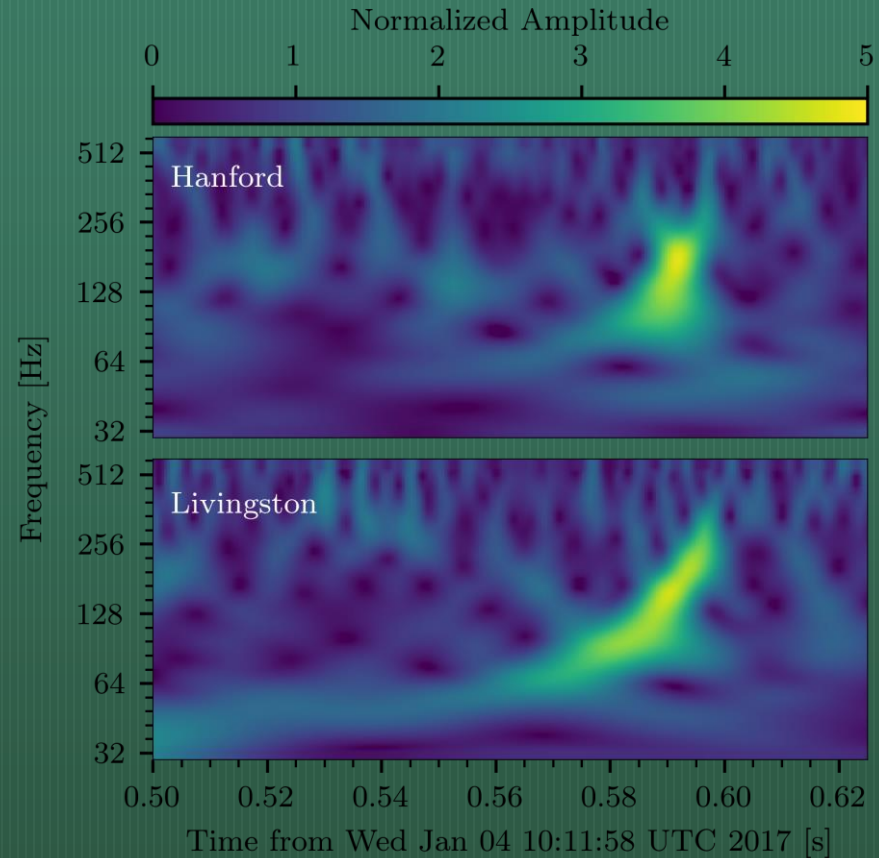
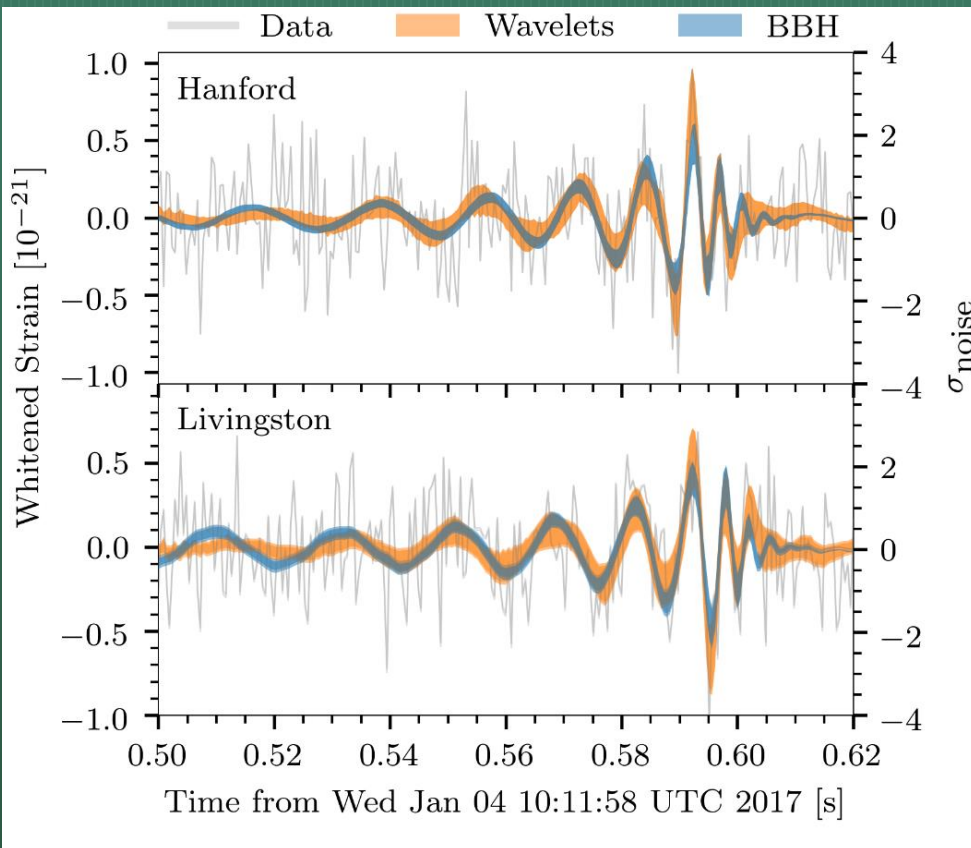


O2

Goal was 80-120 Mpc

Direct Detection of GWs form BBH by Adv.LIGO

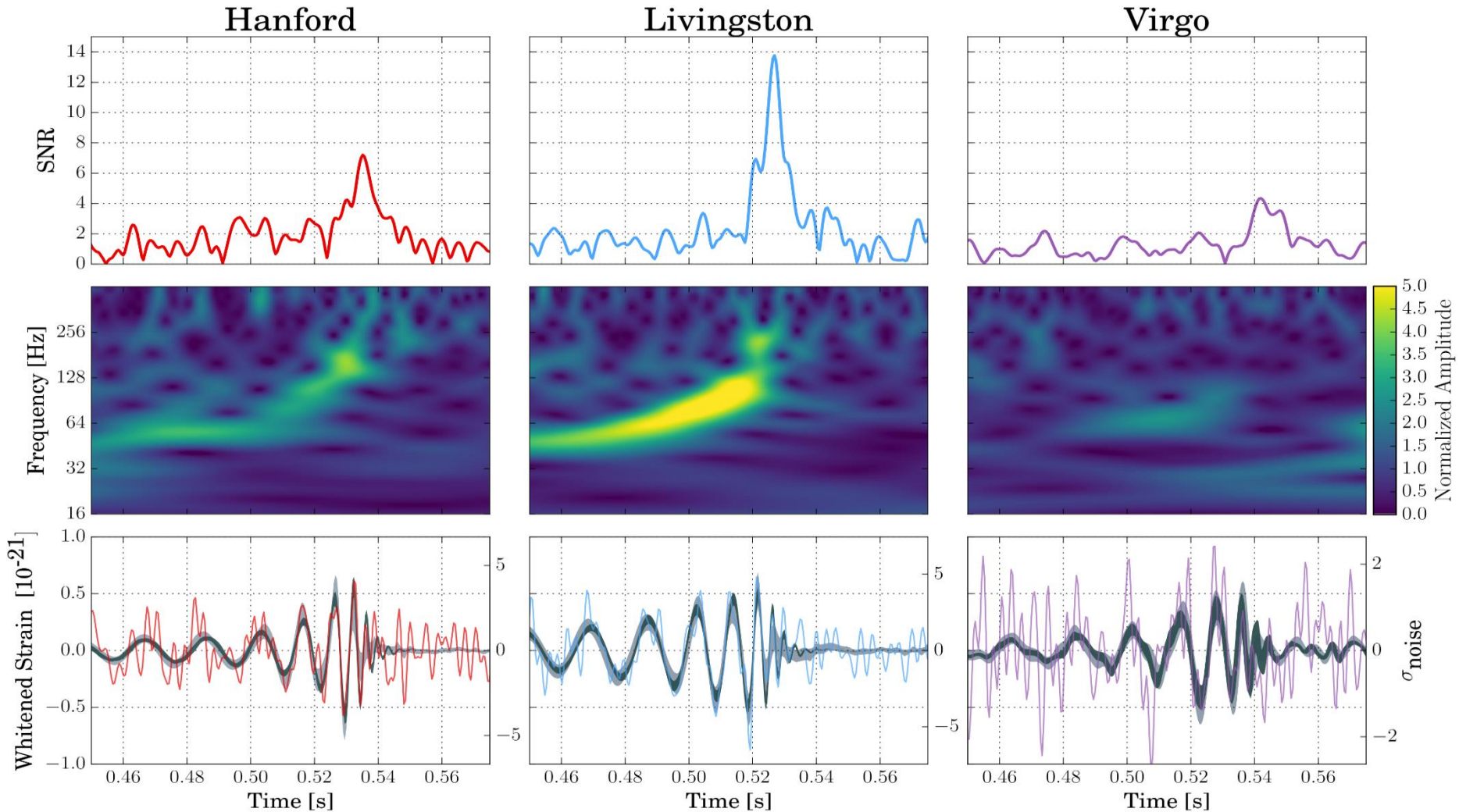
GW170104 ($31.2M_{\odot} - 19.4M_{\odot}$) : SN~14 , D ~ 880Mpc



GW170608 ($12M_{\odot} - 7M_{\odot}$)

Direct Detection of GWs form BBH by Adv.LIGO & Adv. Virgo

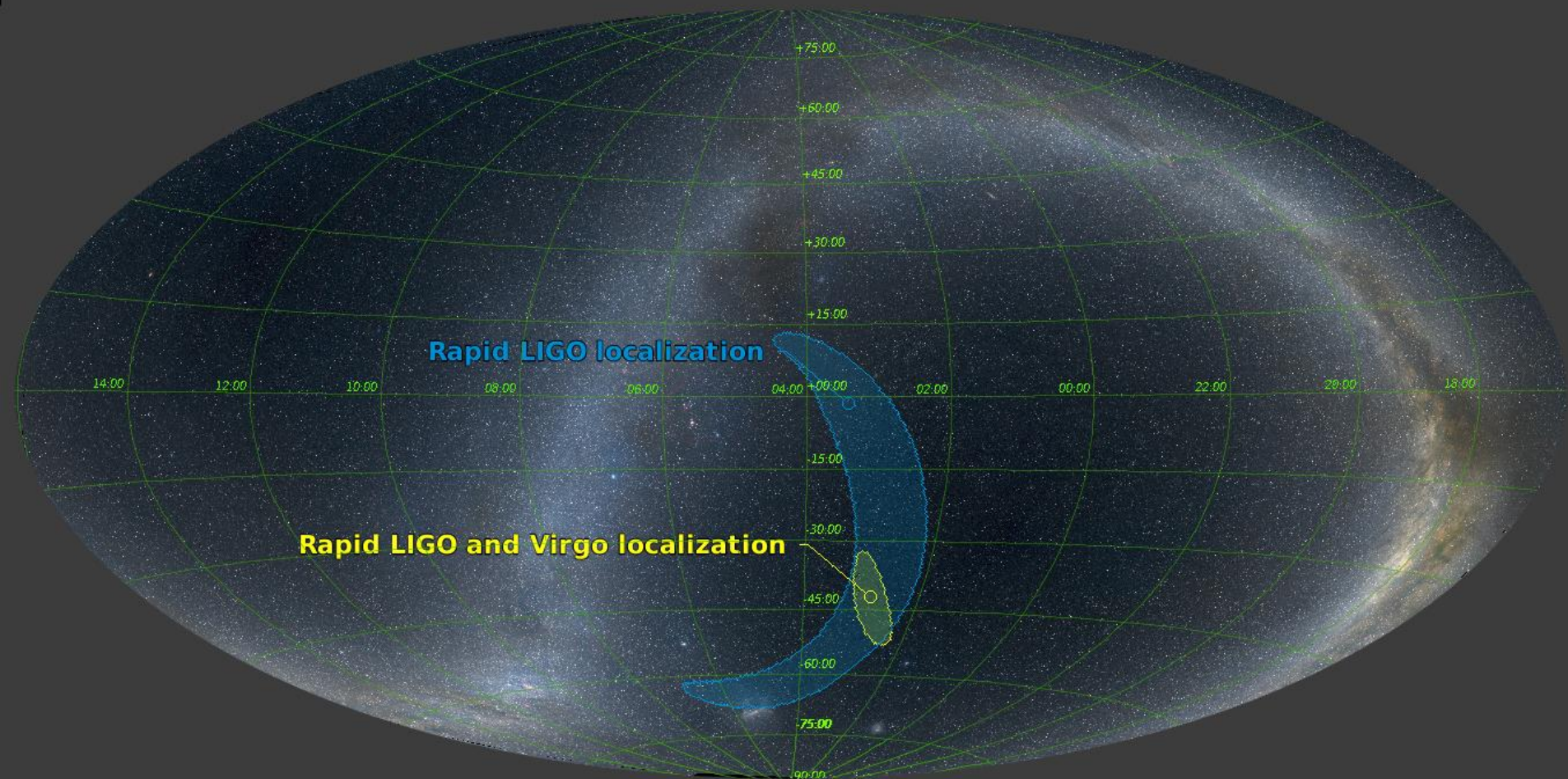
GW170814 ($30.5 M_{\odot} - 25.3 M_{\odot}$), $D \sim 540 \text{Mpc}$



Network Detection by LIGO & Virgo

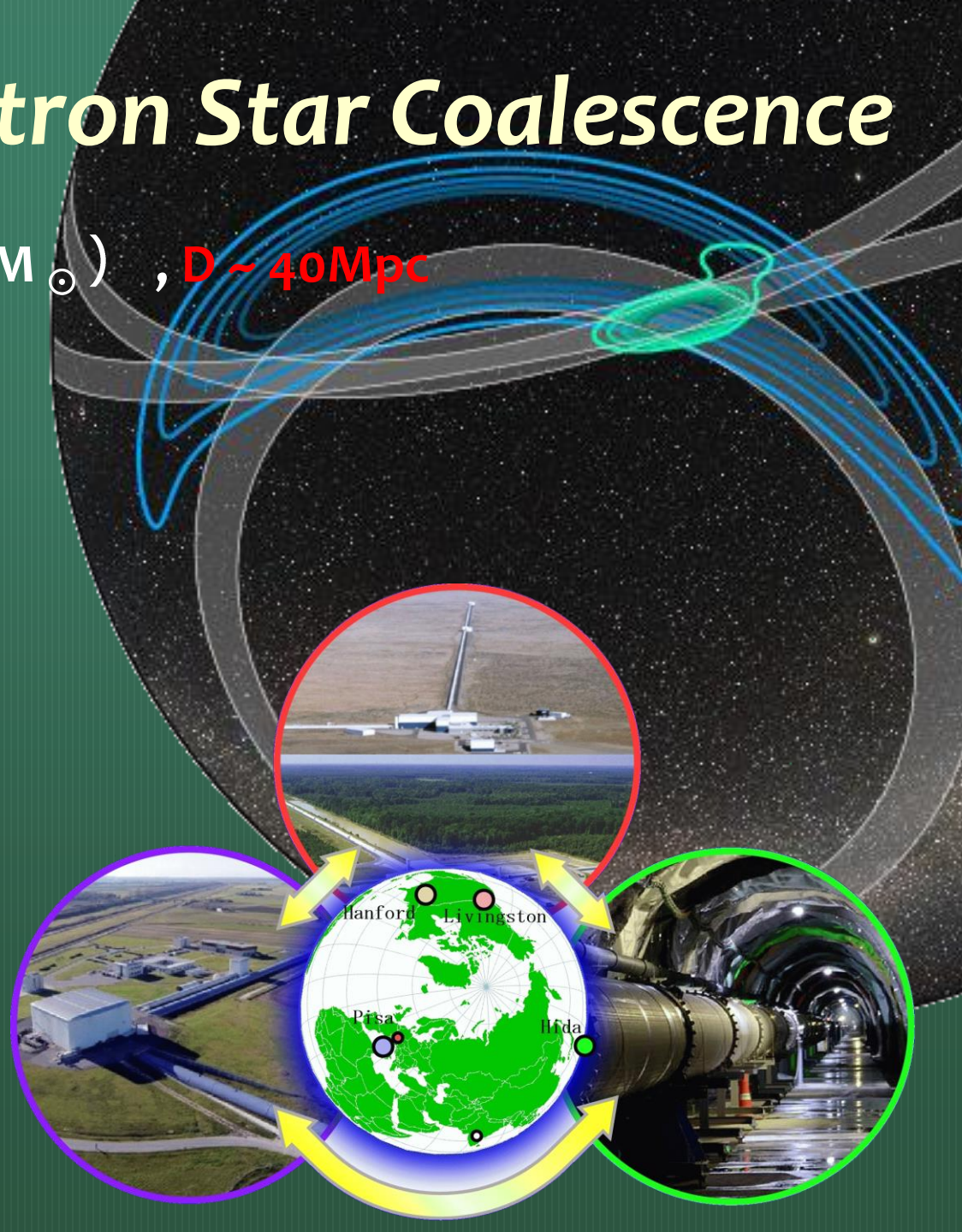
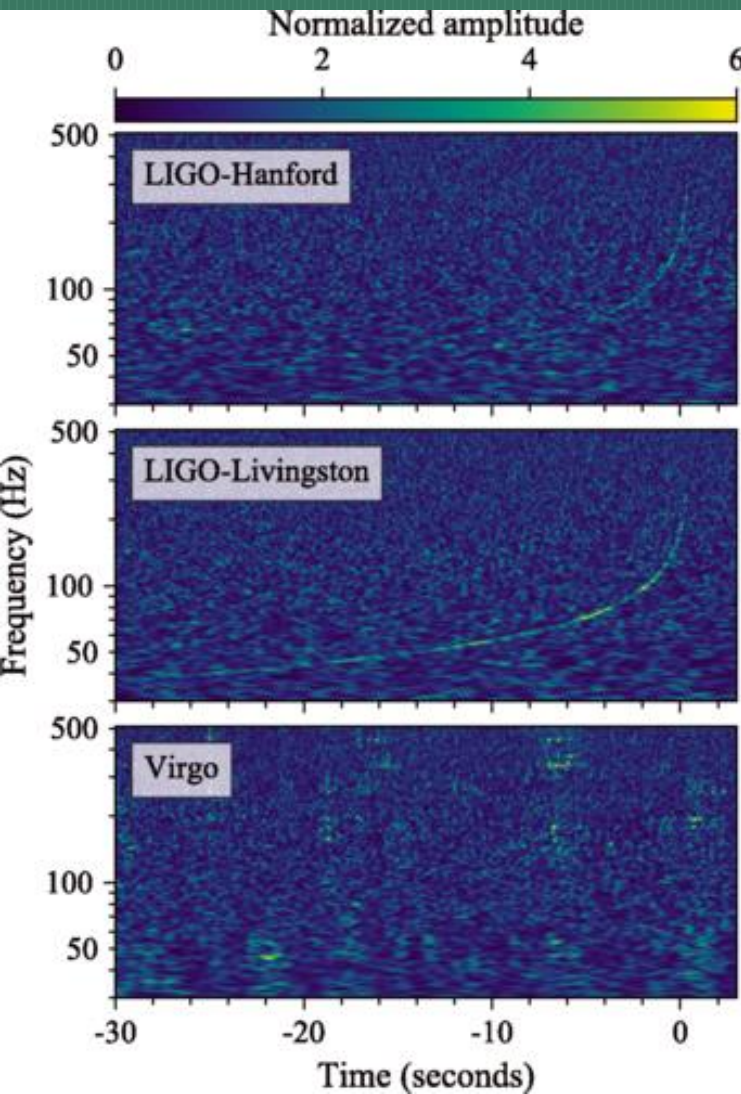
GW170814 ($30.5 M_{\odot} - 25.3 M_{\odot}$) , $D \sim 540\text{Mpc}$

CDS/P/Mellinger/color



GWs from Neutron Star Coalescence

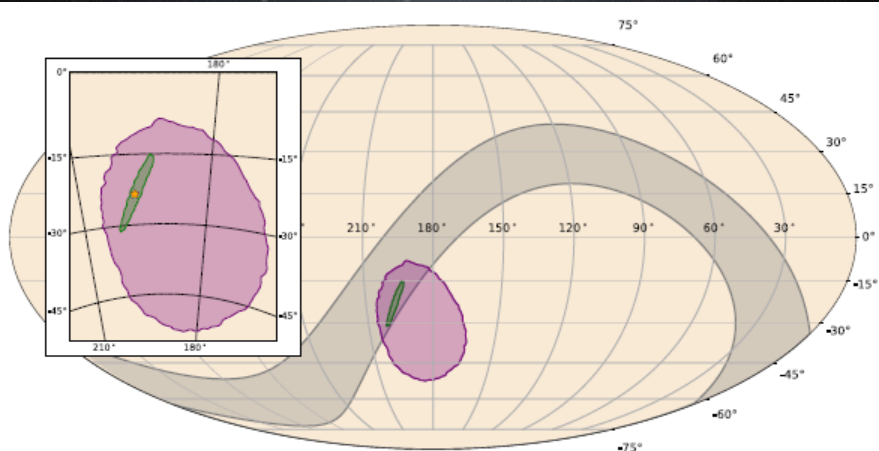
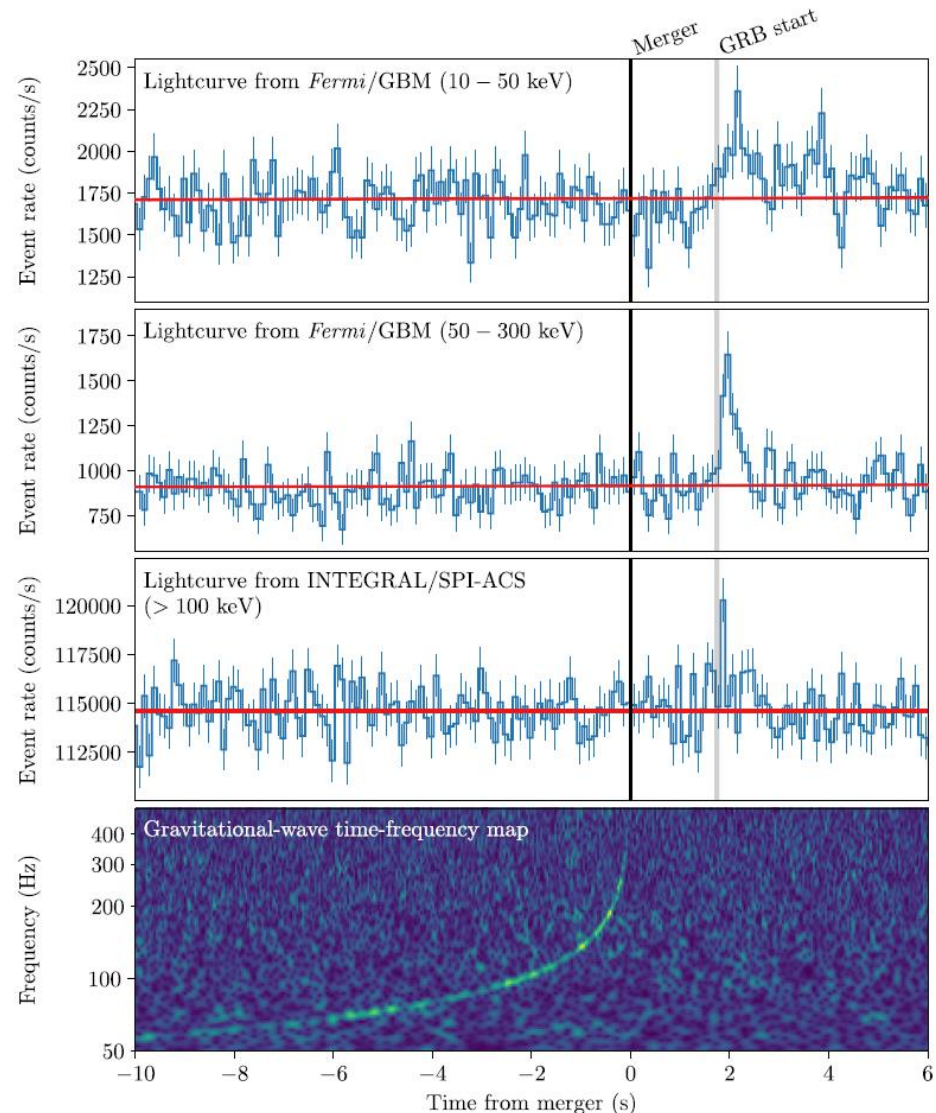
GW170817 (Total Mass $2.74 M_{\odot}$) , $D \sim 40 \text{ Mpc}$



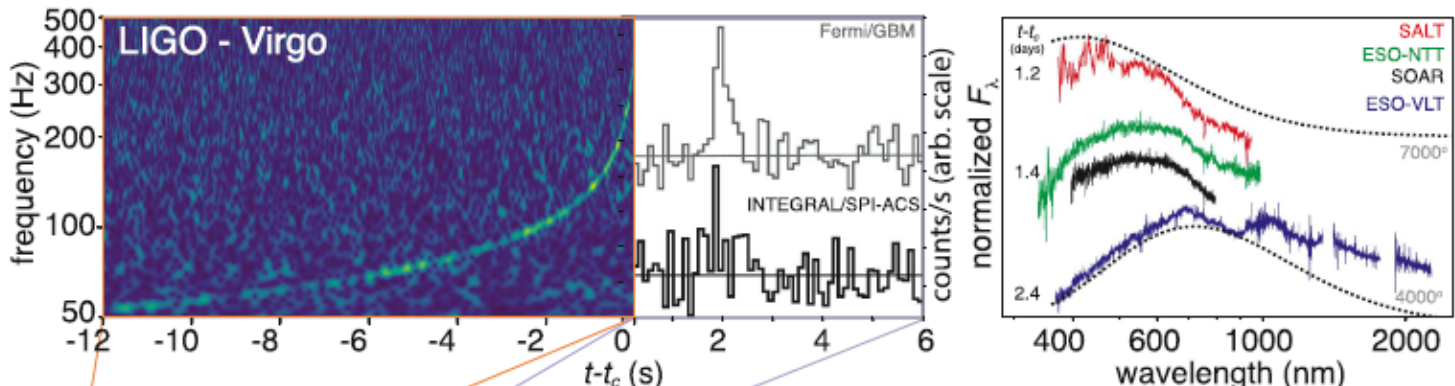
Multi Messenger Astronomy identified GW Source !!

GW170817 and GRB170817A in NGC4993

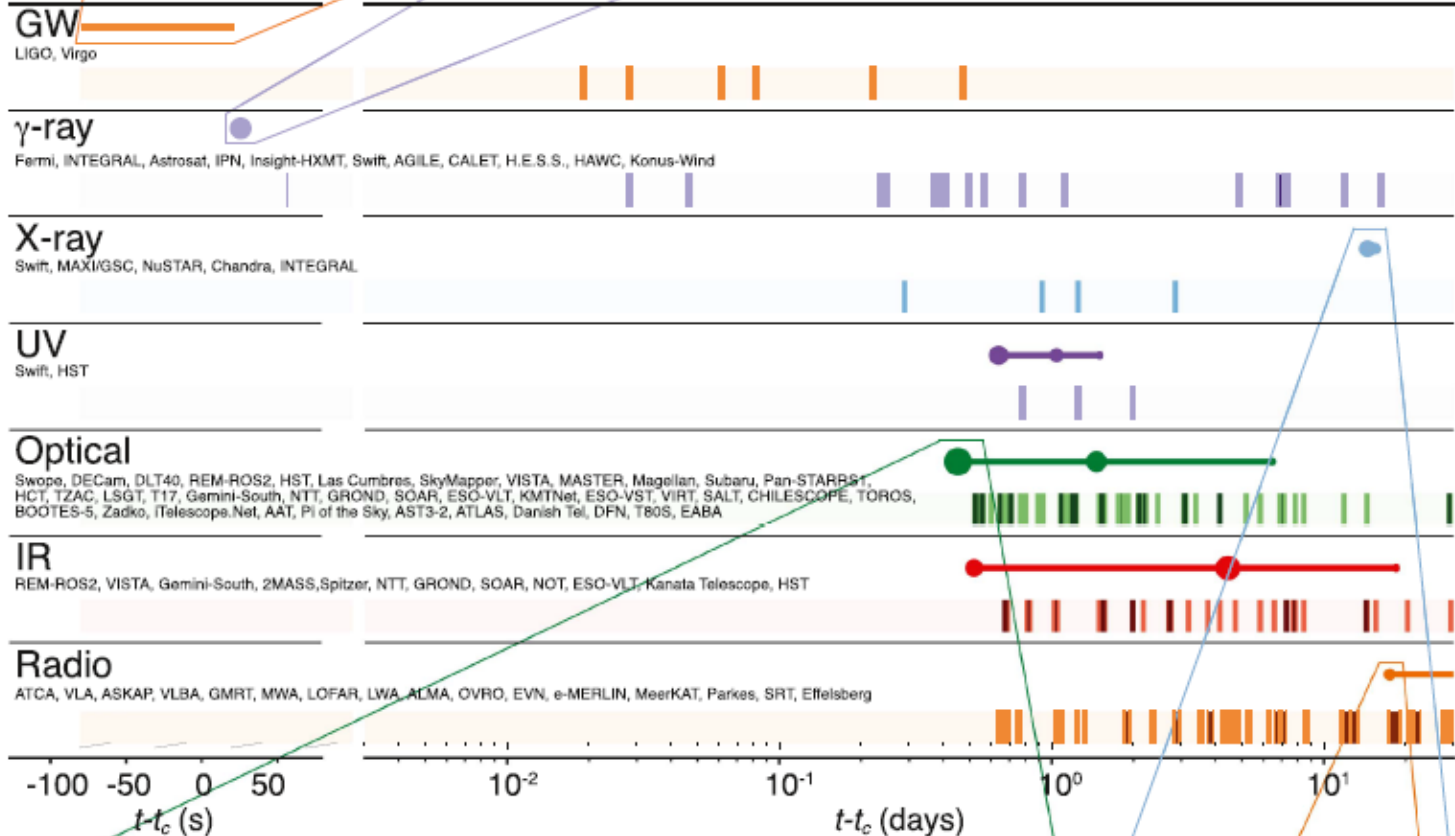
NGC4993



Multi Messenger Astronomy Followed up GW Source



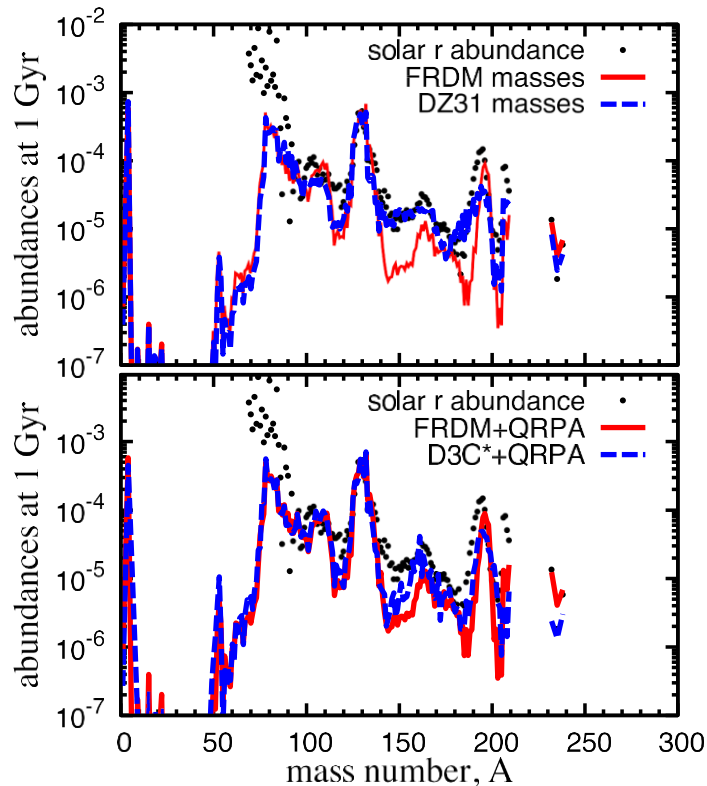
Abbott_2017_ApJL_848_L12



中性子連星合体で、宇宙において金のような重元素が生成される理由と観測事実を説明可

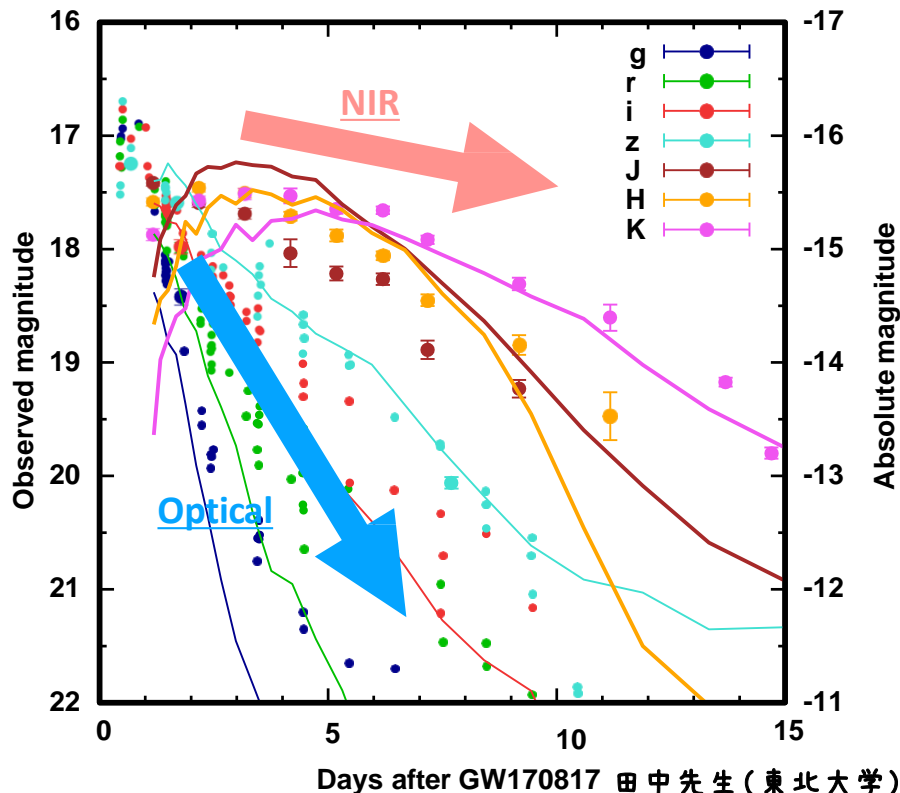
和南城先生(上智大学)

元素量と理論的予想値



Arcavi+17,
Cowperthwaite+17,
Diaz+17,
Drout+17, Evans+17,
Kasliwal+17,
Pian+17,
Smartt+17,
Tanvir+17,
Troja+17,
Utsumi,
MT+17,
Valenti+17

赤外線と可視光線の観測光度変化と理論的予想



田中先生(東北大学)

The First Detection of GWs from BNC

Nobel Prize in Physics 20??



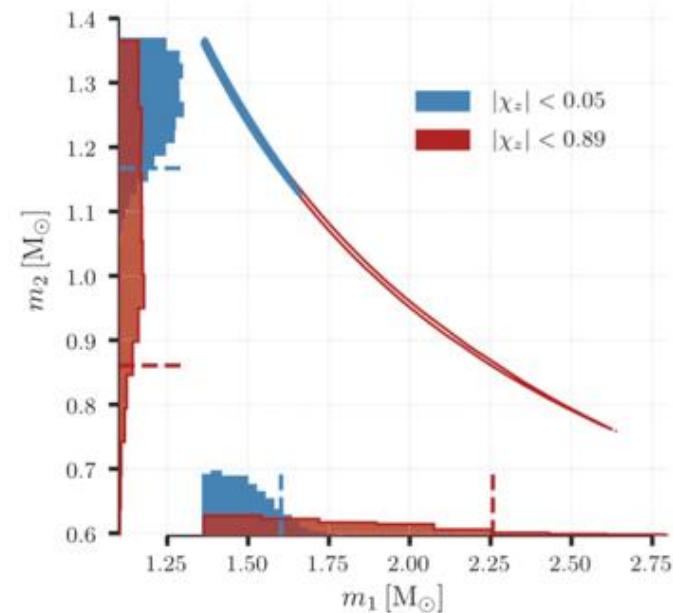
More GWs candidates with low S/N ratios are summarized in the near future report in O1 and O2.

Events with $S/N > 8$ are regarded as GW Events in LIGO/Virgo/KAGRA

Impact of GW170817

	Low-spin priors ($ \chi \leq 0.05$)	High-spin priors ($ \chi \leq 0.89$)
Primary mass m_1	1.36–1.60 M_\odot	1.36–2.26 M_\odot
Secondary mass m_2	1.17–1.36 M_\odot	0.86–1.36 M_\odot
Chirp mass \mathcal{M}	$1.188^{+0.004}_{-0.002} M_\odot$	$1.188^{+0.004}_{-0.002} M_\odot$
Mass ratio m_2/m_1	0.7–1.0	0.4–1.0
Total mass m_{tot}	$2.74^{+0.04}_{-0.01} M_\odot$	$2.82^{+0.47}_{-0.09} M_\odot$
Radiated energy E_{rad}	$> 0.025 M_\odot c^2$	$> 0.025 M_\odot c^2$
Luminosity distance D_L	40^{+8}_{-14} Mpc	40^{+8}_{-14} Mpc
Viewing angle Θ	$\leq 55^\circ$	$\leq 56^\circ$
Using NGC 4993 location	$\leq 28^\circ$	$\leq 28^\circ$
Combined dimensionless tidal deformability $\tilde{\Lambda}$	≤ 800	≤ 700
Dimensionless tidal deformability $\Lambda(1.4M_\odot)$	≤ 800	≤ 1400

- Chirp mass was well decided.
- Mass ratio and spin are degenerated a lot.
- Red shows large errors assuming $|\chi_z| < 0.89$ (EoS Constrain)
- Blue shows narrower errors assuming assuming $|\chi_z| < 0.05$ (Spin of NS that are estimated to coalesce within Hubble time)



Impact of GW170817

- Event rate of NS mergers is 1540 (+3200, - 1200) [1/Gpc³ /Year]
- This value is consistent with that obtained from galactic BNSs.

B. P. Abbott, The Astrophysical Journal Letters, Volume 832, L21, 20

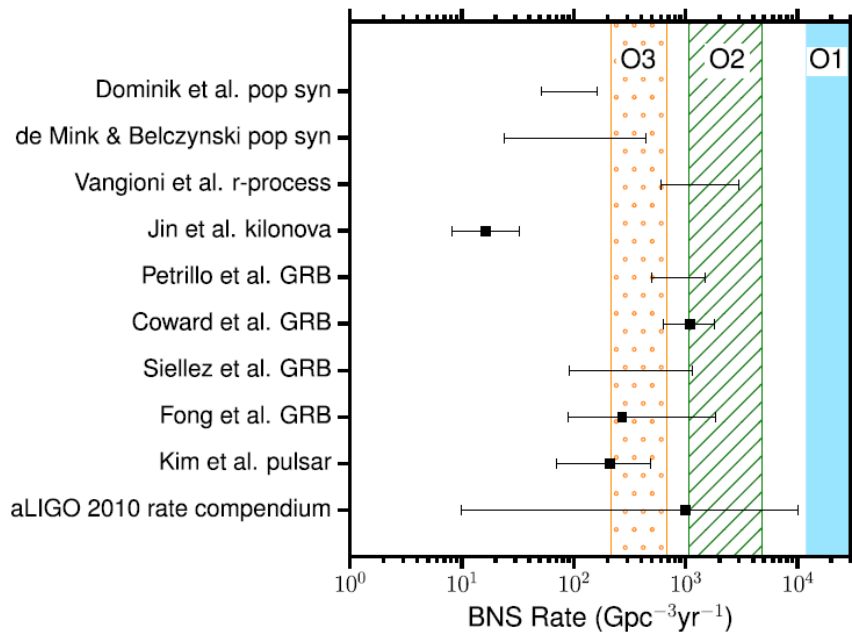


Figure 6. Comparison of the O1 90% upper limit on the BNS merger rate to other rates discussed in the text (Abadie et al. 2010; Coward et al. 2012; Petrillo et al. 2013; Siellez et al. 2014; de Mink & Belczynski 2015; Dominik et al. 2015; Fong et al. 2015; Jin et al. 2015; Kim et al. 2015; Vangioni et al. 2016). The region excluded by the low-spin BNS rate limit is shaded in blue. Continued non-detection in O2 (slash) and O3 (dot) with higher sensitivities and longer operation time would imply stronger upper limits. The O2 and O3 BNS ranges are assumed to be 1–1.9 and 1.9–2.7 times larger than O1. The operation times are assumed to be 6 and 9 months (Aasi et al. 2016) with a duty cycle equal to that of O1 (~40%). For comparison the core-collapse supernova rate in these units is $\sim 10^5 \text{ Gpc}^{-3} \text{ yr}^{-1}$ (Cappellaro et al. 2015 and references therein).

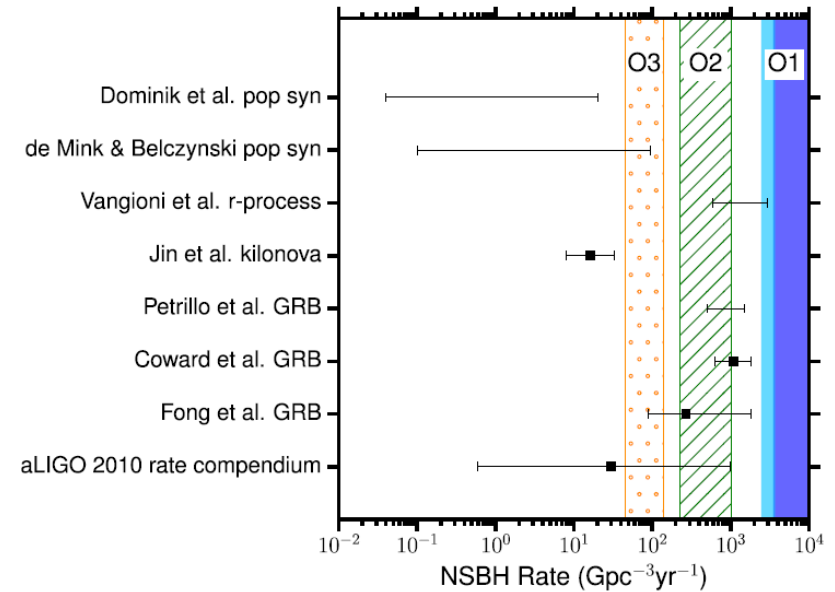


Figure 7. Comparison of the O1 90% upper limit on the NSBH merger rate to other rates discussed in the text (Abadie et al. 2010; Coward et al. 2012; Petrillo et al. 2013; Dominik et al. 2015; de Mink & Belczynski 2015; Fong et al. 2015; Jin et al. 2015; Vangioni et al. 2016). The dark blue region assumes an NSBH population with masses 5–1.4 M_{\odot} , and the light blue region assumes an NSBH population with masses 10–1.4 M_{\odot} . Both assume an isotropic spin distribution. Continued non-detection in O2 (slash) and O3 (dot) with higher sensitivities and longer operation time would imply stronger upper limits (shown for 10–1.4 M_{\odot} NSBH systems). The O2 and O3 ranges are assumed to be 1–1.9 and 1.9–2.7 times larger than O1. The operation times are assumed to be 6 and 9 months (Aasi et al. 2016) with a duty cycle equal to that of O1 (~40%). For comparison the core-collapse supernova rate in these units is $\sim 10^5 \text{ Gpc}^{-3} \text{ yr}^{-1}$ (Cappellaro et al. 2015 and references therein).

Impact of GW170817

B. P. Abbott et al. 2017 ApJL 848 L13 doi:10.3847/2041-8213/aa920c

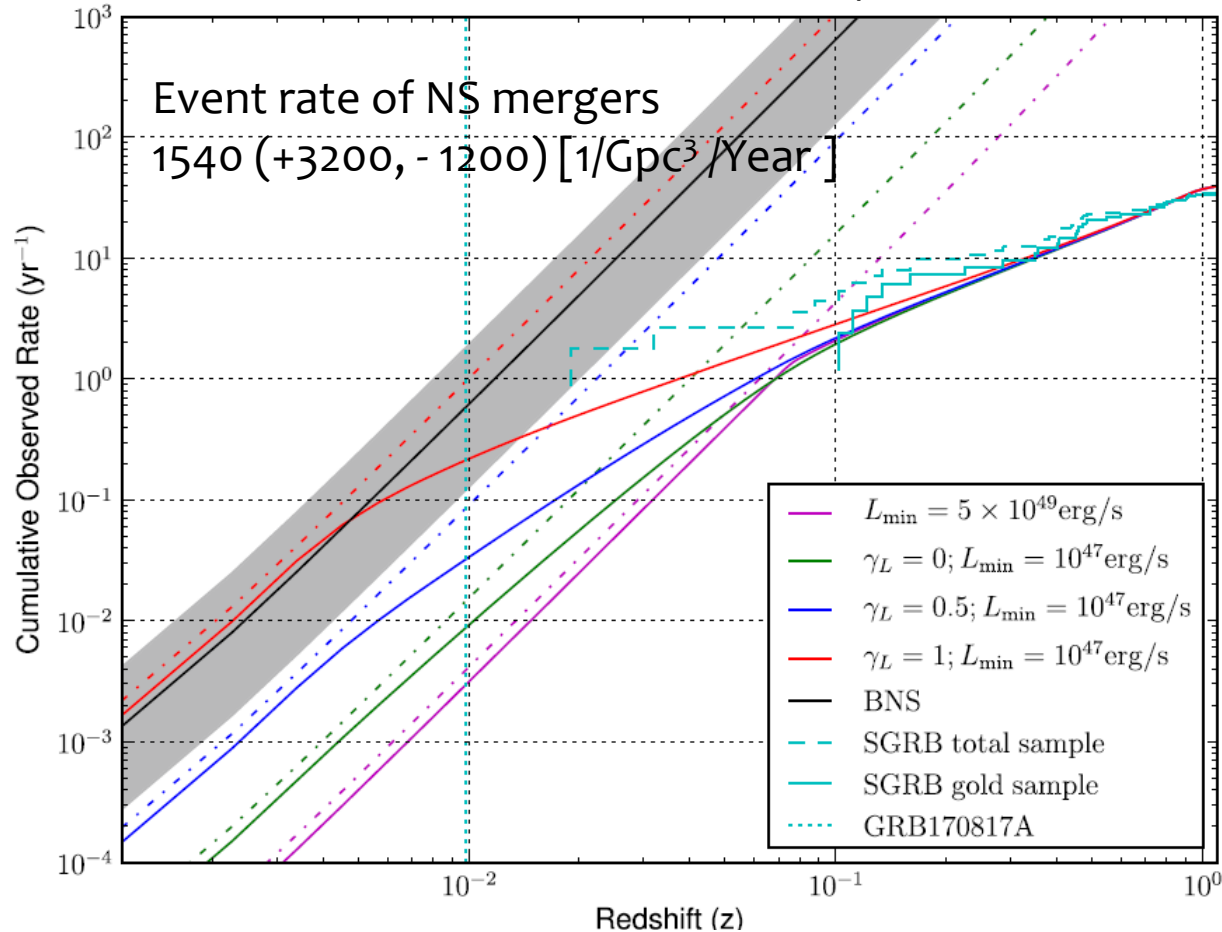
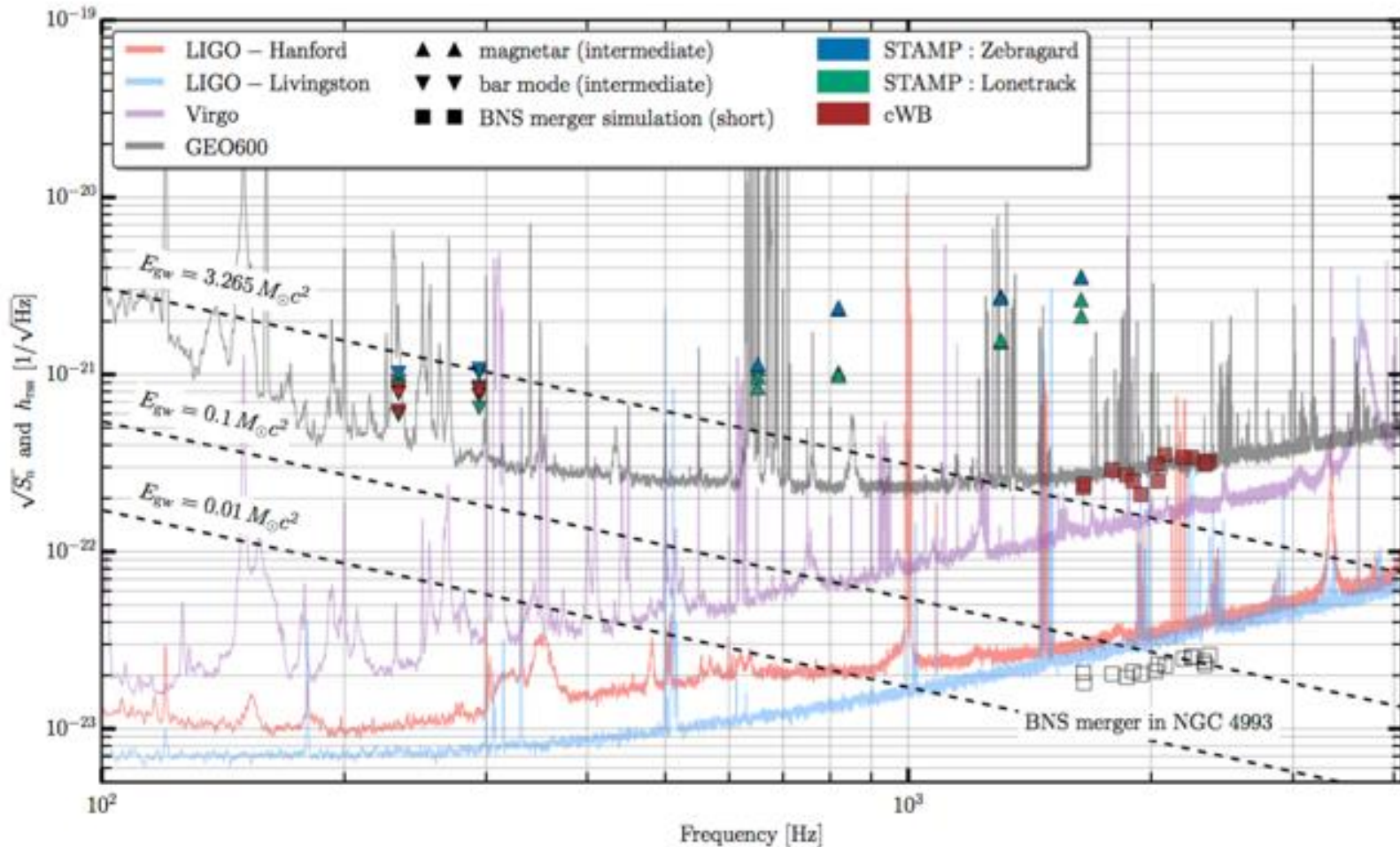


Figure 6. Predicted detection rates per year as a function of redshift. The red, blue, and green solid lines refer to the GBM observed SGRB rate assuming a minimum luminosity L_{\min} of $1 \times 10^{47} \text{ erg s}^{-1}$, and $\alpha_L = 1$, $\beta_L = 2$ and $\gamma_L = \{1, 0.5, 0\}$ in Equation (21), respectively. The purple solid line refers to the base model with L_{\min} of $5 \times 10^{49} \text{ erg s}^{-1}$. The four curves are normalized by imposing 40 triggered SGRB per year. As γ_L increases, the observed rate is no longer volumetric at lower and lower redshifts, because a fraction of SGRBs becomes too dim to be detected. For reference, the red, blue and green dot-dashed curves show the local SGRB occurrence rate for $L_{\min} = 1 \times 10^{47} \text{ erg s}^{-1}$ and $\gamma_L = \{1, 0.5, 0\}$, respectively. The black line and gray band show the BNS merger rate $1540^{+3200}_{-1220} \text{ Gpc}^{-3} \text{ yr}^{-1}$ determined with the detection of GW170817 (Abbott et al. 2017e). For comparison, the measured SGRBs redshift distribution from Table 2 is shown in cyan, and is broadly compatible with all of the models. The dotted vertical cyan line refers to the redshift of GRB 170817A host galaxy.

Impact of GW170817

- Merger state was not detected clearly because of less sensitivity for the high frequency ranges.



Impact of GW170817

- 1.7 seconds difference of arrival time of GW and Gamma ray resulted in strong constrained on the **speed of GW**.

$$\Delta t = D/v_{\text{GW}} - D/v_{\text{EM}} \quad \Delta v := v_{\text{GW}} - v_{\text{EM}}$$

$$-3 \times 10^{-15} \leq \Delta v / v_{\text{EM}} \leq 7 \times 10^{-16}$$

- We can get better constrain on **Principle of Equivalence** because Shapiro delay is same level between GWs and EMs.

$$-2.6 \times 10^{-7} \leq \gamma_{\text{GW}} - \gamma_{\text{EM}} \leq 1.2 \times 10^{-6}$$

Impact of GW170817

B. P. Abbott et al. 2017 ApJL 848 L13 doi:10.3847/2041-8213/aa920c

- Lorentz Invariance (If there is invariance, dispersion has dependency on directions.)

$$\Delta v = -\sum_{lm, l \leq 2} Y_{lm}(\hat{n}) \left[\frac{1}{2} (-1)^{1+l} \bar{s}_{lm}^{(4)} - \bar{c}_{(I)lm}^{(4)} \right]$$

Table 1
Constraints on the Dimensionless Minimal Gravity Sector Coefficients

ℓ	Previous Lower	This Work Lower	Coefficient	This Work Upper	Previous Upper
0	-3×10^{-14}	-2×10^{-14}	$\bar{s}_{00}^{(4)}$	5×10^{-15}	8×10^{-5}
1	-1×10^{-13}	-3×10^{-14}	$\bar{s}_{10}^{(4)}$	7×10^{-15}	7×10^{-14}
	-8×10^{-14}	-1×10^{-14}	$-\text{Re } \bar{s}_{11}^{(4)}$	2×10^{-15}	8×10^{-14}
	-7×10^{-14}	-3×10^{-14}	$\text{Im } \bar{s}_{11}^{(4)}$	7×10^{-15}	9×10^{-14}
2	-1×10^{-13}	-4×10^{-14}	$-\bar{s}_{20}^{(4)}$	8×10^{-15}	7×10^{-14}
	-7×10^{-14}	-1×10^{-14}	$-\text{Re } \bar{s}_{21}^{(4)}$	2×10^{-15}	7×10^{-14}
	-5×10^{-14}	-4×10^{-14}	$\text{Im } \bar{s}_{21}^{(4)}$	8×10^{-15}	8×10^{-14}
	-6×10^{-14}	-1×10^{-14}	$\text{Re } \bar{s}_{22}^{(4)}$	3×10^{-15}	8×10^{-14}
	-7×10^{-14}	-2×10^{-14}	$-\text{Im } \bar{s}_{22}^{(4)}$	4×10^{-15}	7×10^{-14}

Note. Constraints on the dimensionless minimal gravity sector coefficients obtained in this work via Equations (1) and (2) appear in columns 3 and 5. The corresponding limits that predate this work and are reported in columns 2 and 6; all pre-existing limits are taken from Kostelecký & Tasson (2015), with the exception of the upper limit on $\bar{s}_{00}^{(4)}$ from Shao (2014a, 2014b). The isotropic upper bound in the first line shows greater than 10 orders of magnitude improvement. The gravity sector coefficients are constrained one at a time, by setting all other coefficients, including those from the EM sector, to zero.

Impact of GW170817

B. P. Abbott et al. 2017 ApJL 848 L13 doi:10.3847/2041-8213/aa920c

- Constrain on QoS of NS.
- According to gamma ray burst model, we can put loose constrain on EoS.

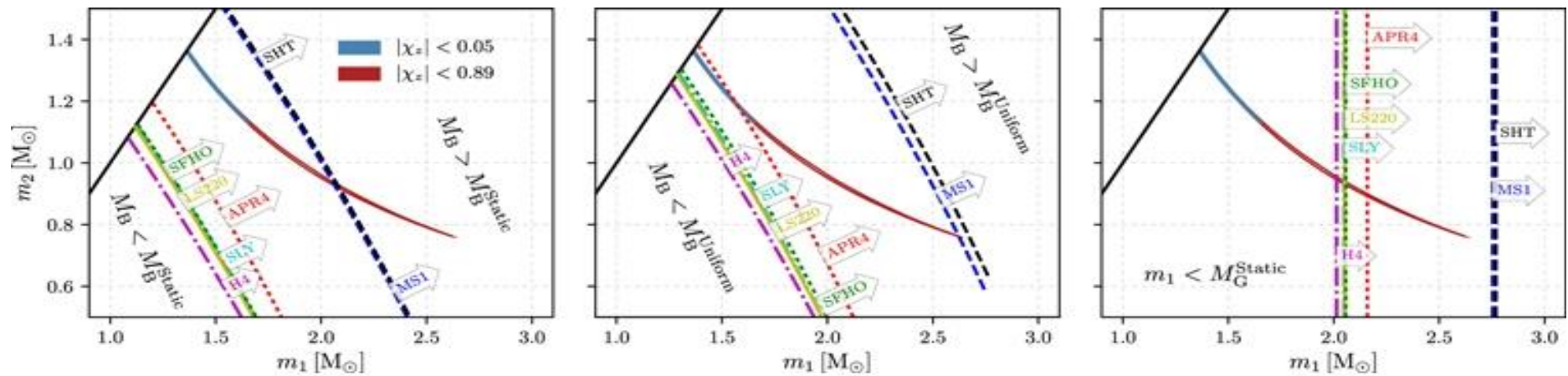


Figure 3. Critical mass boundaries for different EOSs in comparison with the 90% credible region of the gravitational masses inferred from GW170817 (prior limits on the spin magnitude, $|\chi_z|$, given in the legend). The slanted curves in the **left panel and middle panel correspond to the maximum baryonic mass allowed for a single non-rotating NS (left) and for a uniformly rotating NS (middle)**. Arrows indicate for each EOS the region in the parameter space where the total initial baryonic mass exceeds the maximum mass for a single non-rotating or uniformly rotating NS, respectively. The right panel illustrates EOS-dependent cuts on the gravitational mass m_1 of the heavier star, with arrows indicating regions in which m_1 exceeds the maximum possible gravitational mass M^{Static}_G for non-rotating NSs. In all three panels the black solid line marks the $m_1 = m_2$ boundary, and we work in the $m_1 > m_2$ convention.

Impact of GW170817

doi:10.1038/nature24471

- A gravitational-wave standard siren measurement of the Hubble constant

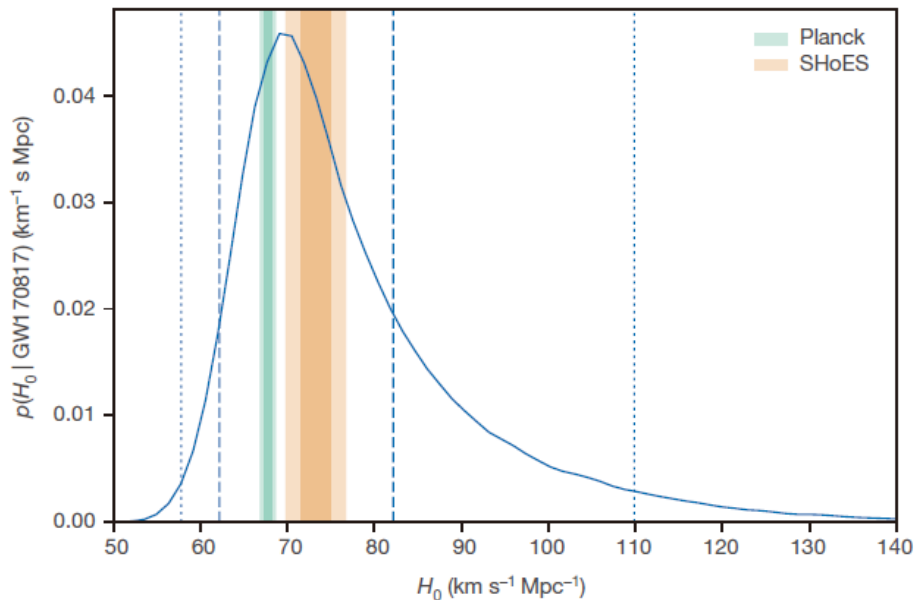


Figure 1 | GW170817 measurement of H_0 . The marginalized posterior density for H_0 , $p(H_0 | \text{GW170817})$, is shown by the blue curve. Constraints at 1σ (darker shading) and 2σ (lighter shading) from Planck²⁰ and SHoES²¹ are shown in green and orange, respectively. The maximum a posteriori value and minimal 68.3% credible interval from this posterior density function is $H_0 = 70.0^{+12.0}_{-8.0} \text{ km s}^{-1} \text{Mpc}^{-1}$. The 68.3% (1σ) and 95.4% (2σ) minimal credible intervals are indicated by dashed and dotted lines, respectively.

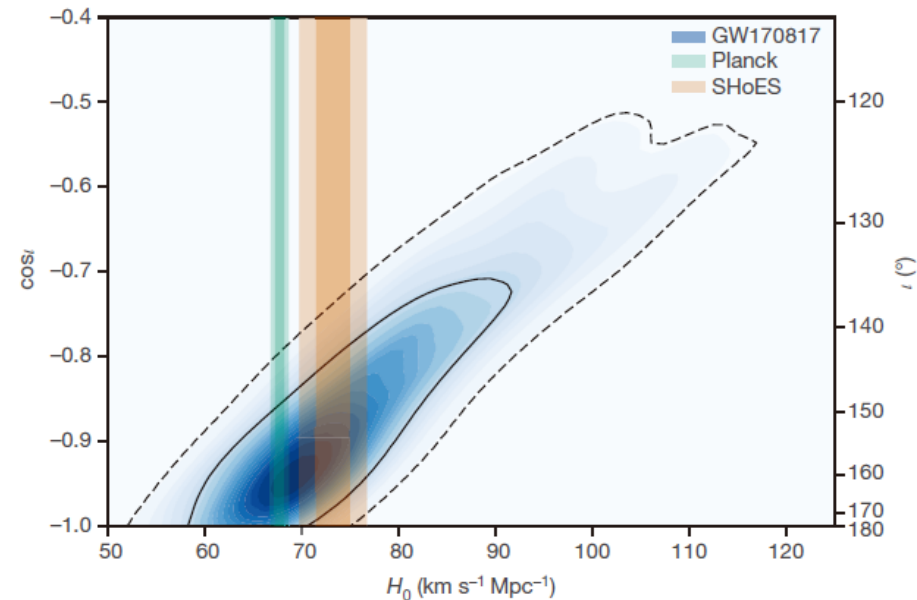


Figure 2 | Inference on H_0 and inclination. The posterior density of H_0 and $\cos i$ from the joint gravitational-wave–electromagnetic analysis are shown as blue contours. Shading levels are drawn at every 5% credible level, with the 68.3% (1σ ; solid) and 95.4% (2σ ; dashed) contours in black. Values of H_0 and 1σ and 2σ error bands are also displayed from Planck²⁰ and SHoES²¹. Inclination angles near 180° ($\cos i = -1$) indicate that the orbital angular momentum is antiparallel to the direction from the source to the detector.

Impact of GW170817

- Stochastic background GWs that compose of many GWs from NS-NS, BH-BH coalescences ever Bigbang might be found just below the level of LVK targeted sensitivity !!

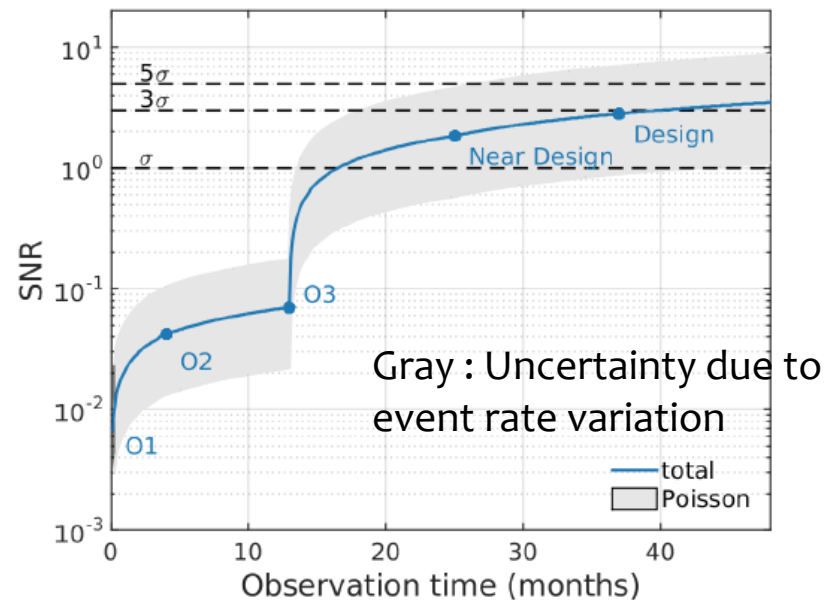
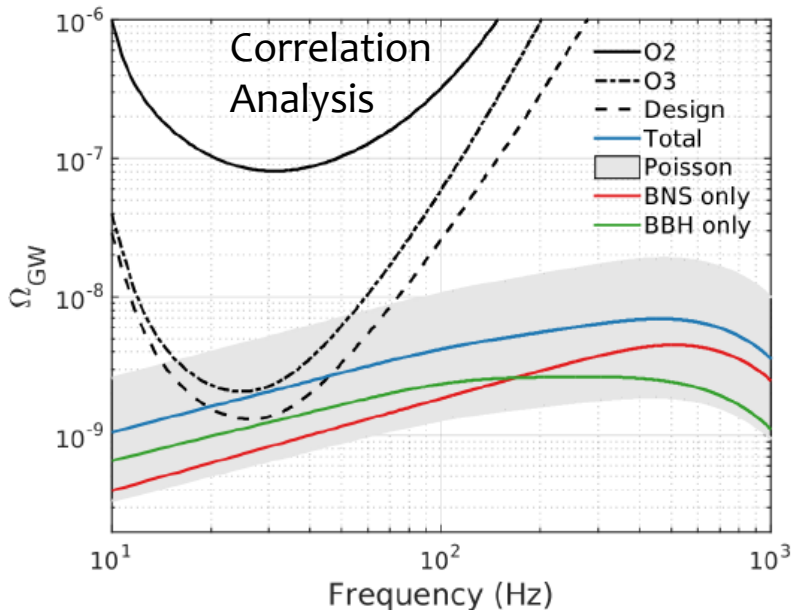
$$\Omega_{\text{GW}}(f = 25 \text{ Hz}) = 1.8_{-1.3}^{+2.7} \times 10^{-9}$$

	$\Omega_{\text{GW}}(25 \text{ Hz})$	τ [s]	λ
BNS	$0.7_{-0.6}^{+1.5} \times 10^{-9}$	13_{-9}^{+49}	15_{-12}^{+30}
BBH	$1.1_{-0.7}^{+1.2} \times 10^{-9}$	223_{-115}^{+352}	$0.06_{-0.04}^{+0.06}$
Total	$1.8_{-1.3}^{+2.7} \times 10^{-9}$	12_{-8}^{+44}	15_{-12}^{+31}

$$\Omega_{\text{GW}} \equiv \frac{1}{\rho_c} \frac{d\rho_{\text{GW}}}{d \ln f}$$

ρ_{GW} : Energy density of GWs
 $\rho_c = 3H_0^2 c^2 / (8\pi G)$
 : Density limit

- 40 months observation with LVK designed sensitivity will enable us to them with $S/N = 3$. Contribution from 10 Hz to 100 Hz is 99% to get $S/N = 3$.



そして、今日12月2日午前1時に新たな発表がありました

Observation 1,2 のデータの精細な解析により02の観測中に、
さらに4個の連星ブラックホール連星合体からの重力波が確認
されました。

2つのBHの質量

自転の可能性

発生場所までの距離

Event	m_1/M_\odot	m_2/M_\odot	M/M_\odot	χ_{eff}	M_f/M_\odot	a_f	$E_{\text{rad}}/(M_\odot c^2)$	$\ell_{\text{peak}}/(\text{erg s}^{-1})$	d_L/Mpc	z	$\Delta\Omega/\text{deg}^2$
GW150914	$35.6^{+4.8}_{-3.0}$	$30.6^{+3.0}_{-4.4}$	$28.6^{+1.6}_{-1.5}$	$-0.01^{+0.12}_{-0.13}$	$63.1^{+3.3}_{-3.0}$	$0.69^{+0.05}_{-0.04}$	$3.1^{+0.4}_{-0.4}$	$3.6^{+0.4}_{-0.4} \times 10^{56}$	430^{+150}_{-170}	$0.09^{+0.03}_{-0.03}$	179
GW151012	$23.3^{+14.0}_{-5.5}$	$13.6^{+4.1}_{-4.8}$	$15.2^{+2.0}_{-1.1}$	$0.04^{+0.28}_{-0.19}$	$35.7^{+9.9}_{-3.8}$	$0.67^{+0.13}_{-0.11}$	$1.5^{+0.5}_{-0.5}$	$3.2^{+0.8}_{-1.7} \times 10^{56}$	1060^{+540}_{-480}	$0.21^{+0.09}_{-0.09}$	1555
GW151226	$13.7^{+8.8}_{-3.2}$	$7.7^{+2.2}_{-2.6}$	$8.9^{+0.3}_{-0.3}$	$0.18^{+0.20}_{-0.12}$	$20.5^{+6.4}_{-1.5}$	$0.74^{+0.07}_{-0.05}$	$1.0^{+0.1}_{-0.2}$	$3.4^{+0.7}_{-1.7} \times 10^{56}$	440^{+180}_{-190}	$0.09^{+0.04}_{-0.04}$	1033
GW170104	$31.0^{+7.2}_{-5.6}$	$20.1^{+4.9}_{-4.5}$	$21.5^{+2.1}_{-1.7}$	$-0.04^{+0.17}_{-0.20}$	$49.1^{+5.2}_{-3.9}$	$0.66^{+0.08}_{-0.10}$	$2.2^{+0.5}_{-0.5}$	$3.3^{+0.6}_{-0.9} \times 10^{56}$	960^{+430}_{-410}	$0.19^{+0.07}_{-0.08}$	924
GW170608	$10.9^{+5.3}_{-1.7}$	$7.6^{+1.3}_{-2.1}$	$7.9^{+0.2}_{-0.2}$	$0.03^{+0.19}_{-0.07}$	$17.8^{+3.2}_{-0.7}$	$0.69^{+0.04}_{-0.04}$	$0.9^{+0.0}_{-0.1}$	$3.5^{+0.4}_{-1.3} \times 10^{56}$	320^{+120}_{-110}	$0.07^{+0.02}_{-0.02}$	396
GW170729	$50.6^{+16.6}_{-10.2}$	$34.3^{+9.1}_{-10.1}$	$35.7^{+6.5}_{-4.7}$	$0.36^{+0.21}_{-0.25}$	$80.3^{+14.6}_{-10.2}$	$0.81^{+0.07}_{-0.13}$	$4.8^{+1.7}_{-1.7}$	$4.2^{+0.9}_{-1.5} \times 10^{56}$	2750^{+1350}_{-1320}	$0.48^{+0.19}_{-0.20}$	1033
GW170809	$35.2^{+8.3}_{-6.0}$	$23.8^{+5.2}_{-5.1}$	$25.0^{+2.1}_{-1.6}$	$0.07^{+0.16}_{-0.16}$	$56.4^{+5.2}_{-3.7}$	$0.70^{+0.08}_{-0.09}$	$2.7^{+0.6}_{-0.6}$	$3.5^{+0.6}_{-0.9} \times 10^{56}$	990^{+320}_{-380}	$0.20^{+0.05}_{-0.07}$	340
GW170814	$30.7^{+5.7}_{-3.0}$	$25.3^{+2.9}_{-4.1}$	$24.2^{+1.4}_{-1.1}$	$0.07^{+0.12}_{-0.11}$	$53.4^{+3.2}_{-2.4}$	$0.72^{+0.07}_{-0.05}$	$2.7^{+0.4}_{-0.3}$	$3.7^{+0.4}_{-0.5} \times 10^{56}$	580^{+160}_{-210}	$0.12^{+0.03}_{-0.04}$	87
GW170817	$1.46^{+0.12}_{-0.10}$	$1.27^{+0.09}_{-0.09}$	$1.186^{+0.001}_{-0.001}$	$0.00^{+0.02}_{-0.01}$	≤ 2.8	≤ 0.89	≥ 0.04	$\geq 0.1 \times 10^{56}$	40^{+10}_{-10}	$0.01^{+0.00}_{-0.00}$	16
GW170818	$35.5^{+7.5}_{-4.7}$	$26.8^{+4.3}_{-5.2}$	$26.7^{+2.1}_{-1.7}$	$-0.09^{+0.18}_{-0.21}$	$59.8^{+4.8}_{-3.8}$	$0.67^{+0.07}_{-0.08}$	$2.7^{+0.5}_{-0.5}$	$3.4^{+0.5}_{-0.7} \times 10^{56}$	1020^{+430}_{-360}	$0.20^{+0.07}_{-0.07}$	39
GW170823	$39.6^{+10.0}_{-6.6}$	$29.4^{+6.3}_{-7.1}$	$29.3^{+4.2}_{-3.2}$	$0.08^{+0.20}_{-0.22}$	$65.6^{+9.4}_{-6.6}$	$0.71^{+0.08}_{-0.10}$	$3.3^{+0.9}_{-0.8}$	$3.6^{+0.6}_{-0.9} \times 10^{56}$	1850^{+840}_{-840}	$0.34^{+0.13}_{-0.14}$	1651

そして、今日12月2日午前1時に新たな発表がありました

Observation 1,2 のデータの中に、もしかしたら連星ブラックホール合体からの重力波かもしれないデータ14個も抽出(ただし、雑音とかぶっていたりしたので、宣言はせず)





重力波発生イベントではないかもしれないことを表す指標(値が大きいほど、嘘である可能性が高まる)

Date	UTC	Search	FAR [y^{-1}]	Network SNR	\mathcal{M}^{det} [M_{\odot}]	Data Quality
151008	14:09:17.5	PyCBC	10.17	8.8	5.12	No artifacts
151012A	06:30:45.2	GstLAL	8.56	9.6	2.01	Artifacts present
151116	22:41:48.7	PyCBC	4.77	9.0	1.24	No artifacts
161202	03:53:44.9	GstLAL	6.00	10.5	1.54	Artifacts can account for
161217	07:16:24.4	GstLAL	10.12	10.7	7.86	Artifacts can account for
170208	10:39:25.8	GstLAL	11.18	10.0	7.39	Artifacts present
170219	14:04:09.0	GstLAL	6.26	9.6	1.53	No artifacts
170405	11:04:52.7	GstLAL	4.55	9.3	1.44	Artifacts present
170412	15:56:39.0	GstLAL	8.22	9.7	4.36	Artifacts can account for
170423	12:10:45.0	GstLAL	6.47	8.9	1.17	No artifacts
170616	19:47:20.8	PyCBC	1.94	9.1	2.75	Artifacts present
170630	16:17:07.8	GstLAL	10.46	9.7	0.90	Artifacts present
170705	08:45:16.3	GstLAL	10.97	9.3	3.40	No artifacts
170720	22:44:31.8	GstLAL	10.75	13.0	5.96	Artifacts can account for

What We Know and Don't Know About the GW Sky

by Salvatore Vitale (MIT) in DAWN II Meeting (Renewed by Miyoki)

Note: some of the searches in O1 data are not finished yet!

	BNS	NSBH	BBH
Detection		$\geq O3$	
Rates	$\geq O3$	$\geq O3$	$\geq O2$
Mass distribution	$\geq O3$	$\geq O3$	Decent in O2
Spin distribution	$\geq O3$	$\geq O3$	$\geq O2$
Formation channels	$\geq O3$	$\geq O3$	$\geq O2$
EOS	$> O3, A+, NF$	$> O3, A+, NF$??
EM connection		$> O3$	O2 w/ Virgo
Detection at $z > 1$	NF	NF	O3
Tests of GR	$\geq O2$	$\geq O3$	

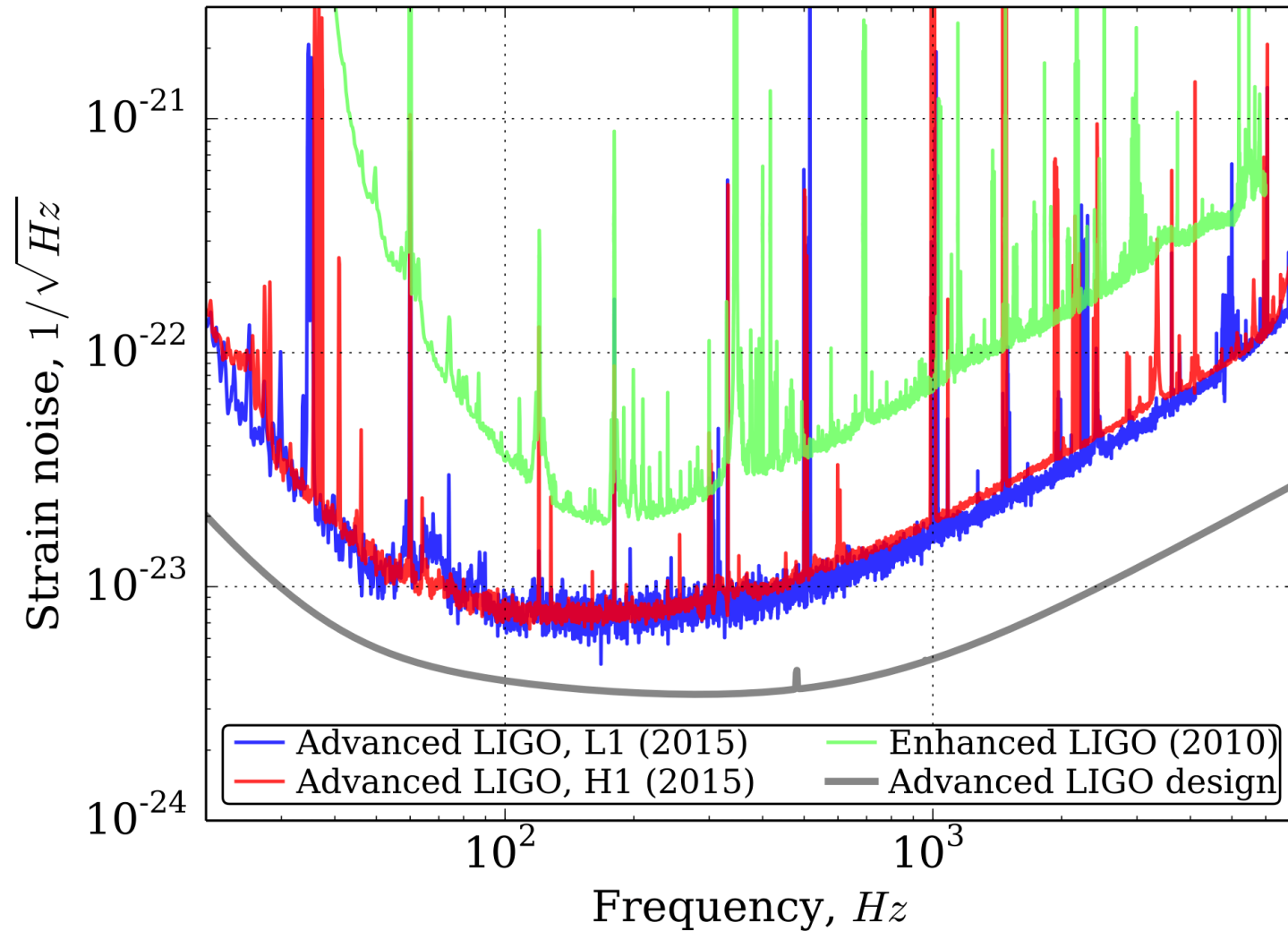
	CC SNe	Other bursts
Detection	O2 - NF	O2- NF
Mechanism	From 1 st detection	??
Mass \rightarrow GW efficiency	From 1 st detection	??

	BBH bgd	Primordial bgd
Detection	O3, O4, A+, NF	\ggg NF
Population studies	A+, NF	Not Relevant

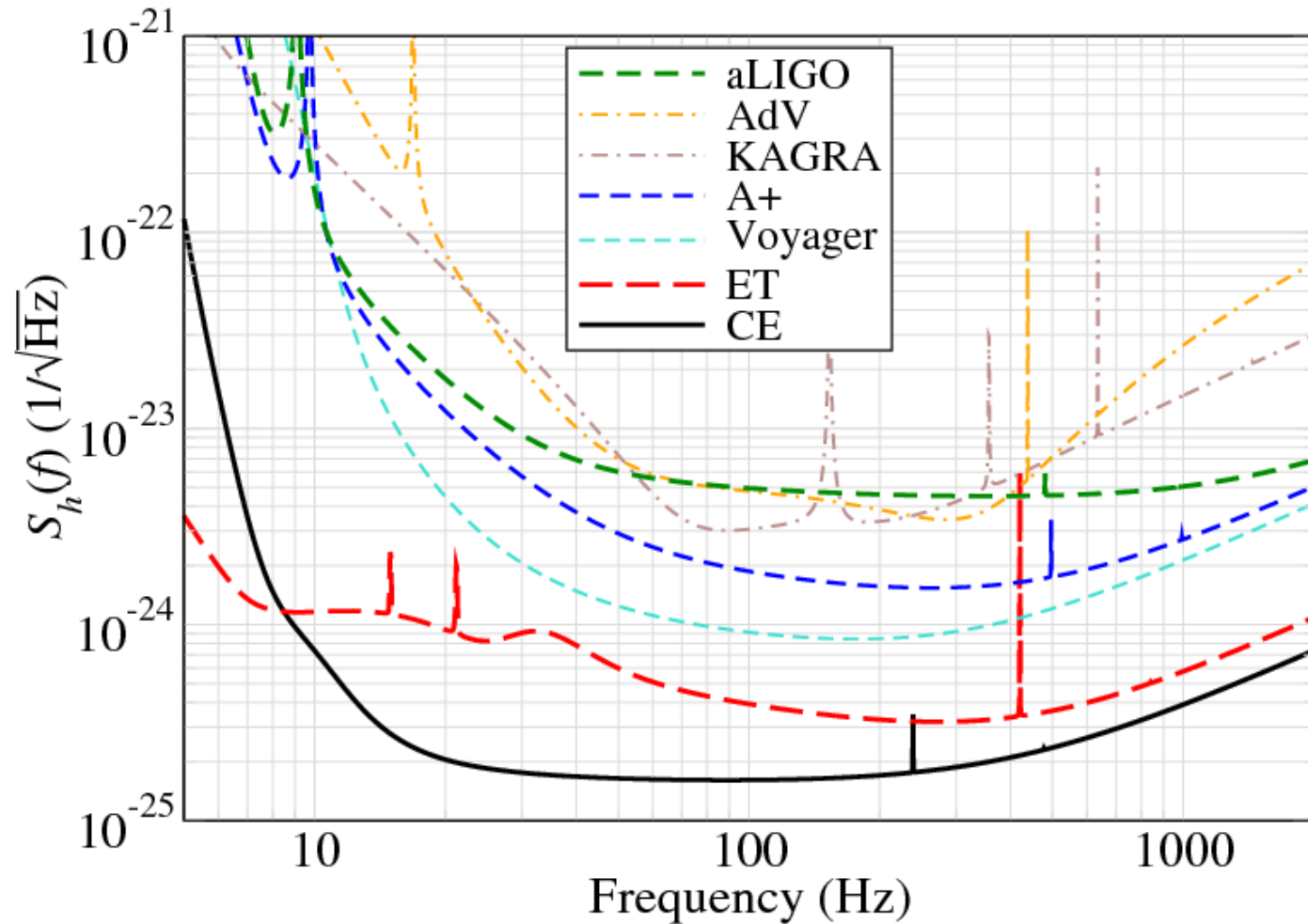
	Targeted CW	Blind CW
Detection	$\geq O3$	$\geq O3$
Ellipticity/EOS	From 1 st detection	From 1 st detection
Population studies	Not relevant	A+, NF

NF= new facilities (CE, ET)

We should realize targeted sensitivity



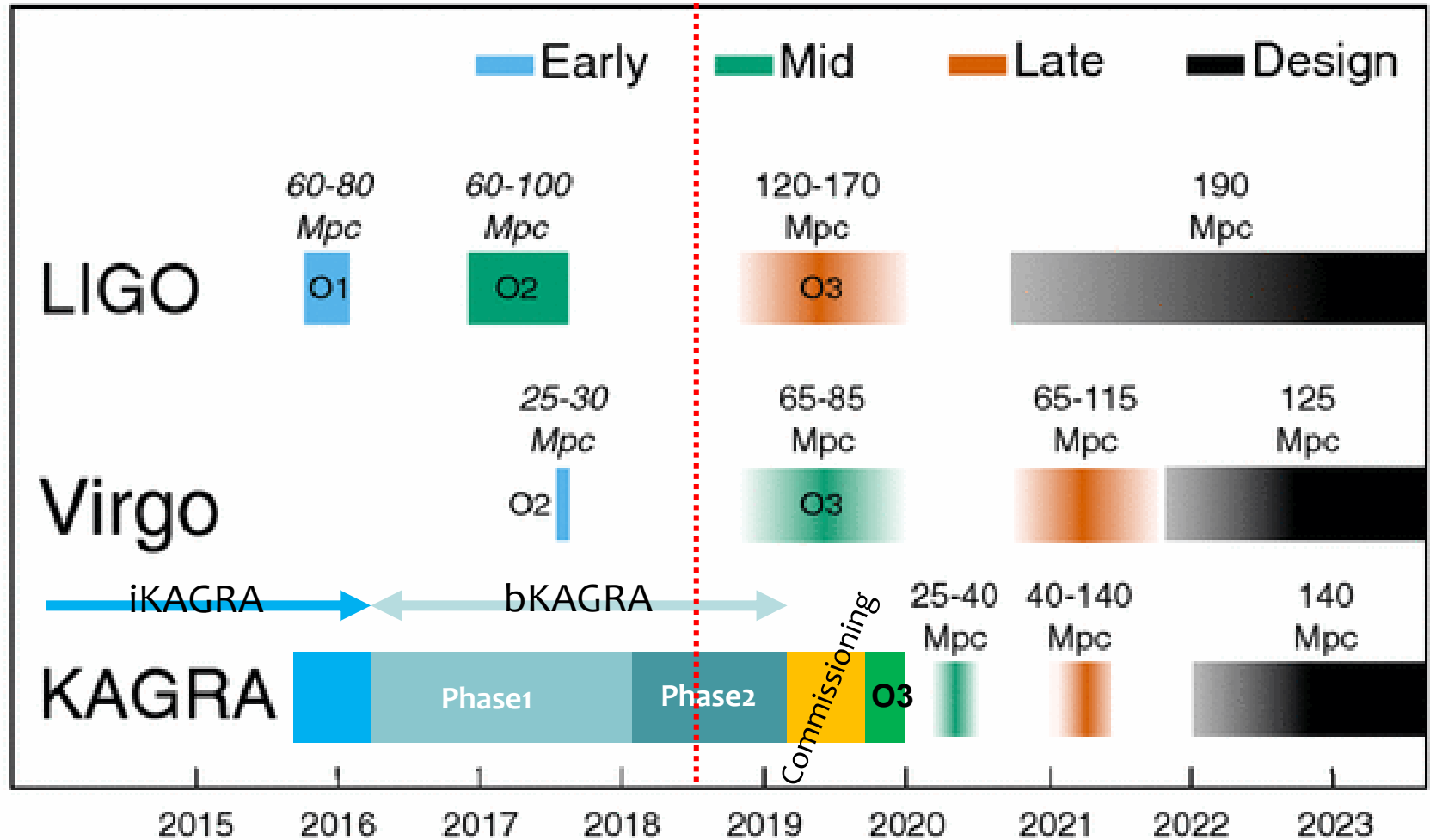
We need Better Sensitivity!



We need more detectors!



Observation Scenario of LVK



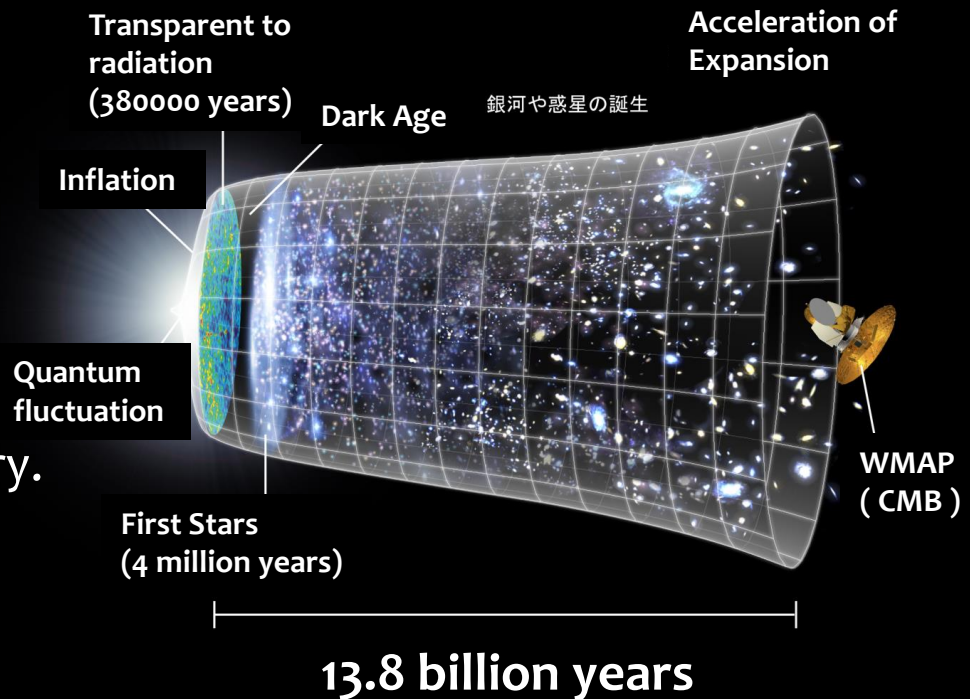
Why direct detection of GWs is important ? (1)

■ New probe to observe the Universe during 380000 years after the Big Bang.

■ We have only EMs and particles as observation method of the Universe.

■ 380000 years cannot be Observed with EMs because the Universe is so hot that EMs were scattered a lot.

■ Only Neutrino and GWs that can be transparent for any material can observe this history.



Why direct detection of GWs is important ? (2)

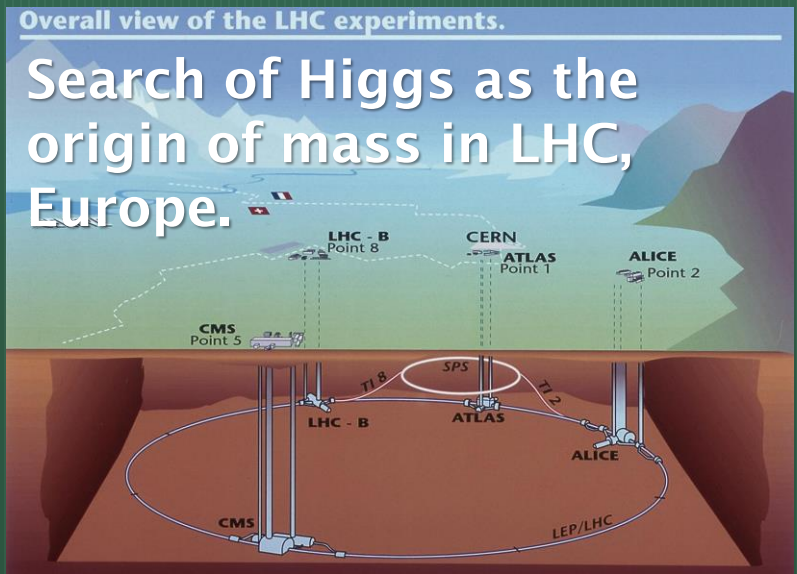
■ Probe of Gravity : Gravity is the most unknown subject in Physics

■ Gravity force is extremely weak ($1/10^{39}$) compared with EM force and atomic forces in the scale of humankind that it is almost impossible to search the property of gravity and its field. The force strength ratio of SF, EMF, WF, GRF is

$$\frac{g^2}{2hc} : \frac{e^2}{2\varepsilon_0 hc} : \frac{4\pi^2 (M_p c^2)^2 G_W}{h^2 c^2} : \frac{2\pi G_N M_p^2}{hc} = 0.1 \sim 10 : \frac{1}{137} : 10^{-5} : 10^{-39}$$

■ Detectable GWs are radiated from so strong gravity field that GWs have unique information about gravity fields and compact stars mechanism.

Gravitational waves search
in several countries (USA,
Europe and Japan)



Why direct detection of GWs is important ?

(3)

■ Gravity rules the structure and fate of the Universe.

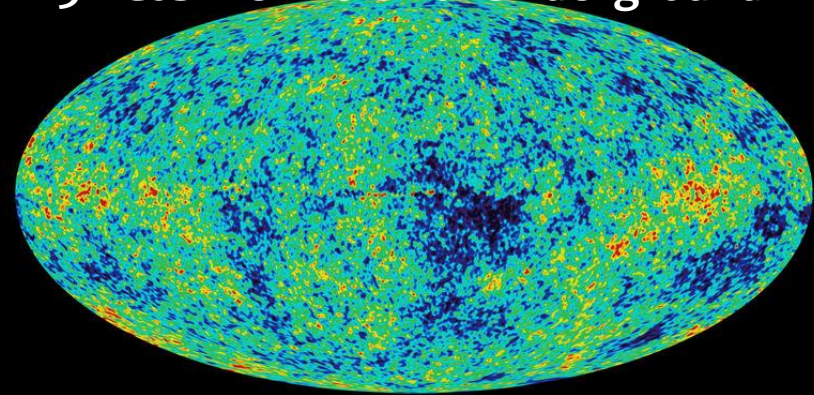
■ Both EM force and Gravity force are long-range force. EM force can be cancelled because of sum of attracting and repulsive forces in the Universe scale. On the other hand, gravity force can be alive.

■ Baryon that we used to recognize as the all component of the Universe was proven to be only 4% of the Universe !!

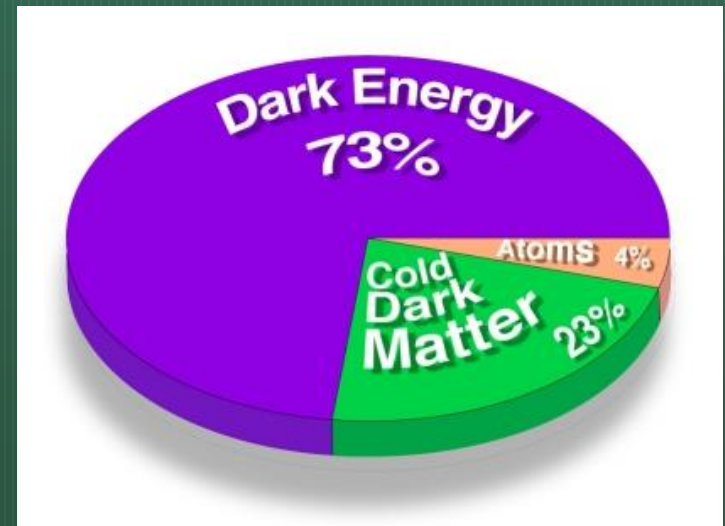
■ Dark matter can be observed by Gravity Effect.

■ It is quite natural motivation to observe the Universe that is dominated by Gravity with Gravitational Waves .

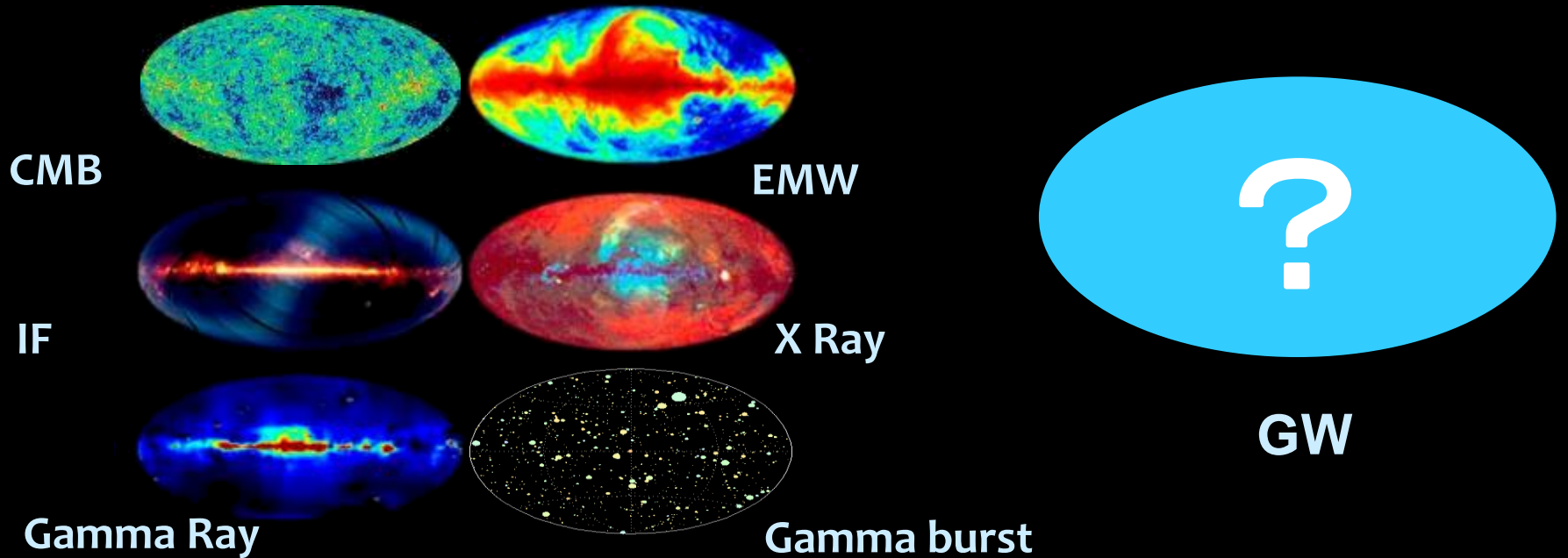
3K Cosmic Microwave Background



WMAP concluded that the Universe must consist of 73% DE, 23% DM and 4% Atoms !!



Gravitational Wave Astronomy



- New method to observe the Universe
- Unexpected Objects ??

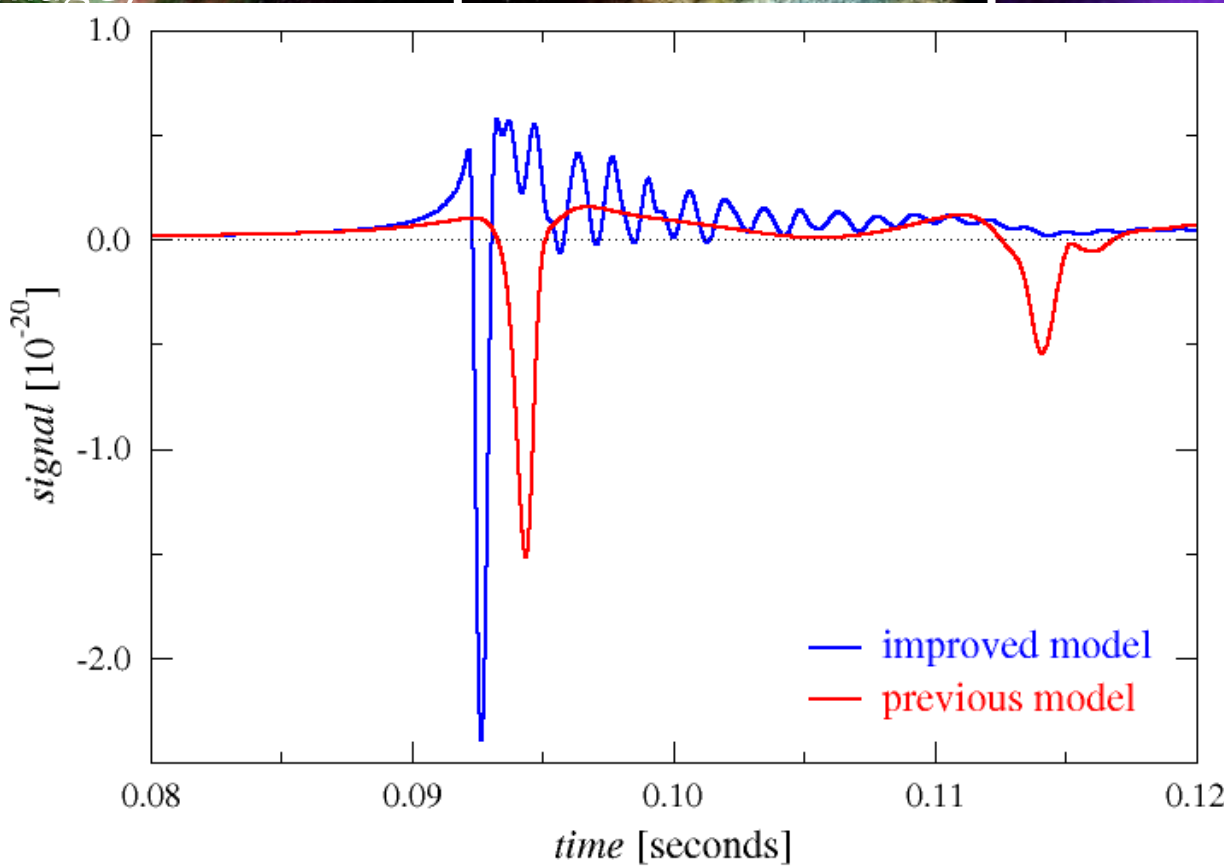
Expected GW Sources

- Big Bang, Compact Stars High Energy Objects-

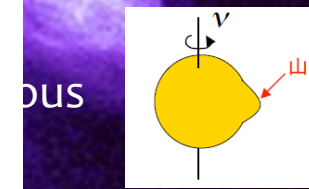
Big Bang and Inflation
(Image)

Supernovae
(NASA)

Pulsar
(NASA)



As GW



Wave

Star Binary
system

And their Coalescences

質量範囲[太陽質量]

0.08以下

主系列星

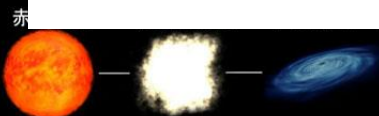
0.08~8

主系列星

8~40

主系列星

40以上



星間ガス

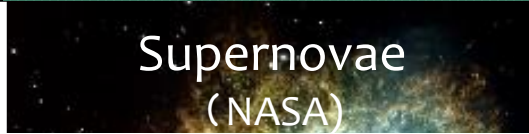
Expected GW Sources

Big Bang and Inflation
(Image)

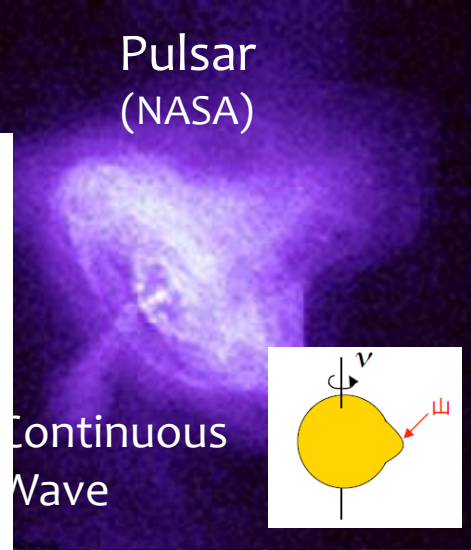


As GW background

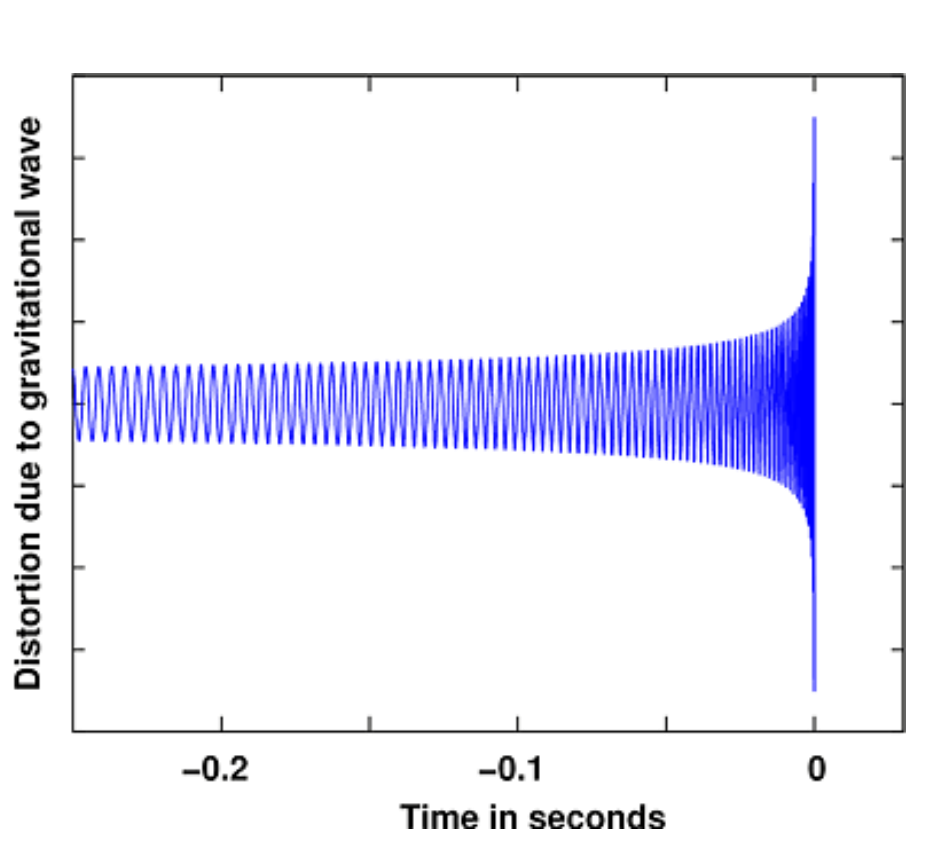
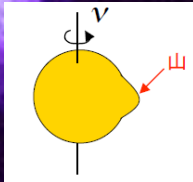
Supernovae
(NASA)



Pulsar
(NASA)



Continuous Wave



Chirp Wave



Neutron Star Binary System
And their Coalescences

質量範囲[太陽質量]

0.08以下

主系列星

赤色巨星

0.08~8

主系列星

赤色巨星

8~40

主系列星

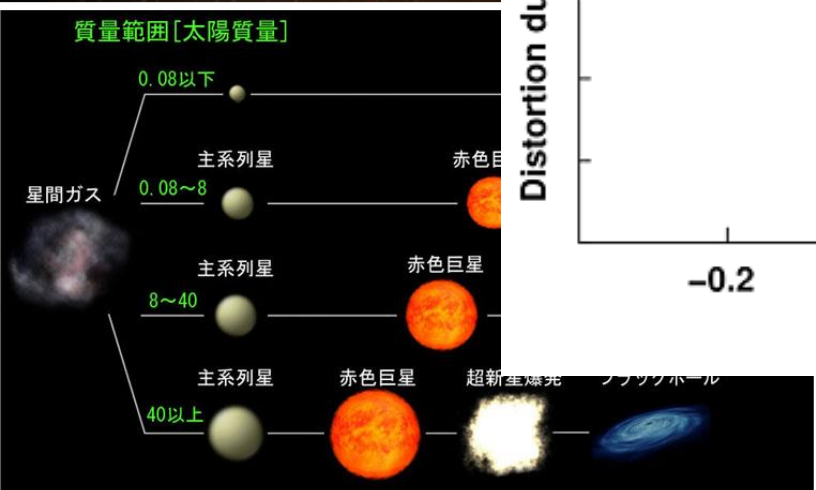
赤色巨星

超新星爆発

ブラックホール

40以上

星間ガス



BIRTH OF BLACK HOLES

Expected GW events Rate

Known compact star binaries in our galaxy

PSR name	P_s (ms)	P_b (hr)	e	τ_{life} (Gyr)
B1913+16	59.03	7.75	0.617	0.37
B1534+12	37.9	10.10	0.274	2.93
J0737-3039A	22.7	2.45	0.088	0.23
J1756-2251	28.46	7.67	0.181	2.03
J1906+0746	144.14	3.98	0.085	0.082
J1227+11C	32.76	8.047	0.681	0.32

Merger Rate of compact star binary and GWD expected detection rate / galaxy/ year

	NS-NS	BH-NS	BH-BH
Merger Rate	$83.0^{+209.1}_{-66.1} \times 10^{-6}$	$10^{-7} \sim 10^{-4}$	$10^{-7} \sim 10^{-5}$
2 nd GWD expected detection rate	$9.2^{+23.2}_{-7.35}$	0.087 ~ 87	0.7 ~ 70

GW Sources

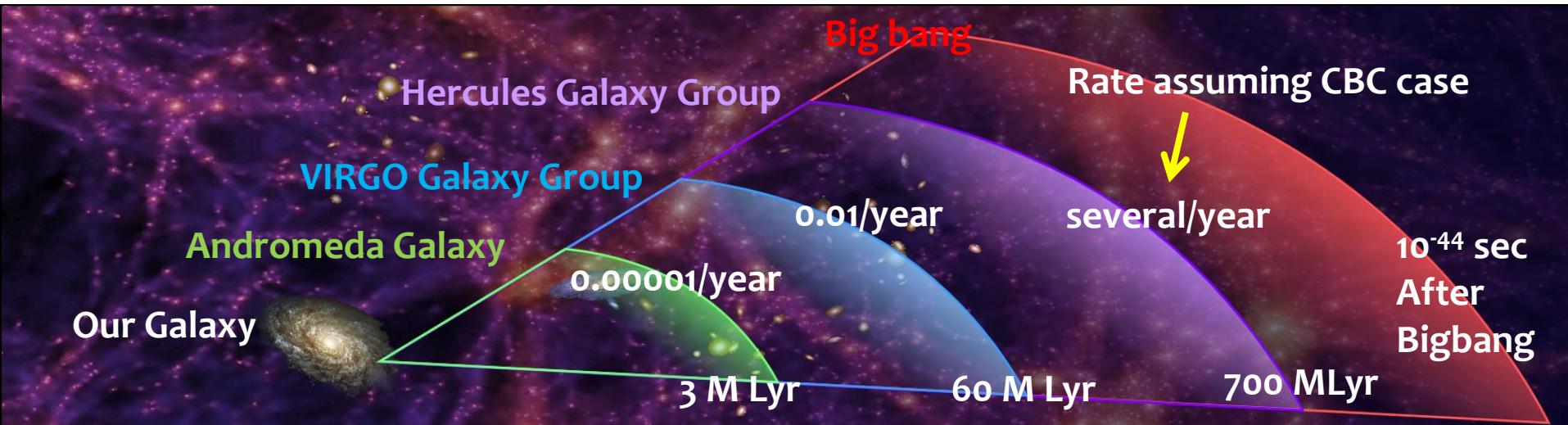
Amplitude, Frequency, Event Rate

GWs from NS-NS coalescences are most reliable sources, and their wave forms can be theoretically predictable.

Estimated Event Rate : 1/100000 years per one Galaxy

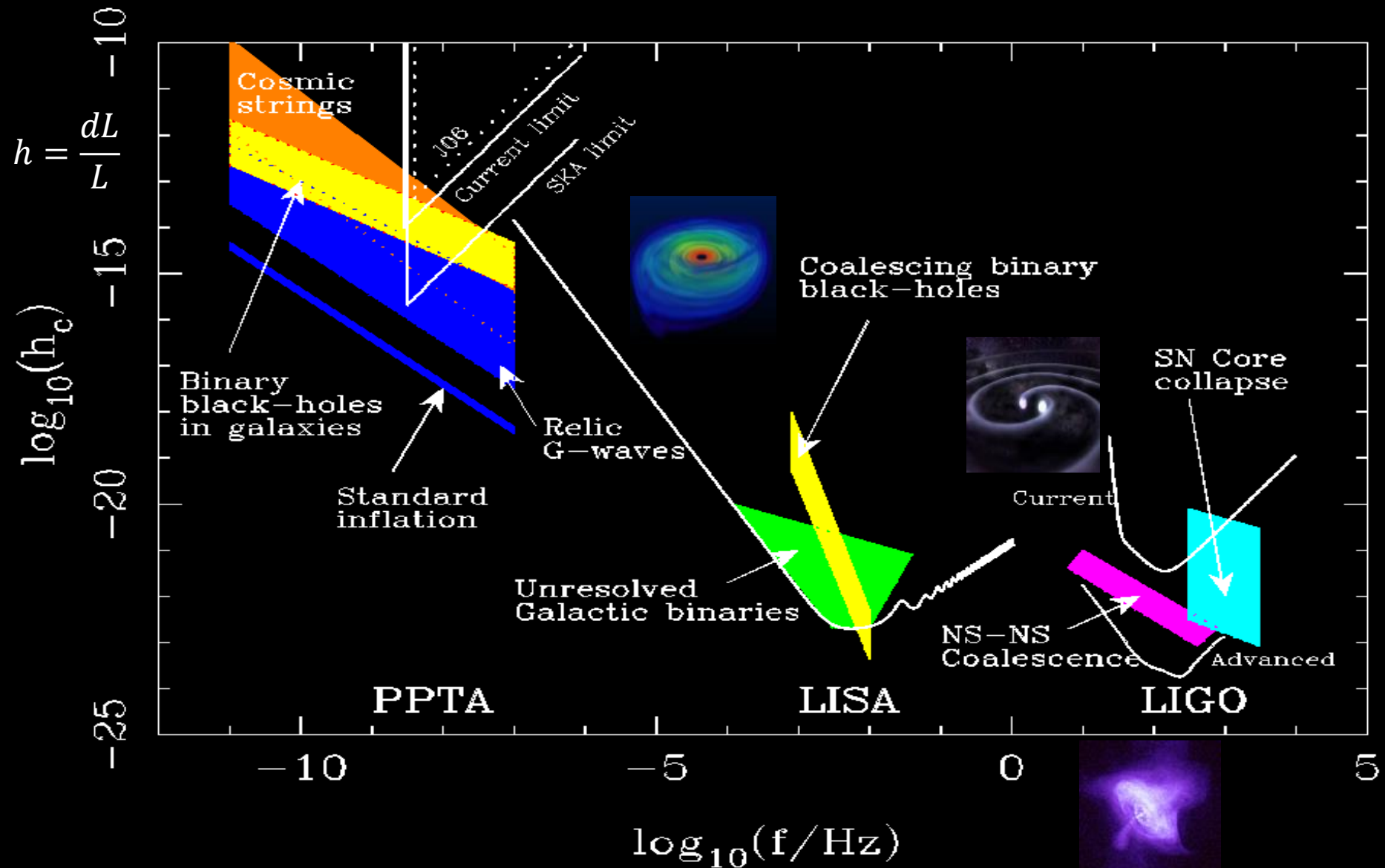
Let's make a GW detector that can observe 100000 galaxies !!

$10^{-23\sim 24}$ [1/rHz] @ 100Hz Sensitivity !!



GW Sources

Amplitude, Frequency, Event Rate



The First GWD

- Pro. J.Weber Maryland Univ. USA (1969) -

■ **Resonant Type GWD** : Detect Excitation of a rigid body resonance due to GWs tidal force.

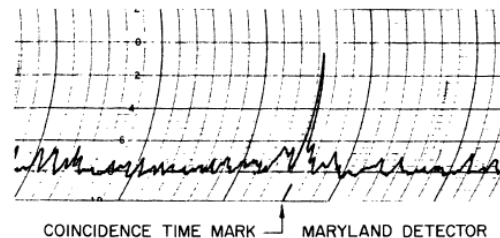
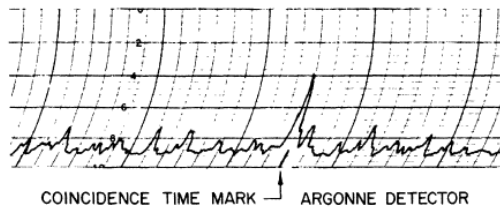
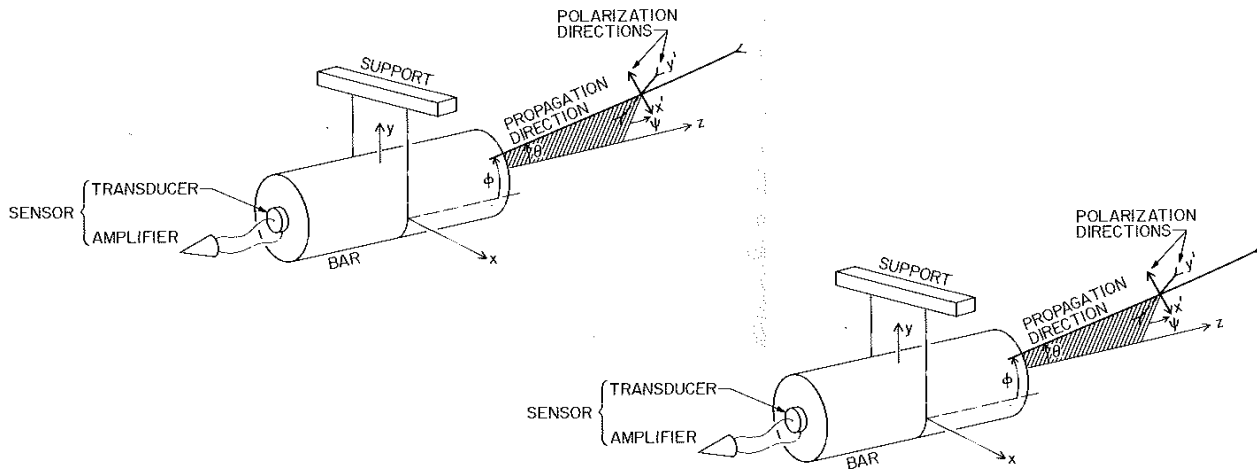


FIG. 2. Argonne National Laboratory and University of Maryland detector coincidence.

- Coincident signals were observed in two GWDs that were set 1000km away.
- The first GWs detection was reported, but... amplitude is too large to destroy the Universe within 10 Mega years !!
- No positive verifications followed his experiment.



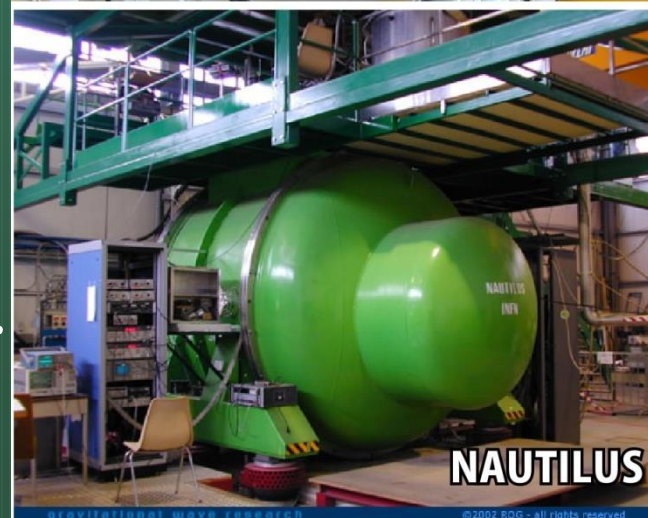
Many Resonant Type GWDs in the world

■ Thermal noise reduction is essential to enhance the sensitivity.

Technical aspects to enhance the sensitivity.

1. Seismic noise isolation
2. Cryogenic operation
3. Low mechanical loss bar
4. Squid for signal extraction

Some of these resonant type GWD performed coincident observation, but no remarkable report about GW signal detection.

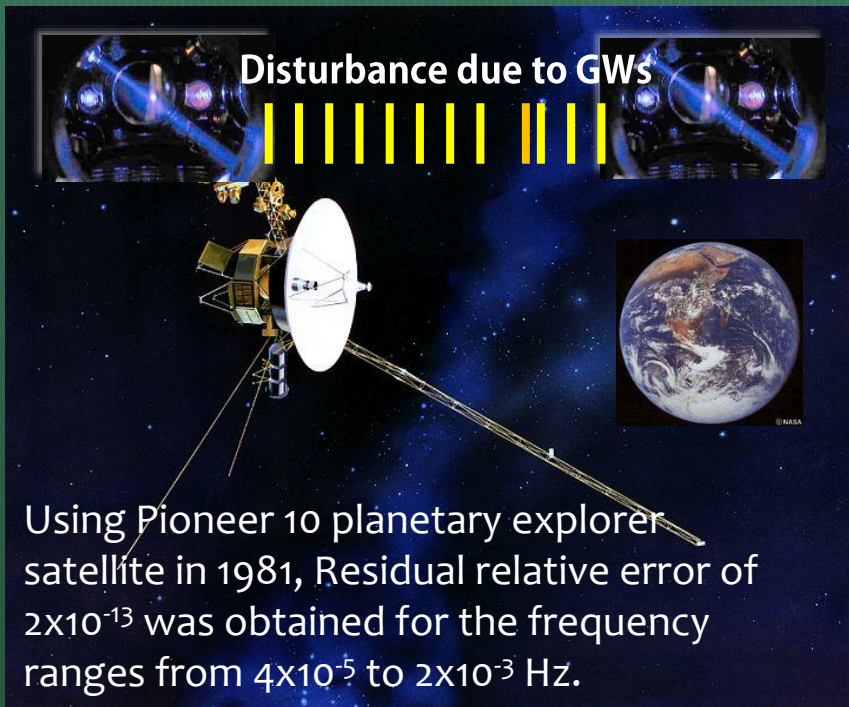


Other ideas for GW detection

■ Doppler Tracking

Monitor the time disturbance from the planetary explorer satellite that has precise atomic clock.

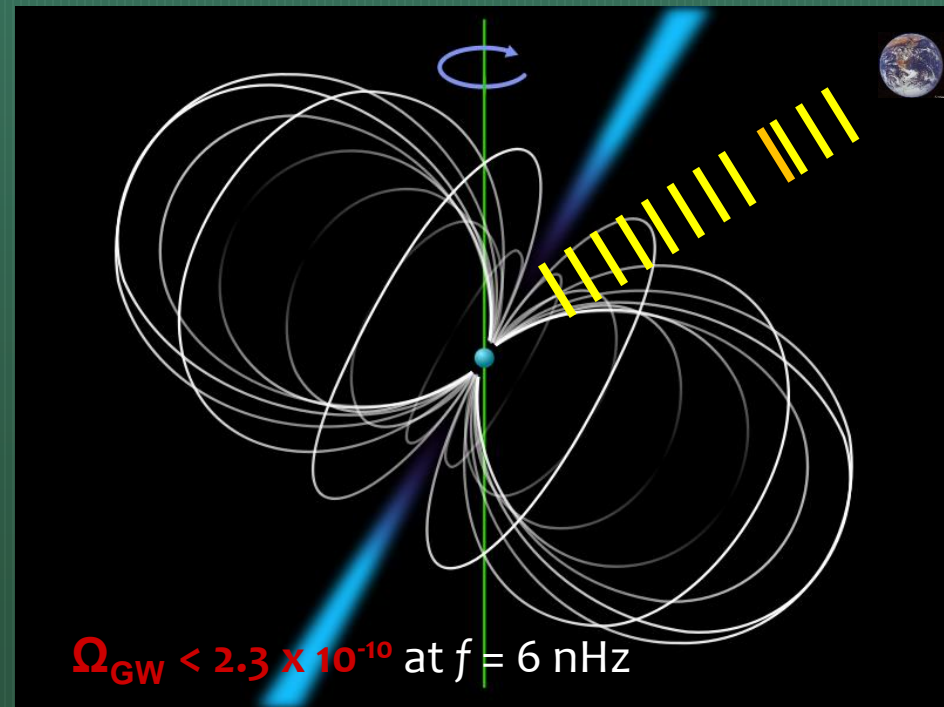
Background GWs ($10^{-5} - 10^{-3}$ Hz)



■ Pulsar Timing

Replace atomic clock with pulsar's pulse signal that can be also good time standard.

Background GWs ($10^{-9} - 10^{-6}$ Hz)

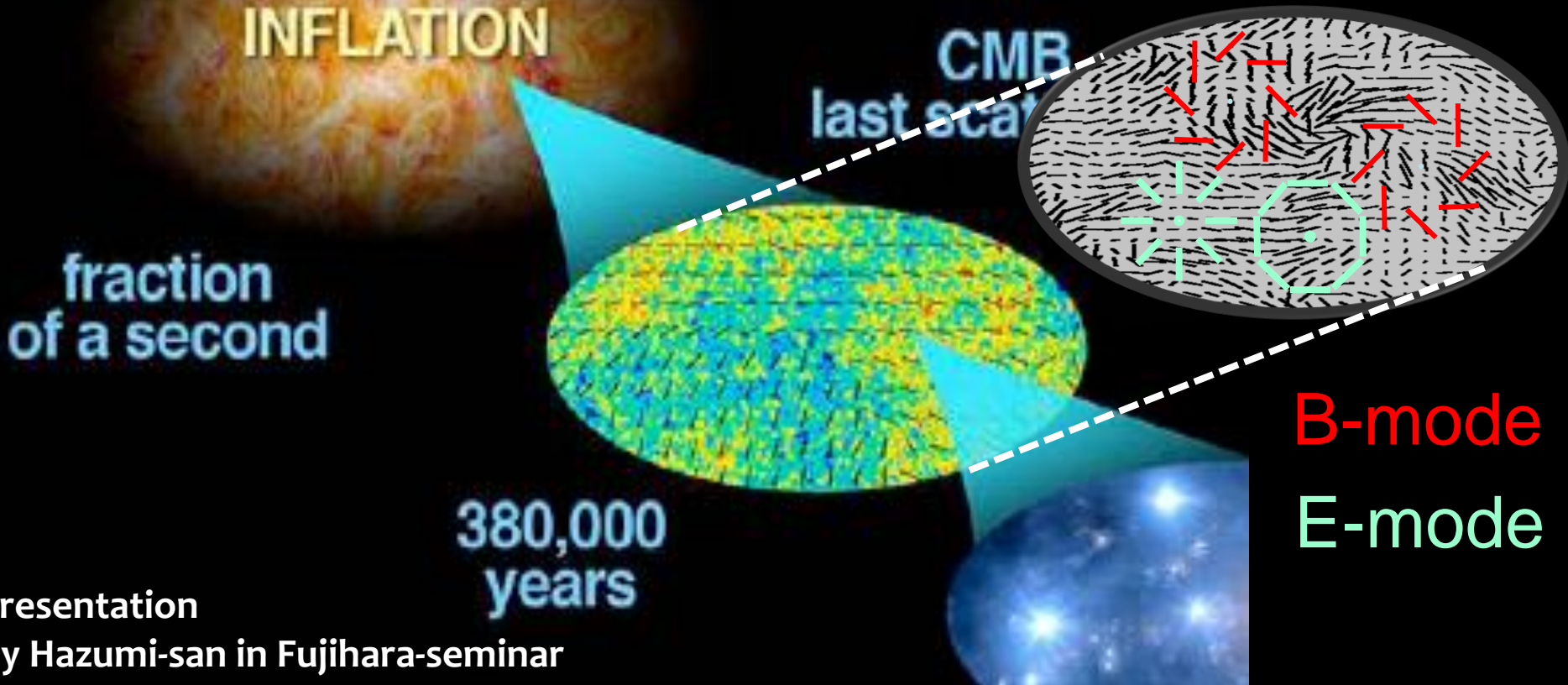


Other ideas for GW detection

■ B mode polarization detection in CMB.

The target is the primordial GWs that are generated by the inflation at the beginning of the Universe.

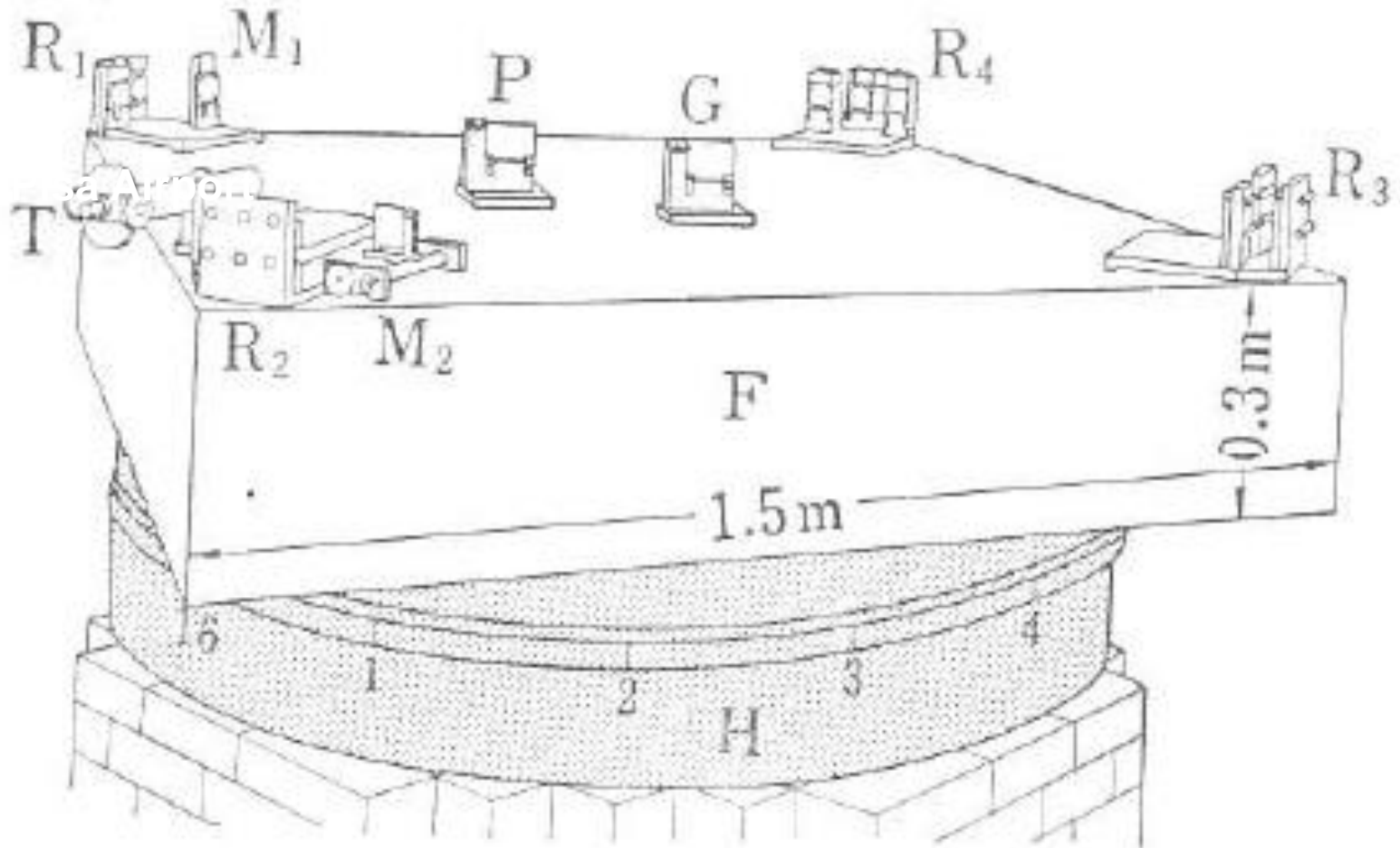
This GWs left B-Mode polarization in CMB.



The Main Stream of GWDs

- Ultra-precise length measurement -

■ Laser interferometer based on the Michelson Interferometer



Let's make GWD

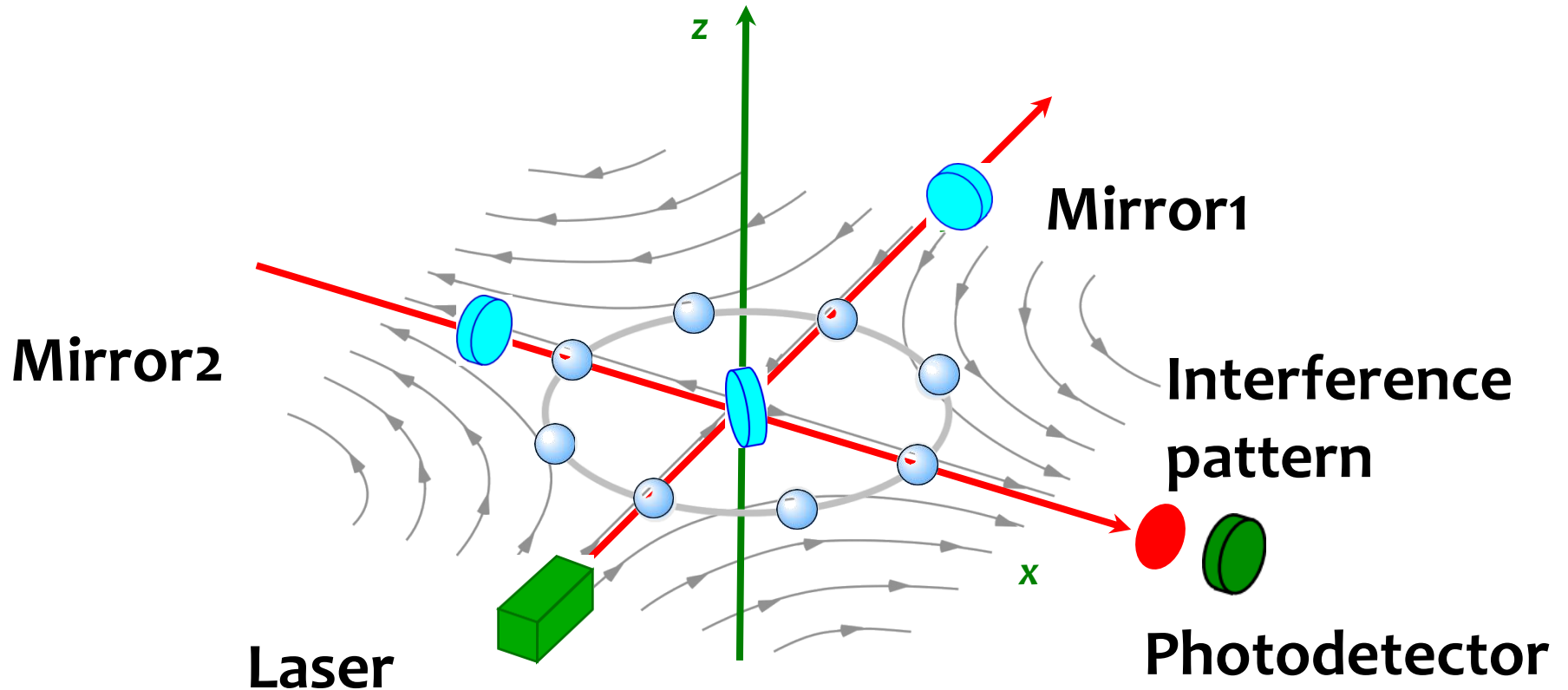
as

**an ultra-precise length measurement
instrument**

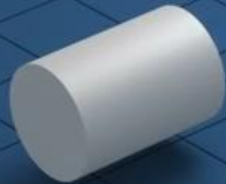
Strategy

**Store a large amount of photon
in the interferometer,
then
enhance the rate of interaction between
Photon and Graviton.**

Differential Motion Measurement

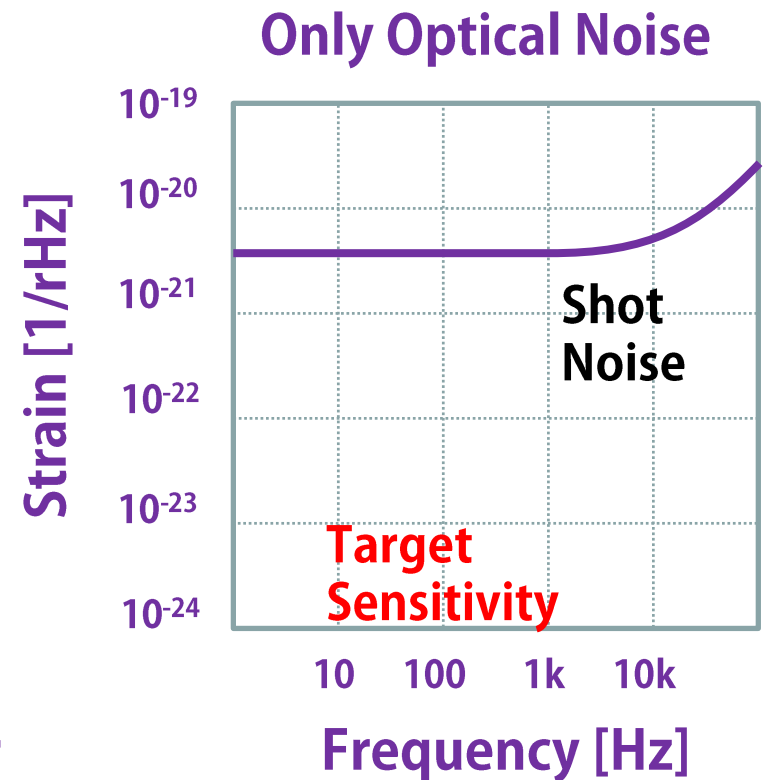
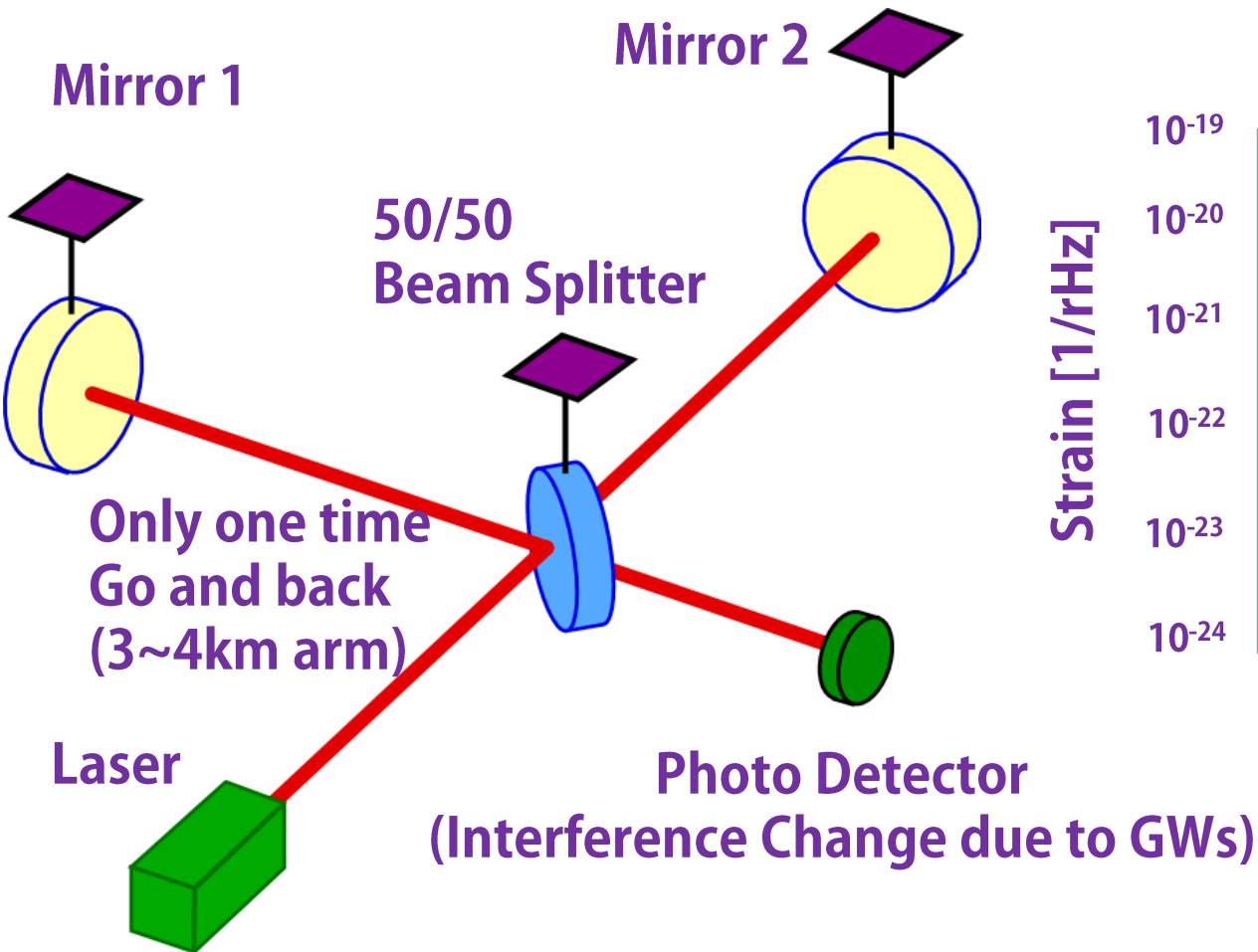


レーザー干渉計で検出する



Principle of a Laser Interferometer

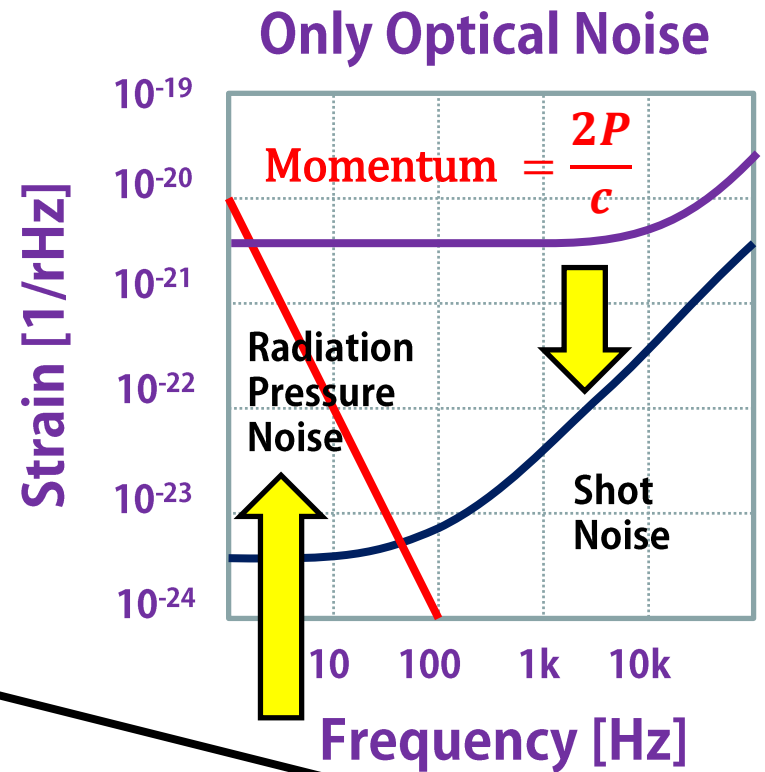
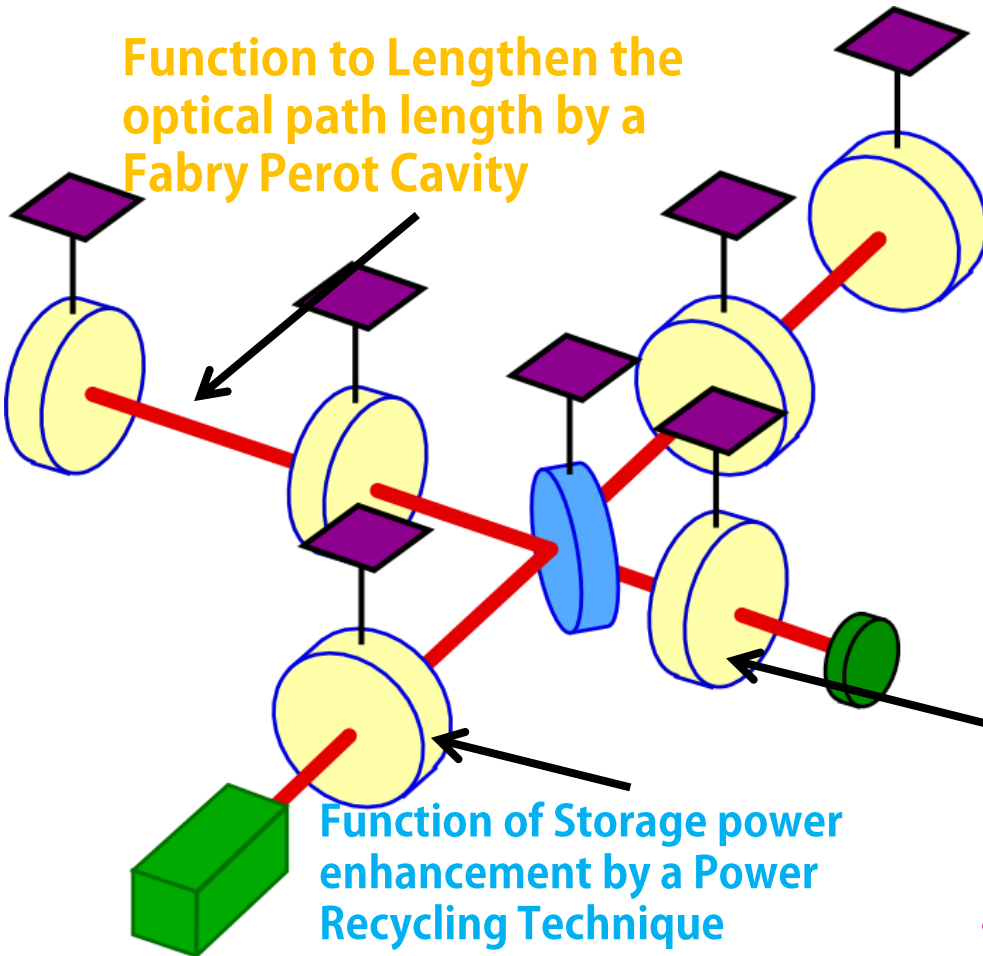
Simple Michelson Laser Interferometer



Ultimate Interferometer

- to obtain 3×10^{-24} [1/rHz] @100Hz-

■ **Power Recycled Fabry-Perot** Michelson Interferometer with **Resonant Sideband Extraction Technique**.

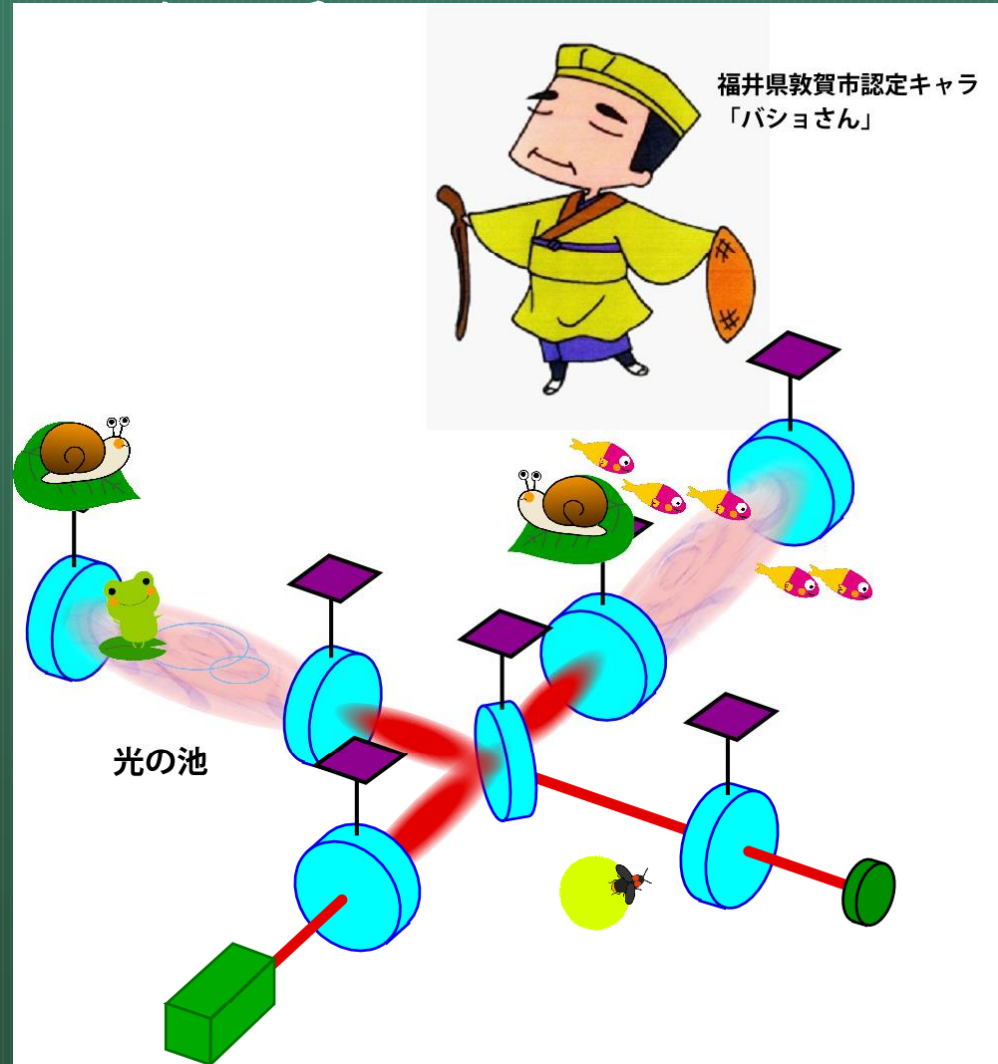


Function of observation frequency band adjustment by a RSE Technique

Practical Noise Sources in GWD

■ GWD Noise Sources

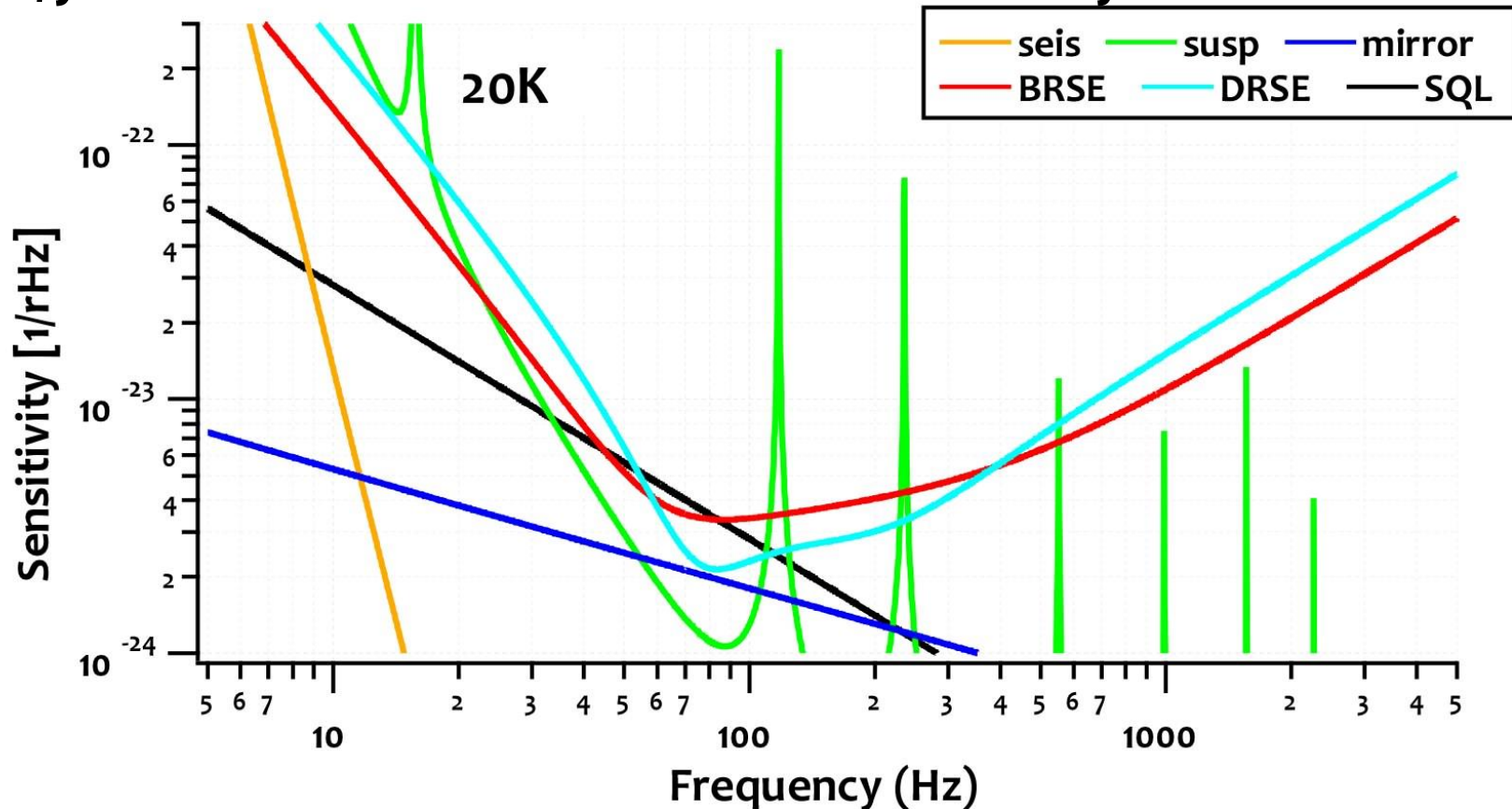
- Shot Noise
- Radiation Pressure Noise
- (Standard Quantum Limit)
- Seismic Noise
- Gravity Gradient Noise
- Residual Gas Fluctuation Noise
- Laser...
 - Frequency Noise
 - Amplitude Noise
 - Beam Jitter Noise
 - Scattered Light Noise
- Thermal Noise (many mechanism) ...
 - of Mirrors
 - of Mirror Suspension
- Control Electrical Noise for mirror length and alignment control
- Length Signal Mixing Noise (Five degrees of freedom)
- Parametric Instability
- Sound Noise



Required Strain Sensitivity

- 3×10^{-24} [1/rHz] @100Hz strain sensitivity -

■ One of targeted GWD strain sensitivity to expect several times/year event rate of GWs from NS-NS binary coalescences



■ Obviously, GWD is ultra-precise length measurement instrument.

Km-scale GWDs in the world

- as GWD network -



LIGO Project since 1994

- Caltech • MIT and GEO600 and LIGO Scientific Collaboration -

Hanford (Washington St.)

Living Stone (Louisiana St.)



Vacuum Chambers

Vibration Isolation Stack

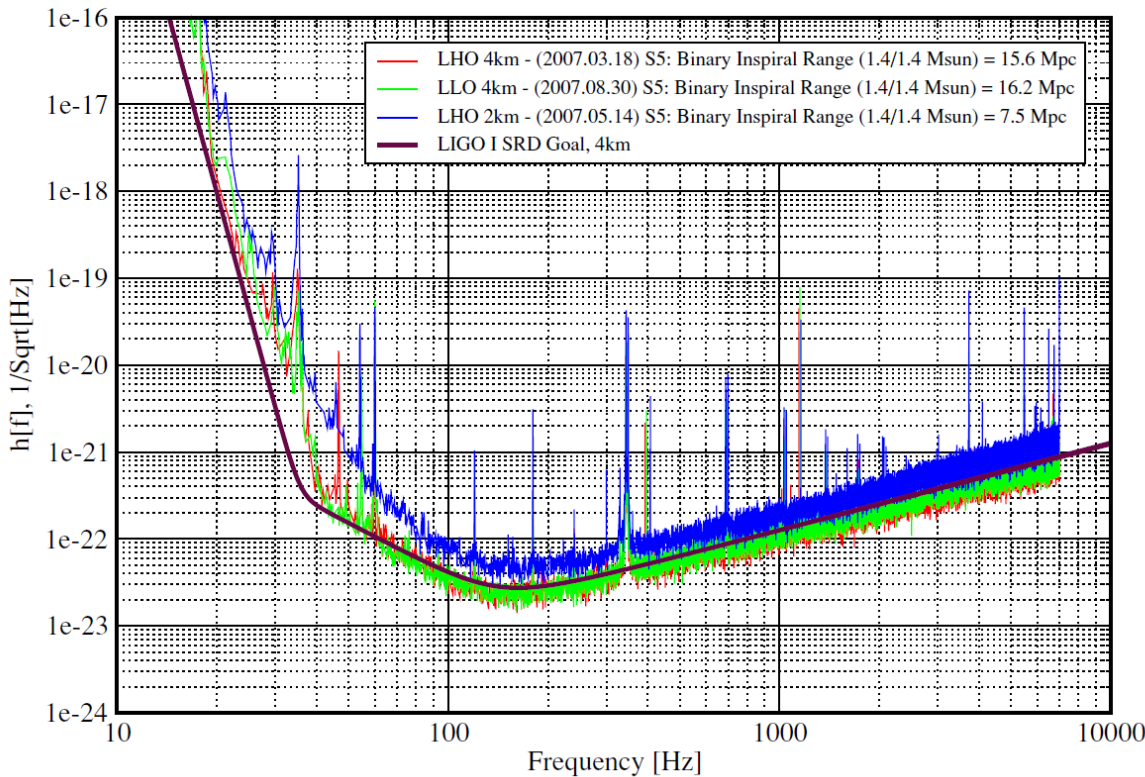
Mirror and Suspension

Highlights of LIGO

- Caltech·MIT and GEO600 and LIGO Scientific Collaboration -

Strain Sensitivity of the LIGO Interferometers

Final S5 Performance LIGO-G0900957-v1



2×10^{-23} [1/rHz] strain sensitivity can detect GWs from 15Mpc away with $S/N = 8$

Coincident observation using two 4km and one 2km GWDs for 3 years.

No remarkable GWs signals. Some new astrophysical upper limits.

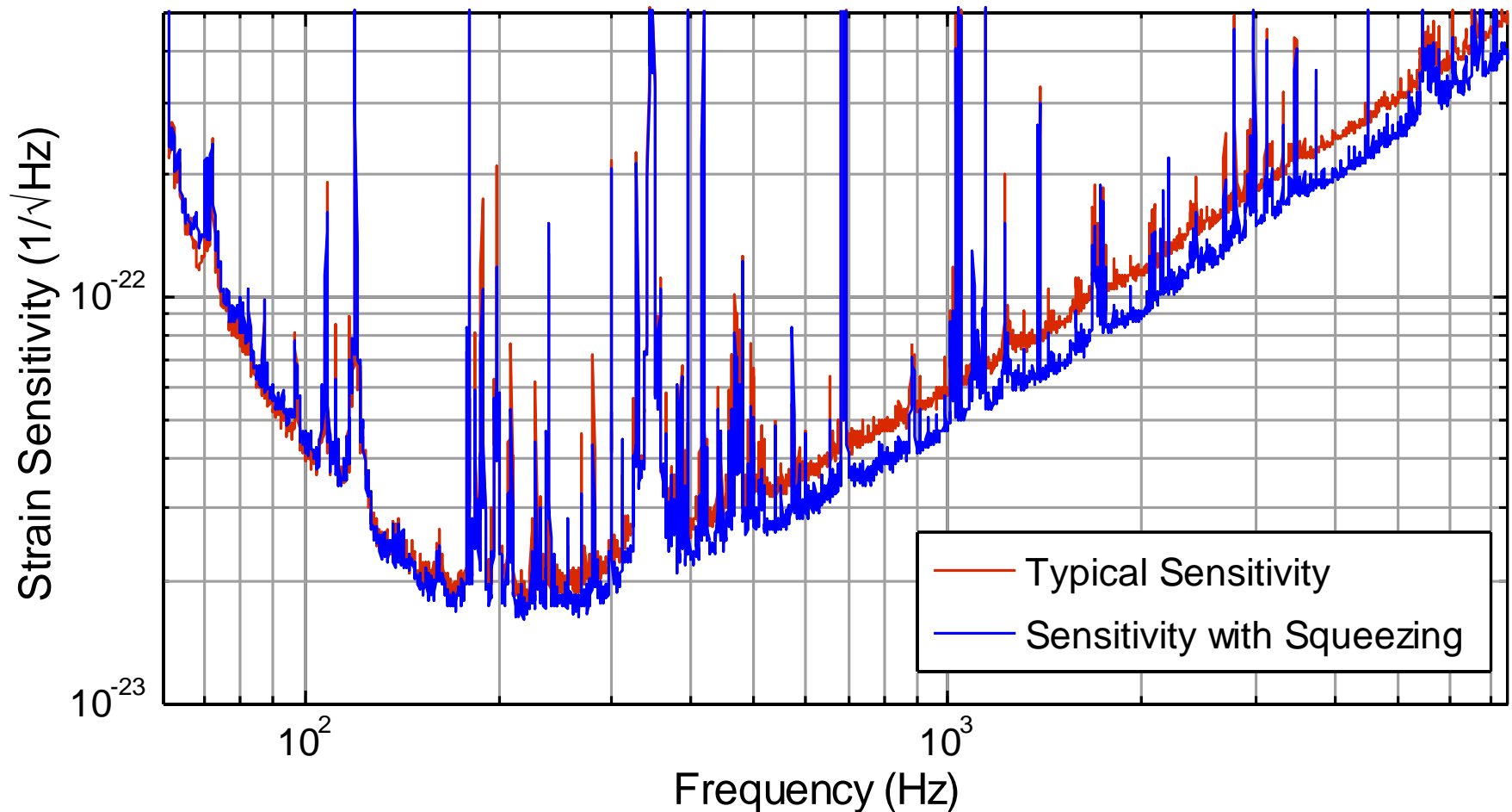
Upgrade for GWs detection is now undergoing.

3rd generation GWD styles are investigated.

Highlights of LIGO

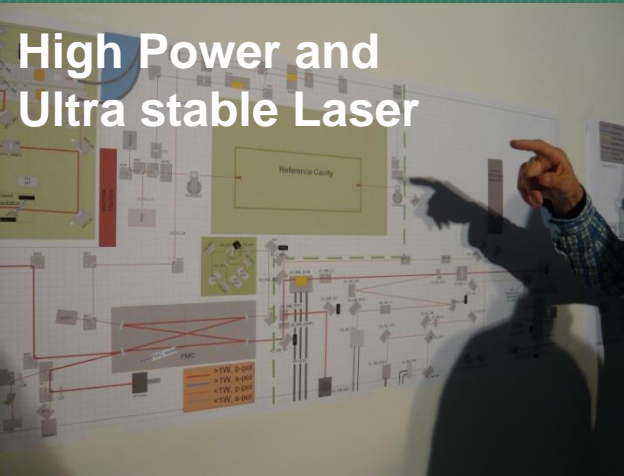
- Caltech·MIT and GEO600 and LIGO Scientific Collaboration -

GEO600 Squeezed Laser Source Introduction in H1 (4km)

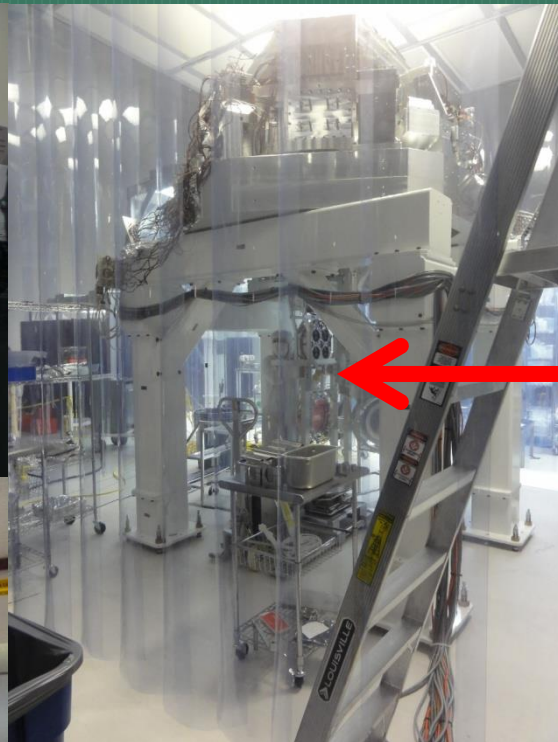


Advanced-LIGO Project

- Caltech • MIT and GEO600 and LIGO Scientific Collaboration -



High Power and Ultra stable Laser



Vibration Isolation using active isolation and 4-stages suspension

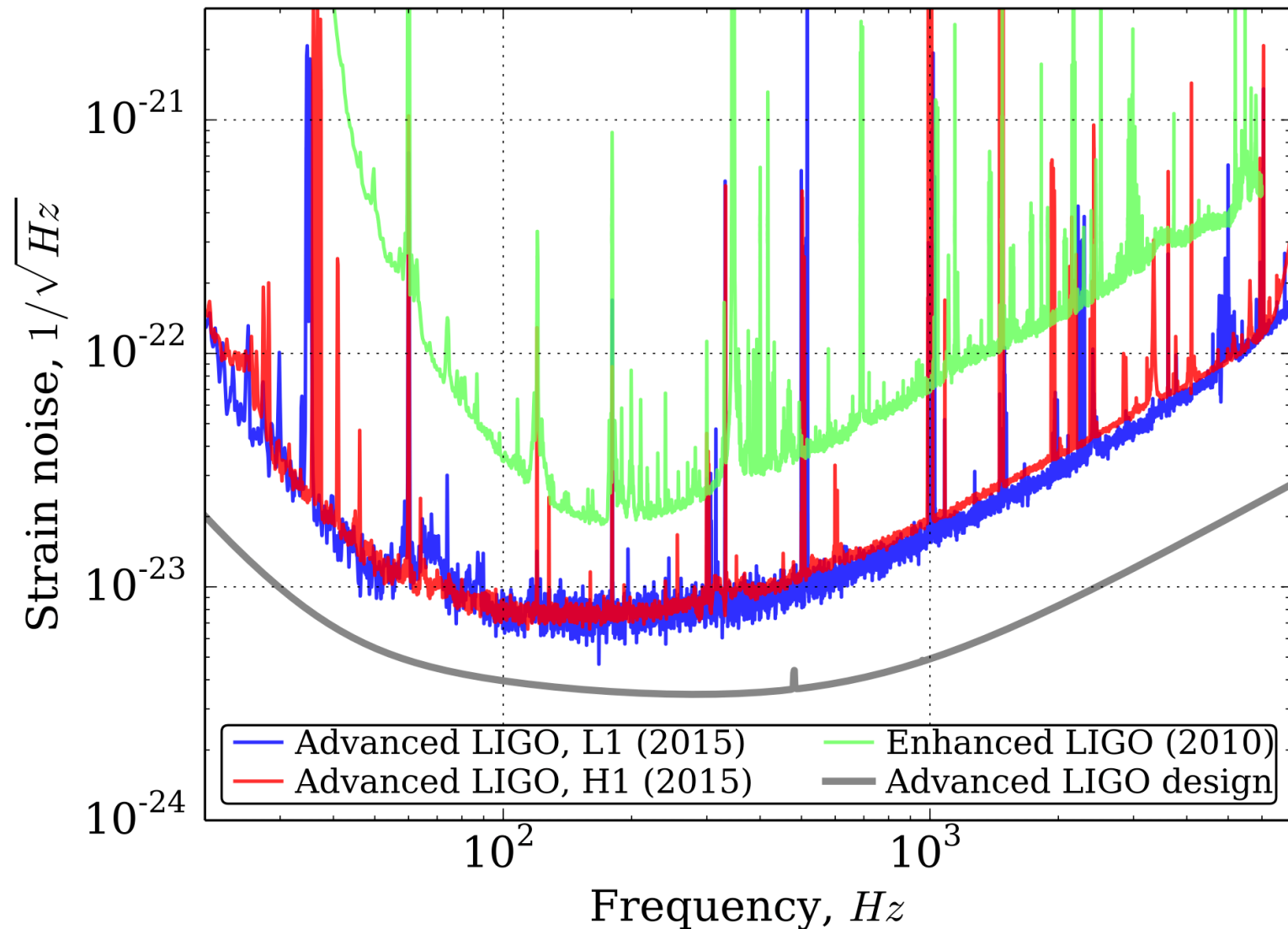


Mirror Assembly



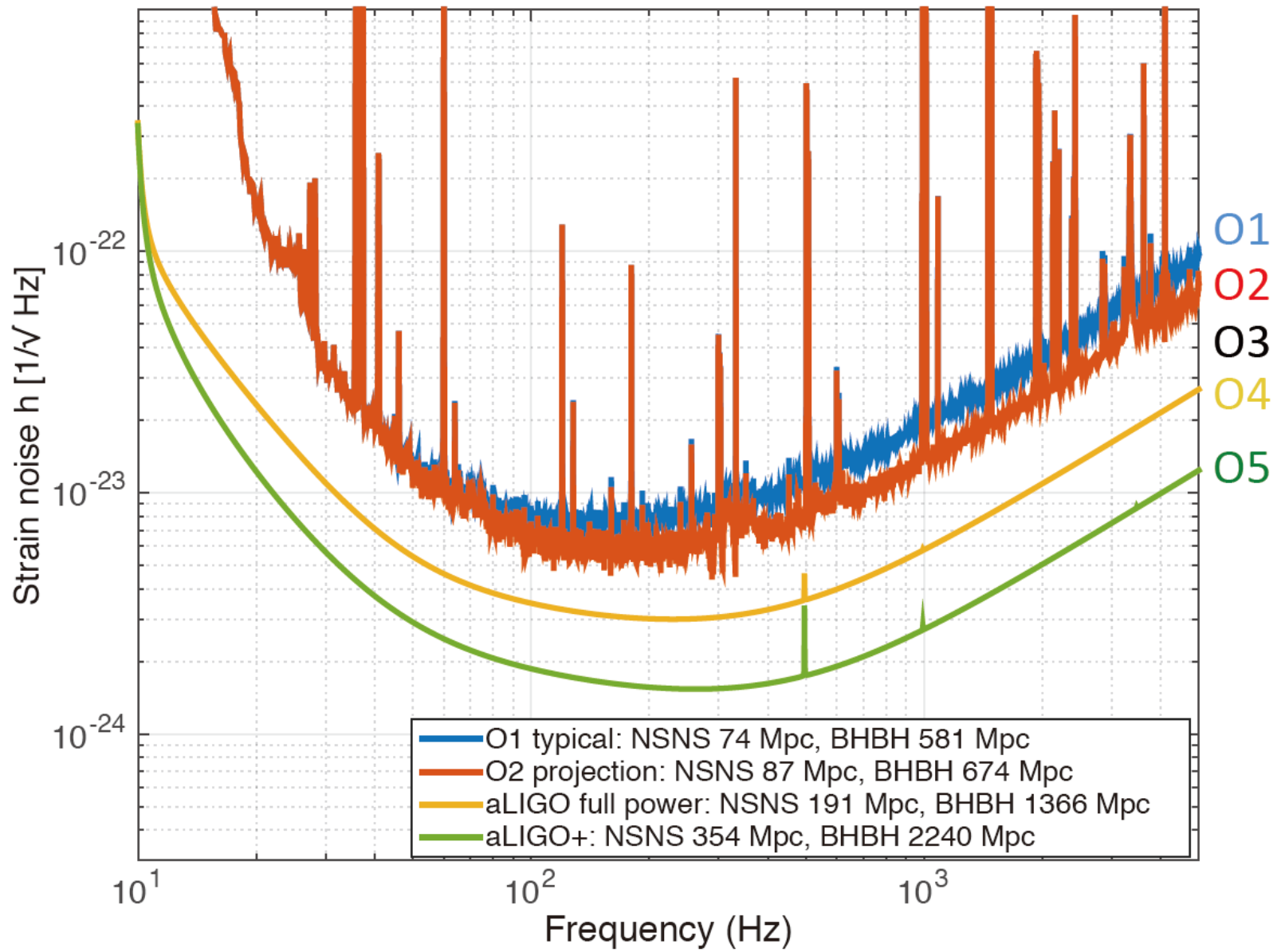
New Vacuum Chambers

Sensitivity of *i*LIGO & Adv.LIGO



Sensitivity Projections

Projections toward aLIGO+ (Comoving Ranges: NSNS 1.4/1.4 M_{\odot} and BHBH 20/20 M_{\odot})



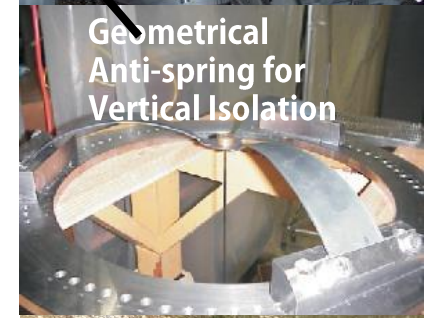
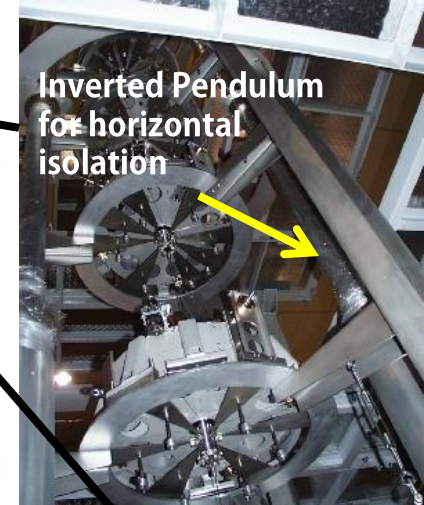
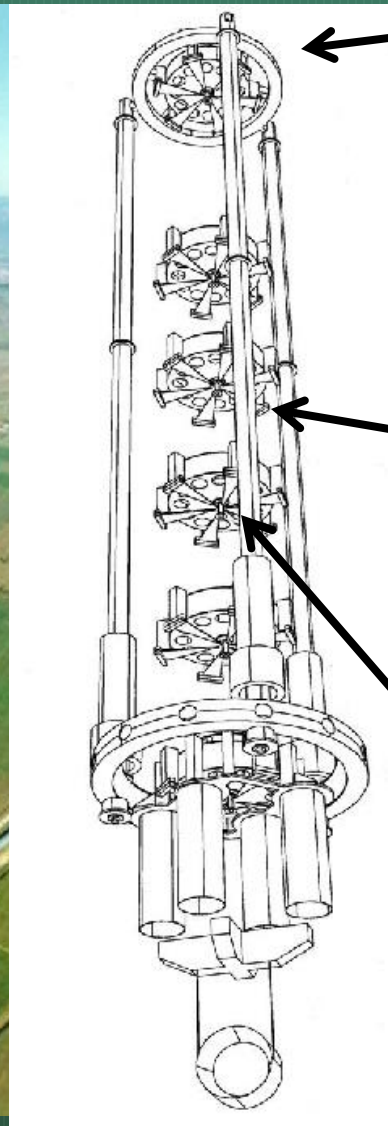
Advanced LIGO Summary

- **Interferometer Commissioning** : The Advanced LIGO interferometers have already exceeded the sensitivity of the initial LIGO interferometers by more than a factor of three and are operating at sensitivities that are interesting from an astrophysical point of view.
- **First Advanced LIGO Science Run**: The LIGO Laboratory and the LIGO Scientific Collaboration started “O1” from Sept 2015. Then Finally detected GWs as GW150914 and GW151226 form BBHs.
- **Second Advanced LIGO Science Run**: “O2” from December? 2016. GW170104, GW170608, GW170804 form BBHs and GW170817 from BNC !! were detected.
- **Network Detection**: GW170814 was also detected Adv. Virgo.
- **Multi Messenger**: GW170817 was also observed many EM observatories, such as Gamma-ray, X-ray, Ultra violet, Visible, Infrared and Radio waves.

VIRGO Project

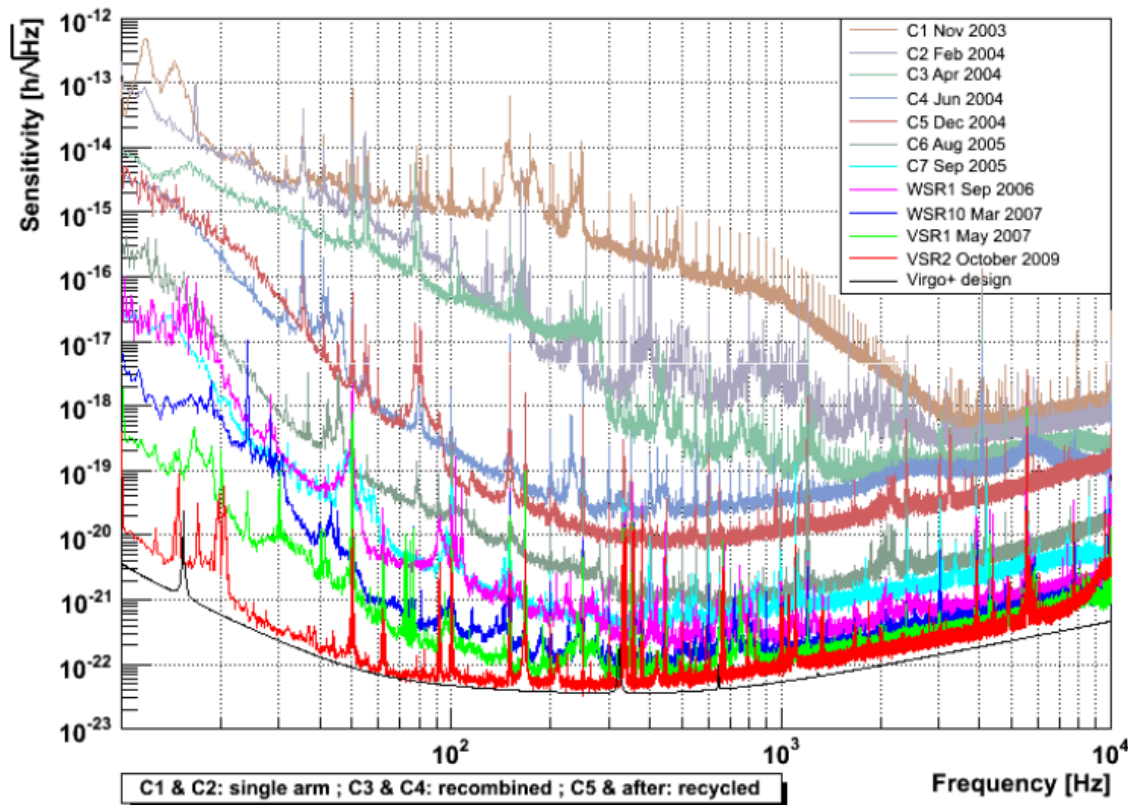
- Mainly France and Italy and Netherland, and EGO -

Italy
Pisa



VIRGO Project

- Maily France and Italy and Netherland, and EGO -



4×10^{-23} [1/rHz] strain sensitivity can detect GWs from 10Mpc away with $S/N = 8$

IP and GAS filters serve a superior strain sensitivity below 100Hz.

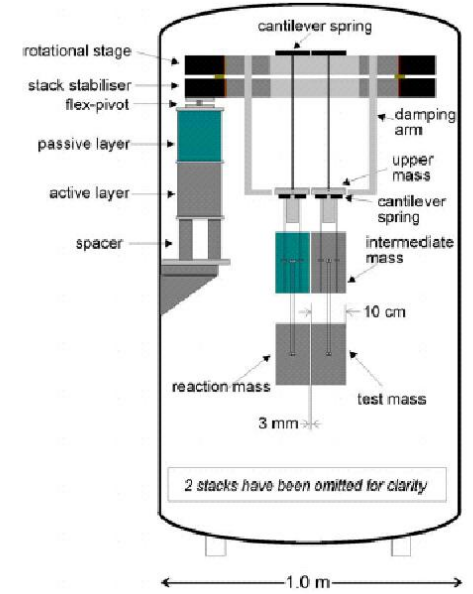
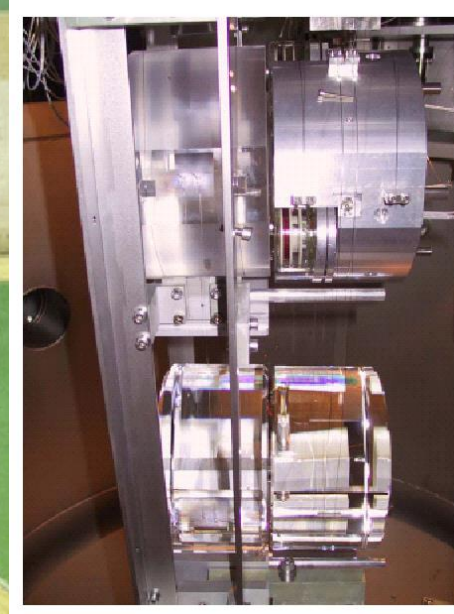
Upgrade for GWs detection is now undergoing.

3rd generation GWD as Einstein Telescope was proposed and some technical investigation have started.

GEO600 Project

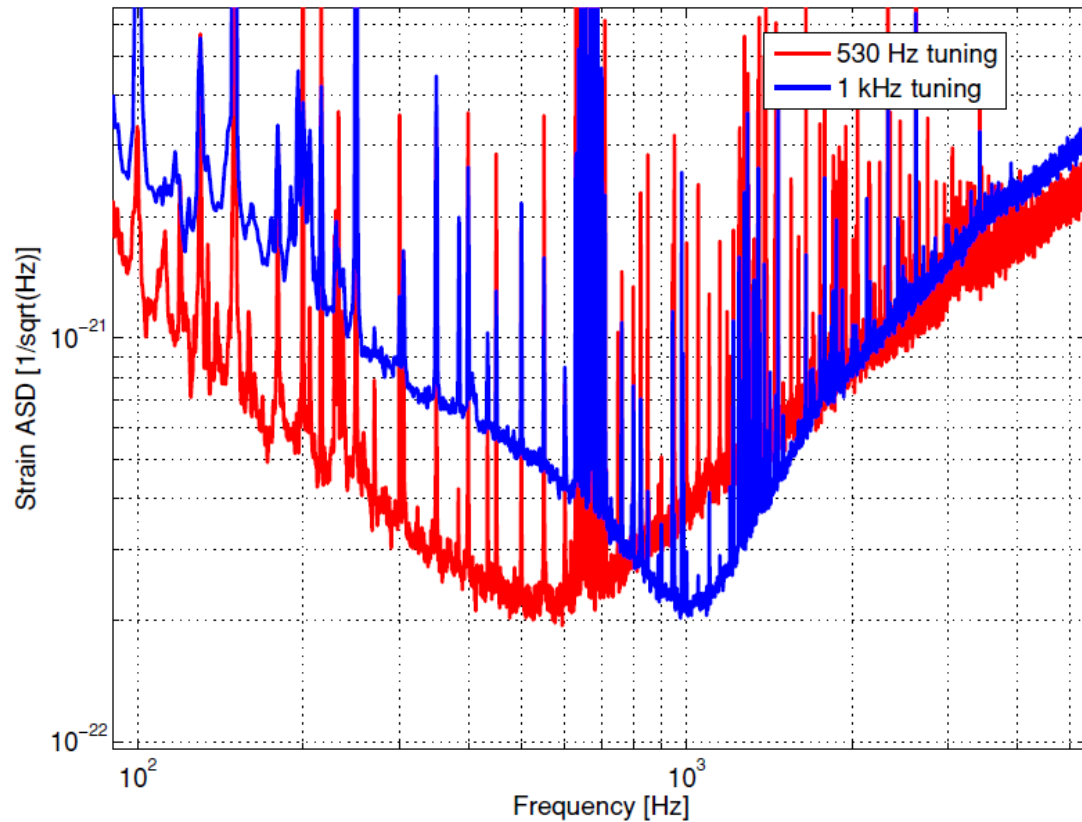
- Germany and Great Britain -

Germany
Hanover



GEO600 Project

- Germany and Great Britain -



Mirror suspension system using low mechanical loss silica fibers are introduced. → Used in Advanced-LIGO

Signal Recycling technique introduction

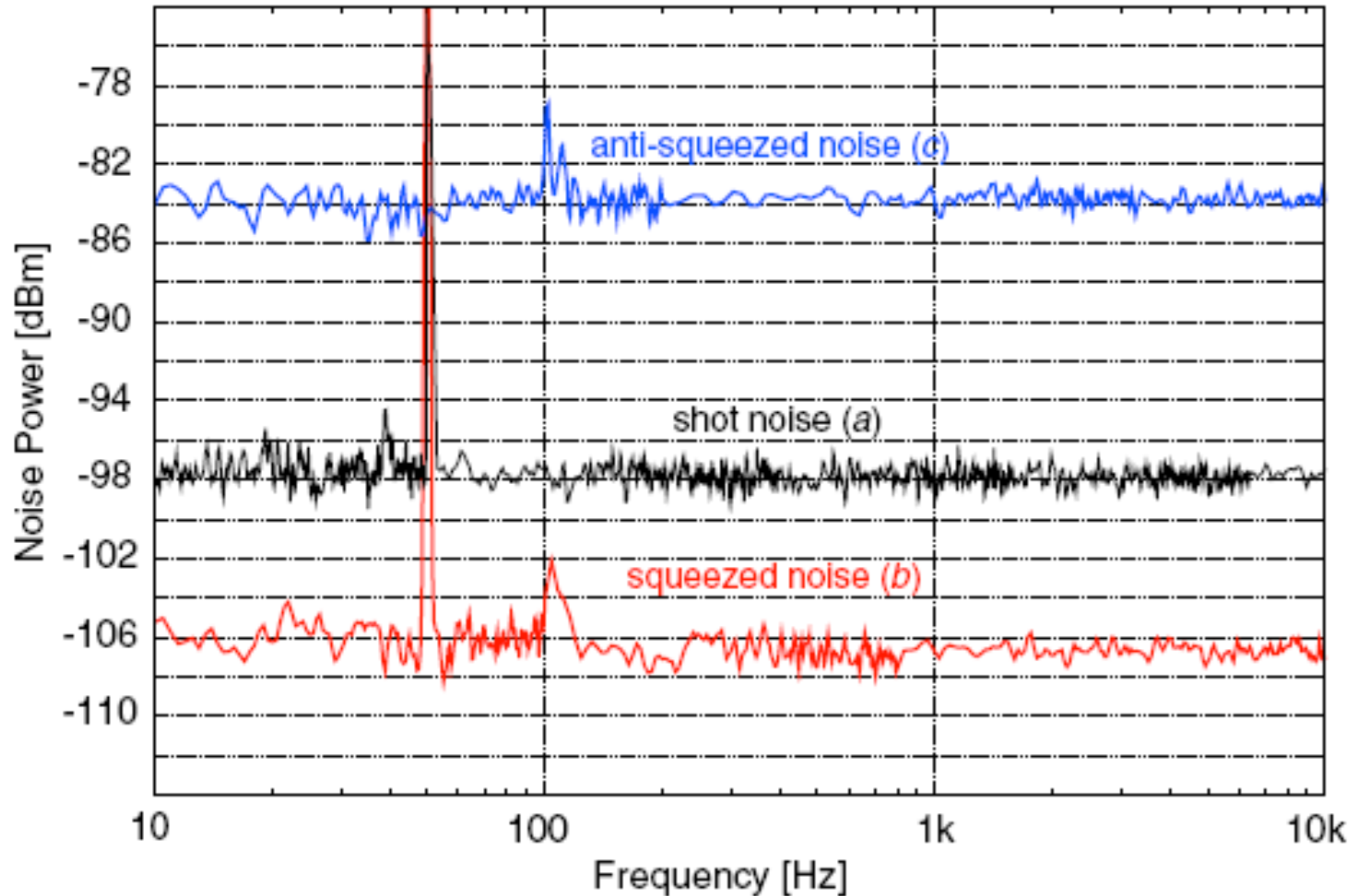
Continuous GW observation for bare possibility during LIGO and VIRGO offline and upgrading time.

Advanced quantum optical technique development and installation, such as Squeezed light source.

GEO600 Project

- Germany and Great Britain -

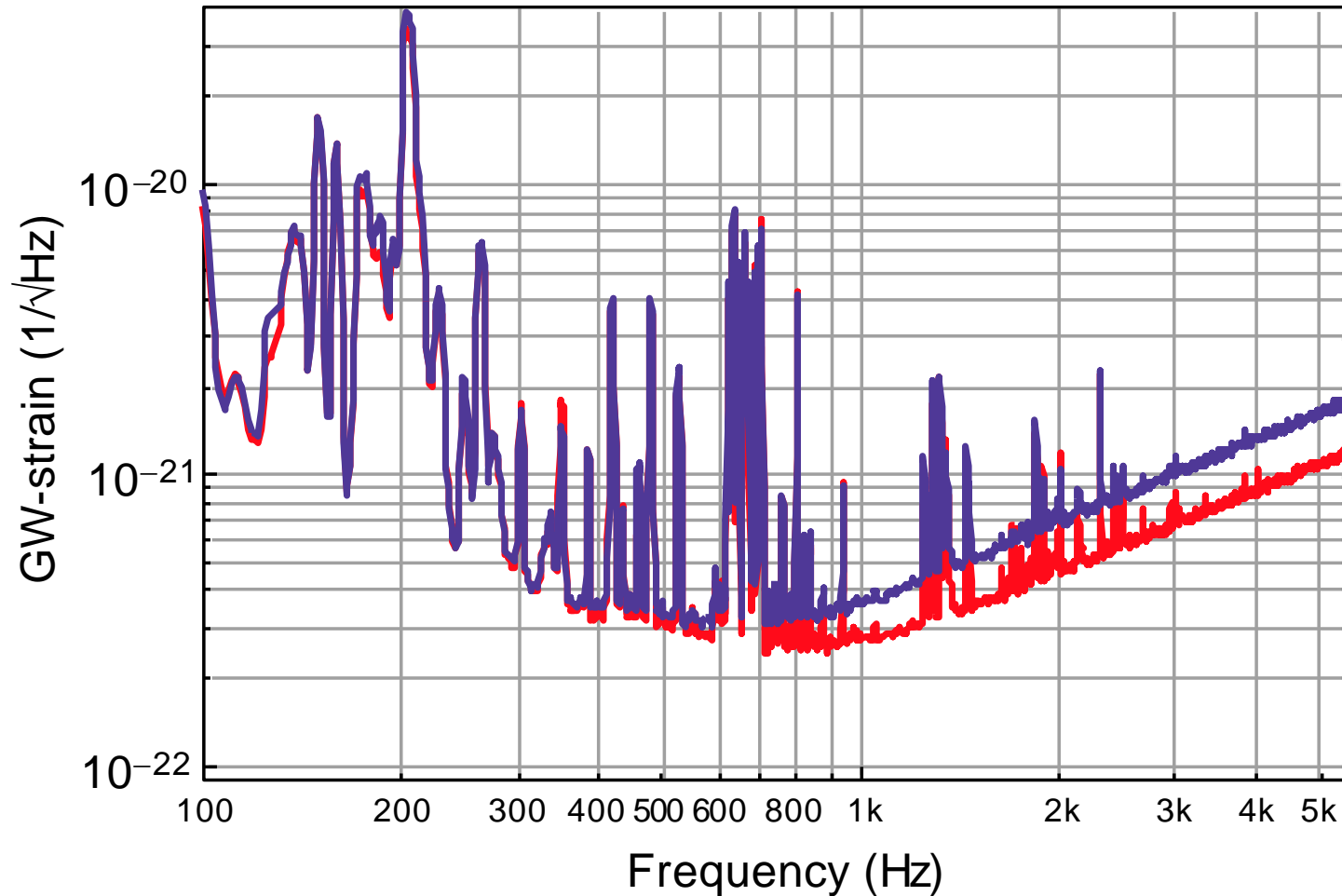
Squeezed Light Source in a table top Experiment



GEO600 Project

- Germany and Great Britain -

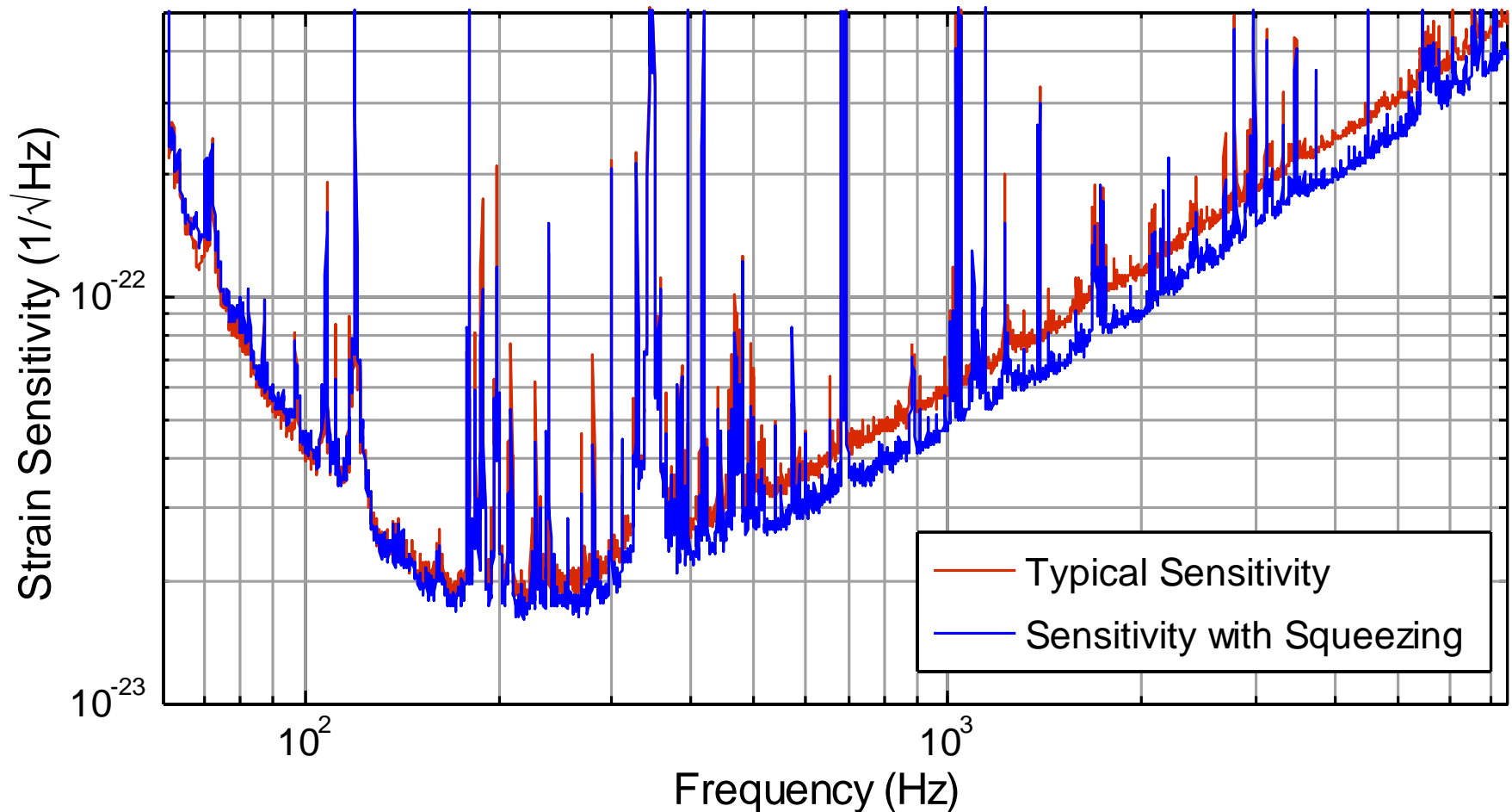
3.5dB Squeezing in GEO600



Highlights of LIGO

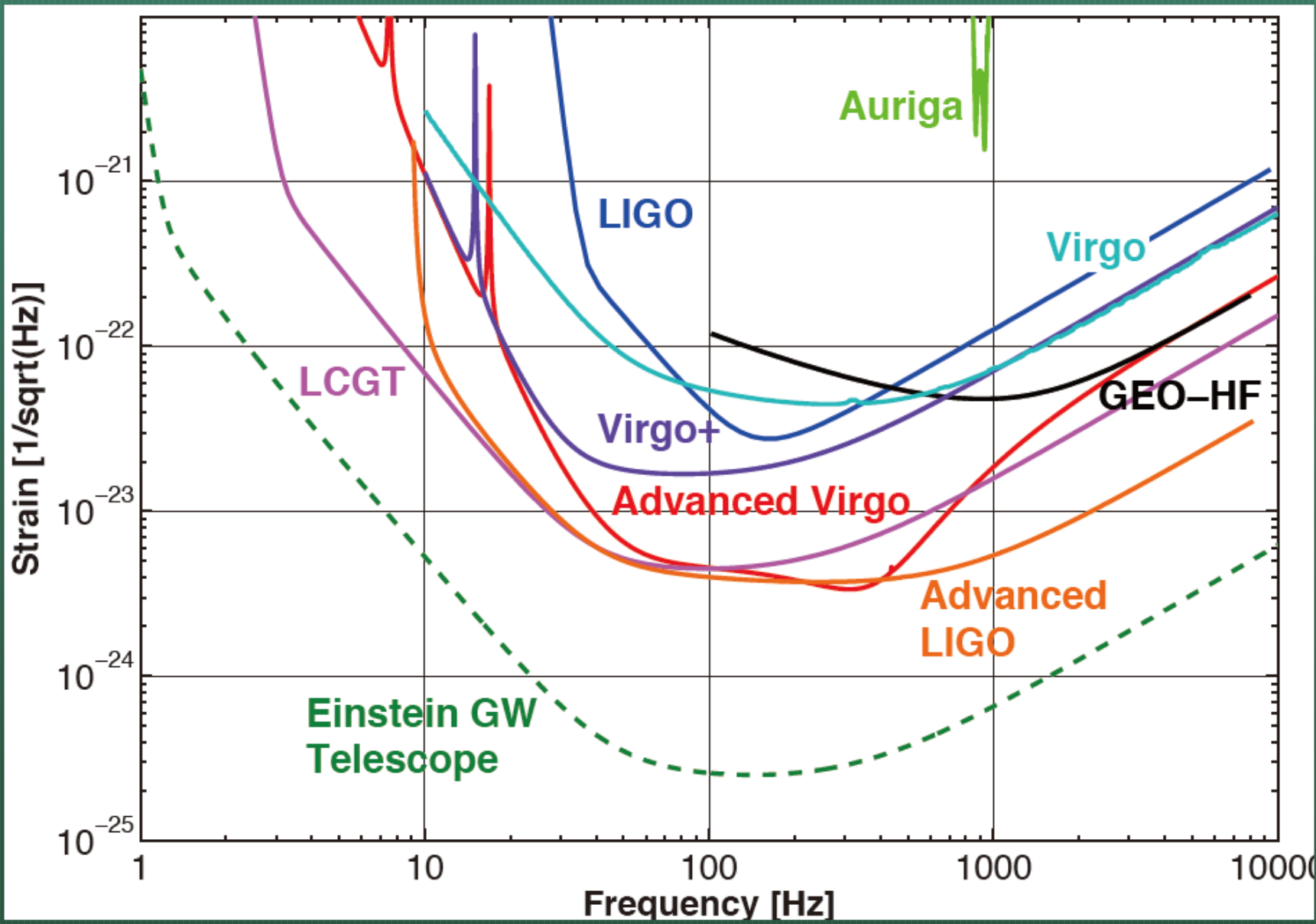
- Caltech·MIT and GEO600 and LIGO Scientific Collaboration -

GEO600 Squeezed Laser Source Introduction in H1 (4km)



Advanced GW Detectors Sensitivity

- Advanced LIGO, Advanced VIRGO, KAGRA, GEOHF, LIGO-India -



KAGRA Project in Japan

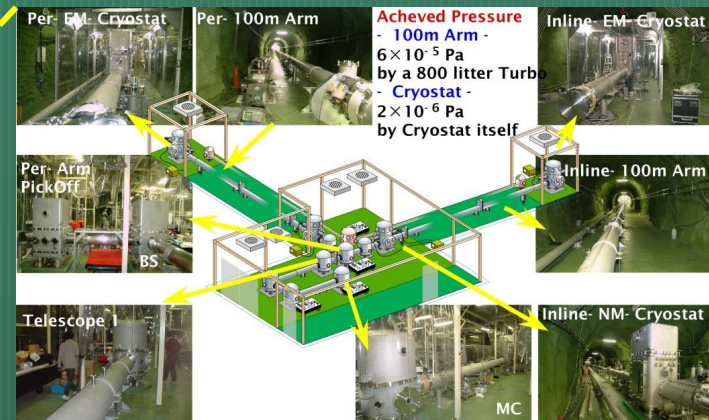
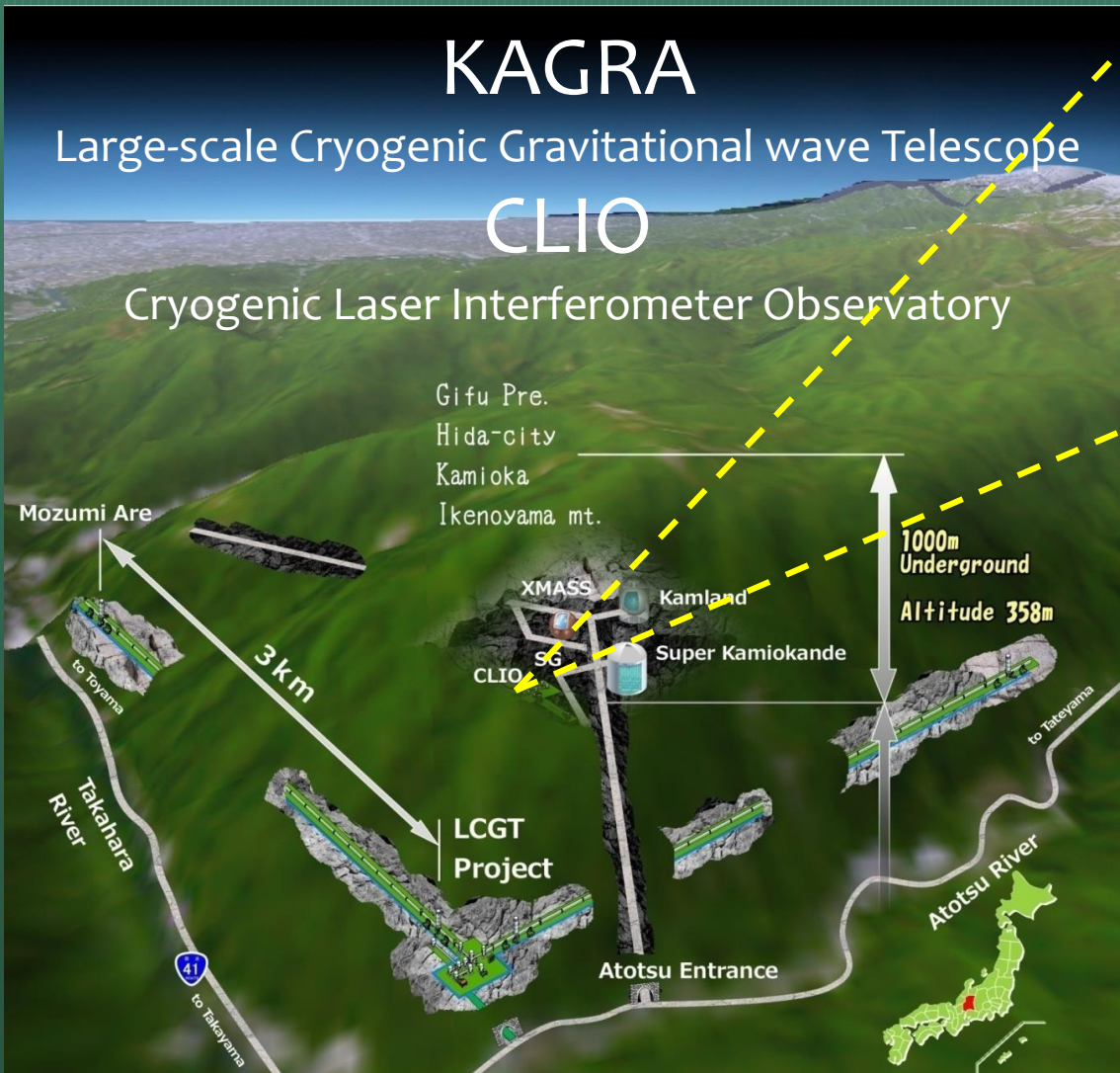
- TAMA300, LISM, CLIO to KAGRA -

KAGRA

Large-scale Cryogenic Gravitational wave Telescope

CLIO

Cryogenic Laser Interferometer Observatory



KAGRA(former called LCGT)

- (1) 200m underground.
- (2) Cryogenic mirror and suspension introduction.
- (3) Collaboration with Geophysics for better understanding about (under)ground motion.

History of GWD Development in Japan

2017
~2018

2015

2010

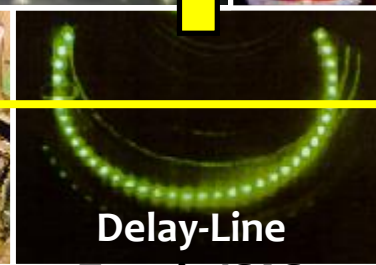
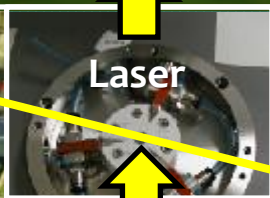
2002

1995
(Ph.D)

1991
(M,D)



RSE



KAGRA Started in 2010

Thermal Noise Reduction Verification in CLIO

Cryogenic IFO Demonstration using CLIK and CLIO

TAMA 300 Development

Underground IFO (LISM)

TAMA LISM Observation

Low Loss High quality mirror Development

FP and Delay-Line Comparison

KAGRA (3km, Underground, Cryogenic)

LSPI

TAMA300

Laser

CLIO

SAS

LISM in Kamioka

CLIK

Cryo R&D

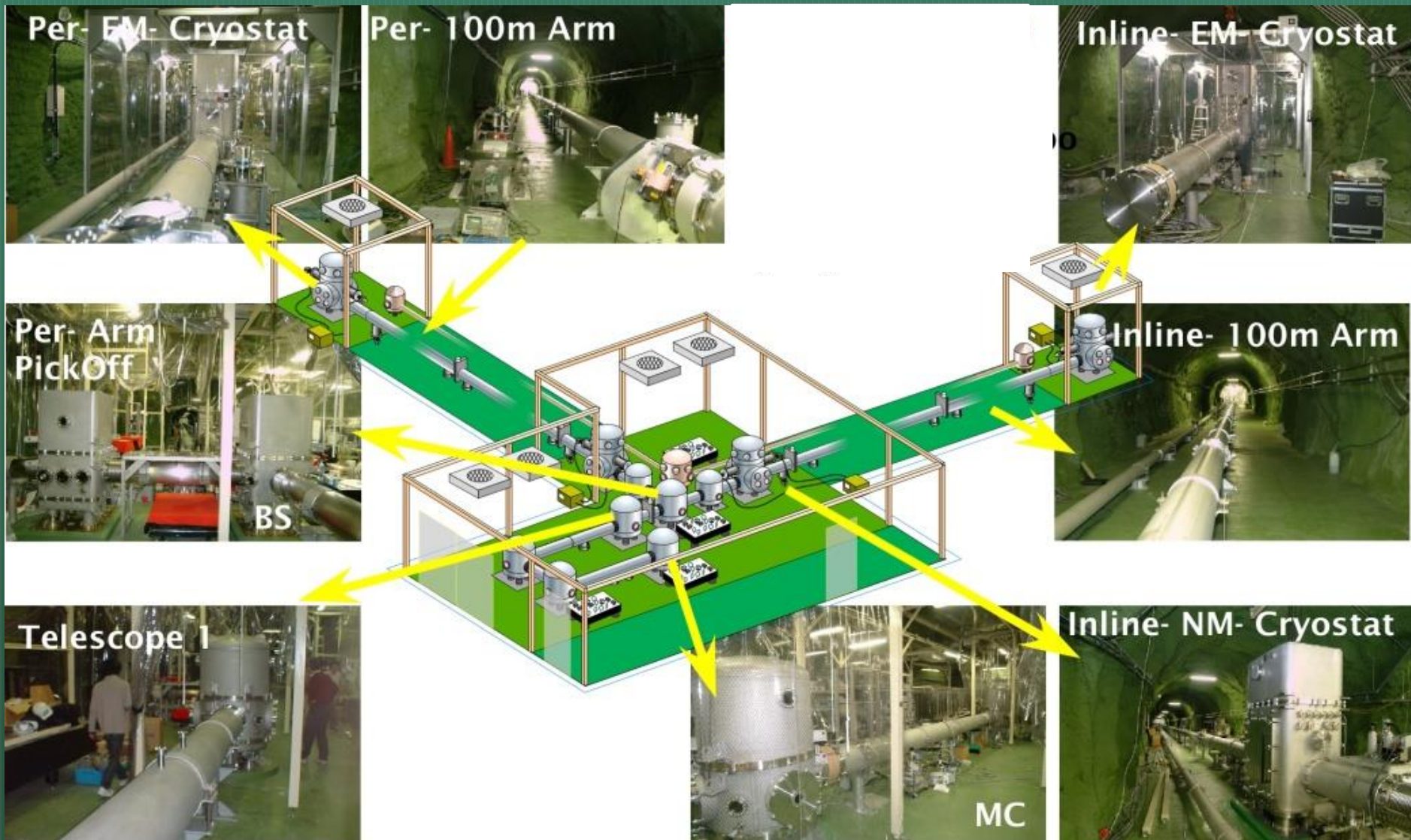
3m FP type Proto-Type

LISM FP type in Tokyo

Delay-Line Type in ISAS

Cryogenic Laser Interferometer Obs.

- Underground, 100m baseline, Cryogenic Sapphire Mirrors -



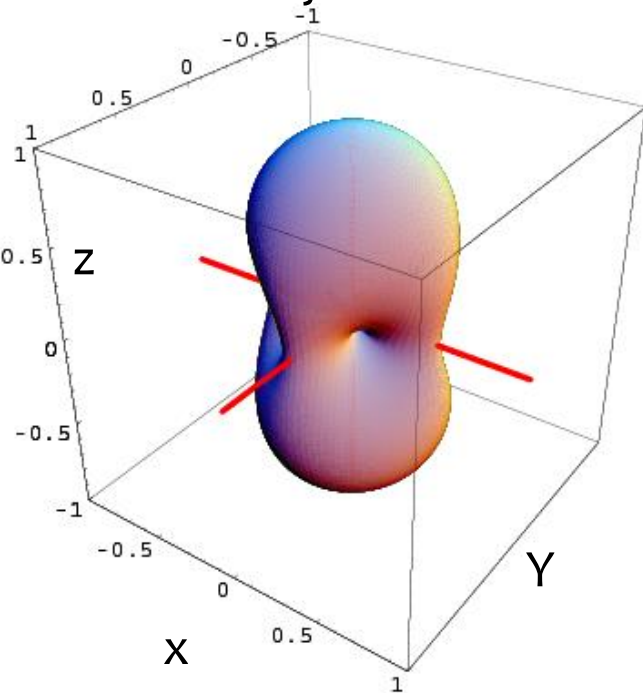
Merits of GW detection network

- **Convincing “True detection”**
 - By coincidence of independent detectors.
- **Determination of**
 - Arrival time,
 - Polarization of GWs,
 - (in case of inspiral binary,) absolute amplitude and inclination angle of orbit.
- **Duty time of observation**
 - More GW events,
 - Chance of follow up observation.
- **Sky coverage enhancement**

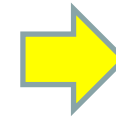
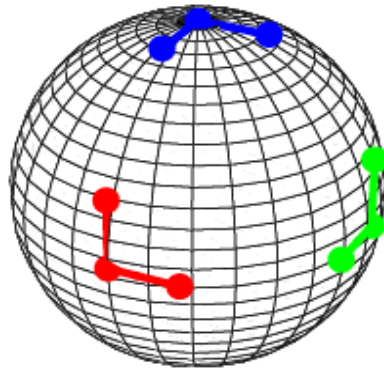
Importance of GWs network detection (1)

(1) Dead angle minimization

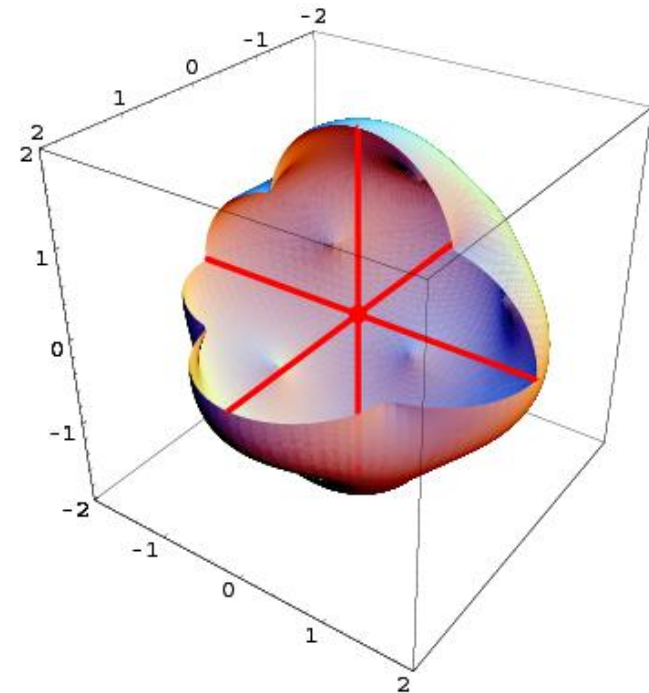
One GWD has insensitive angles because of directionality.



Assuming put 3 GWD on the Earth as shown in this figure...



Good sky coverage can be obtained.



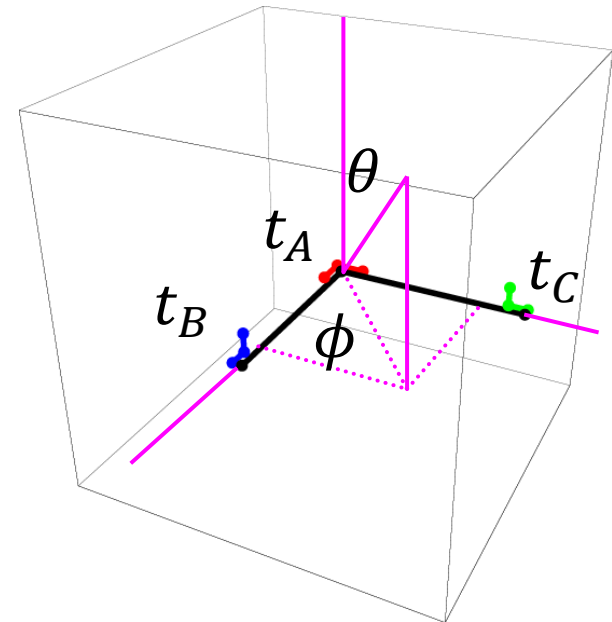
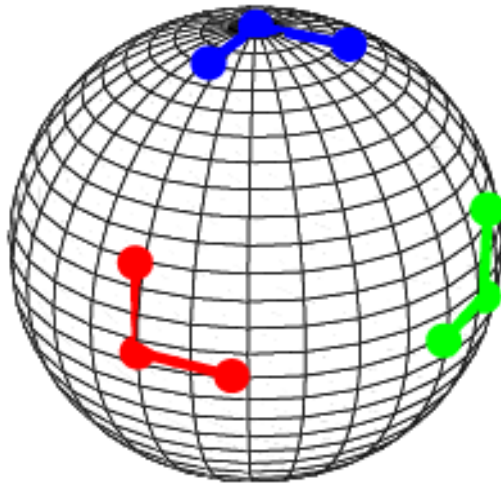
GWD on XY plane has four dead angles

Importance of GWs network detection (2)

(2) Enable source position identification
- angular resolution enhancement -

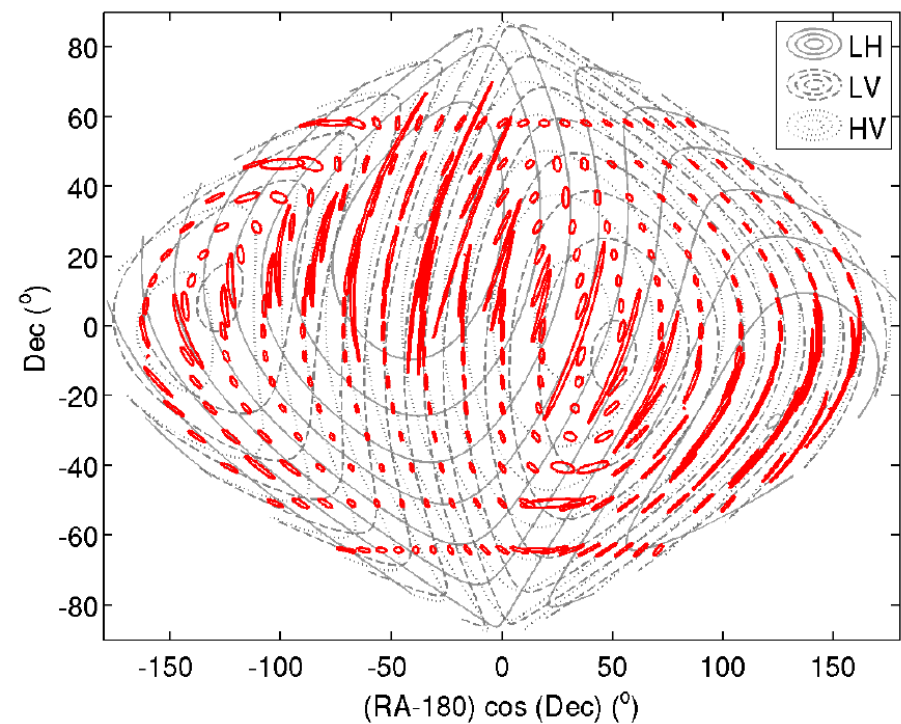
$$\tan \phi = \frac{t_C - t_A}{t_B - t_A}$$

$$\sin \theta = \frac{c}{L} \sqrt{(t_C - t_A)^2 + (t_B - t_A)^2}$$

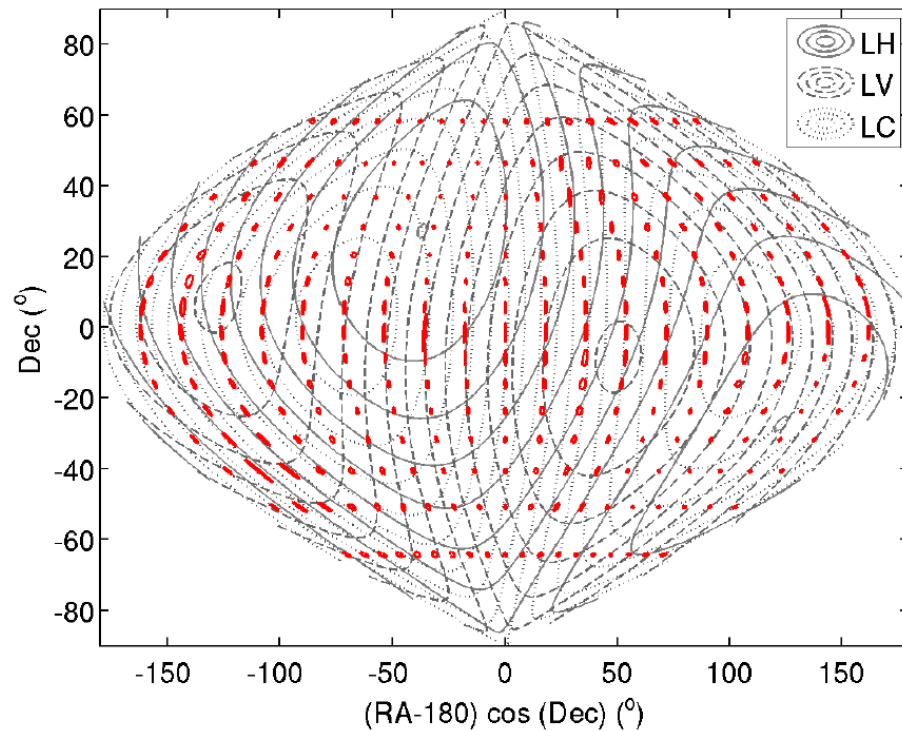


Importance of GWs network detection (3)

- Determination of source sky map : 95% confidence level (CL), SNR = 10.



LIGO (L+H) + VIRGO



LIGO (L+H) + VIRGO + KAGRA

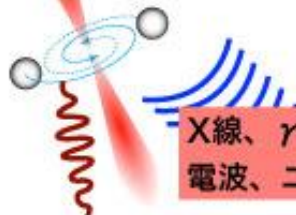
Multi-messenger Astronomy

T.Nakamura
U. kyoto

重力波源

- A. 合体波形
- B. パースト波
- C. 連続波
- D. 背景重力波
- E. 未知の波源

中性子星連星合体



超新星爆発



X線、 γ 線、可視光、赤外線、電波、ニュートリノ...

多様な手段で観測

計画研究A01

大立体角の連続モニター



MAXI

計画研究A02

光・赤外広視野望遠鏡

電波観測



計画研究A03

ニュートリノ検出



連携した観測の構築
重力波事象の理解

計画研究A04

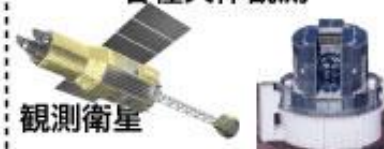
重力波のデータ解析

重力波観測

計画研究A05

理論

各種天体観測



観測衛星

地上の光赤外望遠鏡



海外の重力波検出器
aLIGO, aVirgo